Inaugural-Dissertation

submitted to the

Combined Faculties for the Natural Sciences and for Mathematics

of the Ruperto-Carola University of Heidelberg, Germany

for the degree of

Doctor of Natural Sciences

Presented by

M.Sc. (Mol. Biotechnology) Babitha George

Born in Angamaly, India

Oral Examination: 18 June 2015

Regulation and Function of MYBBP1A in Cellular Senescence and Pathogenesis of Head and Neck Cancer

Referees: Prof. Dr. Peter Angel

PD. Dr. Karin Müller-Decker

“To my parents, brother and loving husband”

Summary

Myb-binding protein 1A (MYBBP1A) is a nucleolar protein implicated in stress response and carcinogenesis. However, its functional contribution to cellular senescence as well as the clinical relevance in head and neck squamous cell carcinoma (HNSCC) have not been addressed so far. In the present study, a cell culture model of genotoxic senescence, which was induced by the topoisomerase II inhibitor VP-16, was established to unravel the role of MYBBP1A in cellular senescence. Interestingly, in response to DNA damage, MYBBP1A first translocate from the nucleolus to the nucleoplasm and subsequently, its protein levels decreased in senescent cells. Loss-of-function approaches in tumor cell lines provided further evidence that silencing of MYBBP1A was not sufficient to trigger senescence, but that it modulated the efficacy of genotoxic-induced senescence and augments resistance to irradiation. Although, the precise molecular mechanism by which MYBBP1A regulates DNA damage-induced senescence remains elusive and warrants further investigation, this study revealed an inverse regulation of MYBBP1A and AKT(Ser473) phosphorylation to be a characteristic feature of senescent tumor cells. Most strikingly, immunohistochemical analysis of tissue microarrays with tumor specimens from primary oropharyngeal squamous cell carcinoma (OPSCC) patients (n=61) revealed that a MYBBP1A^{low}pAKT(Ser473)^{high} staining pattern serves as an independent marker for poor clinical outcome. Remarkably a significant correlation with progression-free or overall survival was not found considering pAKT(Thr308) levels, suggesting a more critical role of the mTOR/AKT pathway for the clinical behavior of OPSCCs with low MYBBP1A levels. In summary, these data demonstrate that tumor cells with a MYBBP1A^{low} but pAkt(Ser473)^{high} protein pattern have a senescent-like phenotype and might critically contribute to tumor progression due to the emergence of highly malignant and/or therapy resistant tumor cells. Moreover, the abundance of MYBBP1A^{low}pAKT(Ser473)^{high} senescent tumor cells in primary tumors as well as following tumor relapse could serve as a reliable biomarker for treatment decision making and to stratify HNSCC patients at high-risk for treatment failure. Thus, restoration of MYBBP1A function or pharmacological inhibition of the PI3K/mTOR/AKT pathway is an attractive new concept not only to sensitize tumor cells for available treatment options, but also to establish new strategies for targeted therapy with the potential of elimination of senescent cells.

Zusammenfasung

Myb-binding protein 1A (MYBBP1A) ist ein Protein im Nuleolus und ist an der zellulären Stressantwort und bei der Karzinogenese beteiligt. Jedoch wurde seine Rolle beim Prozess der Seneszenz sowie die Relevanz von seneszenten Tumorzellen beim Plattenepithelkarzinom der Kopf- und Halsregion (HNSCC) bislang nicht untersucht. In der aktuellen Studie wurde durch die Applikation des Topoisomerase II Inhibitors VP16 ein Zellkulturmodell für genotoxische Seneszenz etabliert, um die Regulation und Funktion von MYBBP1A bei der zellulären Seneszenz aufzuklären. Infolge von DNA-Schädigung wurde zunächst eine Translokation von MYBBP1A vom Nukleolus in das Nukleoplasma nachgewiesen und anschließend ein Verlust von MYBBP1A in seneszenten Zellen beobachtet. Funktionelle Studien in Tumorzelllinien belegten, dass eine Hemmung von MYBBP1A nicht für die Induktion der Seneszenz ausreichend ist, jedoch das Ausmaß der genotoxischen Seneszenz moduliert und die Resistenz gegenüber Bestrahlung steigert. Obwohl die zugrundeliegenden Mechanismen noch aufgeklärt werden müssen, zeigt diese Studie eine inverse Regulation zwischen MYBBP1A und AKT(Ser473) Phosphorylierung als charakteristische Eigenschaft von seneszenten Tumorzellen. Die klinische Relevanz dieser Ergebnisse konnte mittels immunhistochemischer Analysen von Gewebearrays mit Tumorproben von Patienten mit einem Oropharynxkarzinom (OPSCC, n=61) gezeigt werden. Ein MYBBP1A^{low}pAKT(Ser473)^{high} Färbemuster stellte sich als unabhängiger Marker für eine schlechte Prognose heraus. Interessanterweise wurde keine vergleichbare Korrelation für pAKT(Thr308) nachgewiesen, was auf eine kritischere Rolle der mTOR/AKT Signalkaskade für das klinische Verhalten von OPSCC Patienten mit einer geringen MYBBP1A Proteinexpression hindeutet. Zusammenfassend demonstrieren die gezeigten Daten, dass Tumorzellen mit MYBBP1A^{low} aber pAKT(Ser473)^{high} Proteinlevel einen Seneszenz-ähnlichen Phänotyp aufweisen und aufgrund ihrer malignen und therapieresistenten Eigenschaften maßgeblich zur Tumorprogression beitragen könnten. Die Häufigkeit von MYBBP1A^{low}pAKT(Ser473)^{high} Tumorzellen im Primärtumor bzw. im Tumorrezidiv könnte als zuverlässiger Biomarker für die Therapieentscheidung oder zur Stratifizierung von Risikopatienten für Therapieversagen beitragen. Somit stellt die Widerherstellung der MYBBP1A Funktion oder eine pharmakologische Hemmung der PI3K/mTOR/AKT Signalkaskade ein attraktives Konzept dar,

um Tumorzellen für etablierte Therapieoptionen zu sensitivieren. Alternativ könnten sie die Grundlage für neue Strategien der zielgerichteten Therapie bilden mit dem Ziel seneszente Zellen zu eliminieren.

Acknowledgments

The research presented in this thesis was carried out in the Division of Experimental and Translational Oncology at the German Cancer Research Center (DKFZ) and in the University Hospital Heidelberg. Hence, I would like to thank all the people who contributed to this work and supported me during this time. In particular, I would like to thank:

- PD Dr. Jochen Hess, my mentor, for providing the opportunity to perform my PhD thesis in his group and for his substantial contribution to the conceptual design of this work. He supported my work not only by his wide knowledge but also by his constant positive attitude and many encouraging discussions.
- Prof. Dr. Peter Angel for giving me the opportunity to be a part of A100 group, for his valuable discussions throughout my research project and finally for being first referee.
- PD Dr. Karin Müller-Decker for her valuable ideas and helpful suggestions as a member of the advisory committee and for being second examiner in my disputation.
- Prof. Dr. Michael Boutros for chairing the examination committee.

During this time I have collaborated with many colleagues who greatly contributed to this work. Especially, I would like to thank:

- Dr. Valery Krizhanovsky and Anat Biran for our fruitful collaboration within the DKFZ-MOST research program and for many exciting discussions.
- Dr. Gustavo Acuna Sanhueza for introducing me to the field of MYBBP1A.
- Dr. Vinko Misetic and Dr. Peter Hofner for introducing me to the workflow in the laboratory.
- Ingeborg Vogt, Antje Schuhmann, Leoni Erdinger, Ines Kaden and Nataly Henfling for excellent technical assistance.
- Dr. Maria Llamazares Prada, Dr. Barbara Costa, Dr. Pilar Bayo and Aurora De Ponti for being constant and exceptionally helpful discussion partners.
- Dr. Jochen Hess, Jennifer Grünow and Vinod Paremal for comments and critical reading of this thesis.

I would like to extend my thanks to all current and former members at DKFZ and in the clinic for the great time spent in the lab, especially to:

- Aurora, Maria, Barbara, Laura, Christine, Tanja, Sebastian, Leoni, Pilar, Effie, Regina, Vinko and Jenni for being awesome lab members, and for our friendship.
- Antje and Ingeborg for being an important source of motivation and support.

This work would certainly not be possible without good friends and a lovely family. I am deeply grateful to:

- My friends, particularly Aparna, Shruthi, Milene, Yammuna, Vidhya and Corina, for their invaluable friendship.
- My family in Angamaly, Wayand, Amsterdam, Singapore and Germany, specially my German Mom, for their enduring support and encouragement throughout my entire studies. Your prayer for me was what sustained me thus far.
- My parents who always encouraged and supported me. My brother and best friend, Bibin, for all of the sacrifices that you have made on my behalf.
- Words cannot express how grateful I am to my husband Vipin, for going with me through all the ups and downs of a PhD's life and for his loving support and understanding.

Table of Contents

List of Figures

List of Tables

Abbreviations

˚C	Degree Celcius
aa	Amino acid
AhR	Aryl hydrocarbon receptor
AP-1	Activator protein-1
APS	Ammonium peroxodisulfate
ATM	Ataxia telangiectasia mutated
ATP	Adenosine 5'-triphosphate
ATR	Ataxia telangiectasia and Rad3-related protein
BCA	Bicinchoninic acid
BCL	B-cell lymphoma
bp	Base pairs
BCA	Bicinchoninic acid
BP-1	Binding protein 1
BrdU	Bromodeoxyuridine
BSA	Bovine serum albumine
$CaCl_2$	Calcium chloride
CASP8	Caspase-8
CCND1	Cyclin D1
CDKN2A	Cyclin-dependent kinase inhibitor 2A
CDK2	Cyclin-dependent kinase 2
CFA	Colony forming assay
CHK	Cell-cycle checkpoint kinase
COX	Cyclooxygenase
CRY1	Cryptochrome circadian clock1
CT	Cycle of threshold
cDNA	Complementary desoxyribonucleic acid
ddH2O	Deionized water
DCR2	Decoy receptor 2
DDR	DNA damage response
DMEM	Dulbecco´s Modified Eagles Medium
DMSO	Dimethylsulfoxide
DNA	Desoxyribonucleic acid
DNA-PK	DNA-dependent protein kinase
DNase	Desoxyribonuclease

dNTP	Desoxynucleoside triphosphate
DTT	Dithiothreitol
E6	HPV early gene 6
E7	HPV early gene 7
ECL	Enhanced chemoluminescence
ECM	Extracellular matrix
EDTA	Ethylenediamine-tetraacetate
EGFR	Epidermal growth factor receptor
ERK	Extracellular signal-regulated kinase
EtOH	Ethanol
GM-CSF	Granulocyte-macrophage colony-stimulating factor
FCS	Fetal calf serum
gDNA	Genomic DNA
GOI	Gene of interest
GRO1	chemokine (C-X-C motif) ligand 1
h	Hour
H_2O_2	Hydrogen peroxide
H&E	Hematoxilin and eosin
HKG	Housekeeping gene
HRP	Horseraddish peroxidase
HNSCC	Head and neck squamous cell carcinoma
HP-1	Heterochromatin protein-1
HPV	Human papilloma virus
IF	Immunofluorescence
IHC	Immunohistochemistry
INPP4B	Inositol polyphosphate-4-phosphatase, type II
IL	Interleukin
JAK	Janus kinase
kb	Kilobase pairs
KCl	Potassium chloride
kDa	Kilo dalton
KH_2PO_4	Potassium hydrogen phosphate
mM	Millimolar
mg	Milligram
µl	Microliter
MAPK	Mitogen-activated protein kinase
MEF	Mouse embryonic fibroblast
$MgCl_2$	Magnesium chloride

MMP	Matrix metalloproteinase
mRNA	Messenger RNA
mTOR	Mammalian target of rapamycin
MYBBP1A	Myb-binding protein 1A
MW	Molecular weight
NaCl	Sodium chloride
NaOH	Sodium hydroxyde
NGS	Next-generation sequencing
NIH3T3	Mouse embryonic fibroblast cell line
NF1	Neurofibromin 1
NF-κB	Nuclear factor-kappaB
NK cell	Natural killer cell
NLS	Nucleolar localization sequences
NP-40	Nonidet P-40
n.s.	Not significant
o/n	Overnight
OPSCC	Oropharyngeal squamous cell carcinoma
OS	Overall survival
PAGE	Polyacrylamide gel electrophoresis
PBS	Phosphate buffered saline
PCNA	Proliferating cell nuclear antigen
PCR	Polymerase chain reaction
PDK1	Phosphoinositoside-dependent protein-kinase 1
PFA	Paraformaldehyde
PFS	Progression free survival
PGC-1α	Peroxisome proliferator-activated receptor gamma coactivator 1-alpha
pH	Pondus hydrogenii
PI3K	Phosphoinositide 3-kinase
PIP_2	Phosphotidylinositol 1,4-biphosphate
PIP_3	Phosphotidylinositol 1,4, 5-triphosphate
PKC	Protein kinase C
Prep1	Pbx-regulating protein-1
PTEN	Phosphatase and tensin homolog
qRT-PCR	Quantitative real-time PCR
RNA	Ribonucleic acid
ROS	Reactive oxygen species
rpm	Rounds per minute
Rb	Retinoblastoma

RT	Room temperature
RT-PCR	Reverse transcriptase PCR
RTK	Receptor tyrosine kinase
SA-β-gal	Senescence-associated β-galactosidase
SAHF	Senescence-associated heterochromatic foci
SASP	Senescence-associated secretory phenotype
SCC	Squamous cell carcinoma
SD	Standard deviation
SDS	Sodium dodecyl sulfate
SIPS	Stress-induced premature senescence
siRNA	Small interfering RNA
STAT	Signal transducers and activators of transcription
T	Tumor stage
T_A	Annealing temperature
T_M	Melting temperature
Taq	Thermus aquaticus
TCS	Therapy-induced cellular senescence
TEMED	N, N, N', N', Tetramethylethylendiamine
TGF-β	Transforming growth factor-β
TMA	Tissue microarray
TNF	Tumor necrosis factor
TPPII	Tripeptidyl-peptidase II
U	Unit
UV	Ultraviolet
V	Volt
VEGF	Vascular endothelial growth factor
VHL	Von Hippel-Lindau
v/v	Volume to volume
w/v	Weight in volume

Introduction

1 Introduction

1.1 Head and neck squamous cell carcinoma

Head and neck cancer encompasses a heterogeneous group of epithelial malignancies arising within the upper aerodigestive tract, and presents the sixth common cancer in the world by incidence (1, 2). Over 90% of head and neck cancers are of squamous cell histology (HNSCC), which originates from the mucosal surfaces of the oral cavity, pharynx, larynx or nasal cavity (Fig. 1.1).

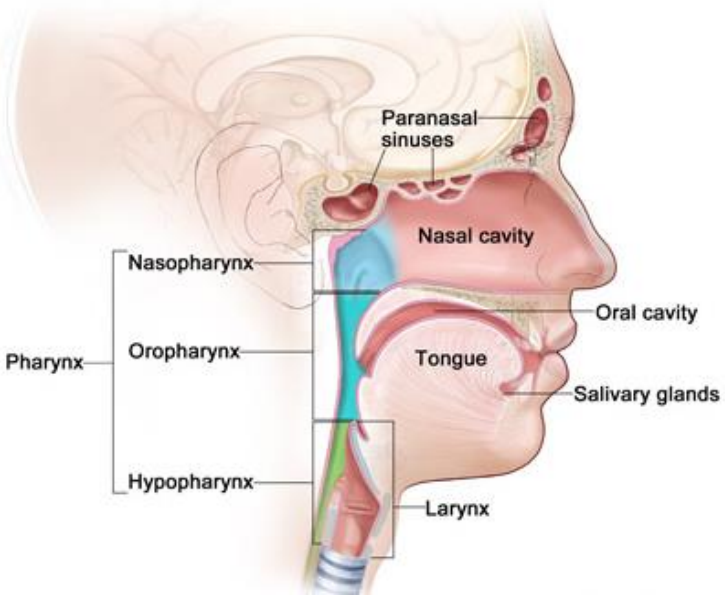

Figure 1.1: Anatomic sites and subunits of head and neck. HNSCC includes following subsites: oral cavity, pharynx, larynx, paranasal sinuses, nasal cavity and salivary glands. Image source: www.cancer.gov/PublishedContent/ Images/ cancertopics/factsheet/ Sites-Types/headandneck-diagram.jpg.

Worldwide, an estimated 644.000 new cases are diagnosed each year and a high incidence is seen in the Indian subcontinent, Australia, France and Brazil (Fig. 1.2) (3, 4). Mortality expected

to rise in South East Asia by 2030, whereas in Europe is expected to remain stable (5). Moreover, studies in both low- and high-income countries have revealed that the patients with low socio-economic class and low educational attainment had a greater risk for the development of HNSCC, particularly oral cancer (6). The incidence of HNSCC is three-fold higher in men than women and reported to increases with age (3, 4). According to the large scale epidemiological studies, in Europe 98% of patients diagnosed are over 40 and 50% are over 60 years of age (3).

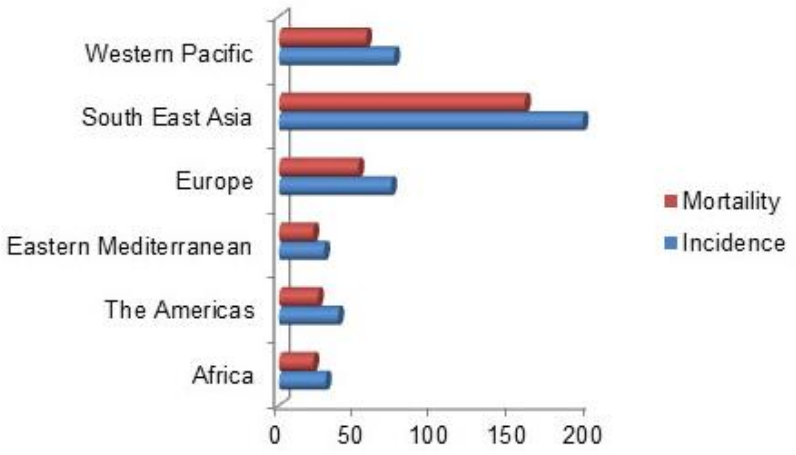

Figure 1.2: Worldwide mortality and incidence figures of head and neck cancer. Estimated figures in 2008 for head and neck cancers. Population number should be multiplied by 1000**.** (Data taken from Mehanna et al. 2010 (3)).

The major risk factors so far identified are tobacco (smoking and smoke-less products such as betal quid) and alcohol consumption, account for about 75% cases with HNSCC. The combined effect of tobacco and alcohol causes a synergistic increase in risk (7). In the western world, public health measures have been successful in reducing the use of tobacco, and therefore attributed to a decrease in the incidence of HNSCC during the past decade. However, there has been a dramatic increase in the incidence rates of oropharyngeal squamous cell carcinoma (OPSCC), which may be related to an increase in oral and oropharyngeal human papilloma viruses (HPVs) infections especially with HPV subtype 16 (HPV-16) (8, 9). Importantly, the HPV status was found to have a profound influence on patient survival. Patients with HPV-positive HNSCC showed improved survival outcomes compared to those with HPV-negative HNSCC irrespective of treatment modality (10). Although Epstein-Bar virus infection (for

nasopharyngeal cancer) and inherited disorders such as Fanconi anemia render a predisposition for the disease, they play only a minor role (11, 12). A diet rich in fruits and vegetables has also been shown to have the most promising effect to reduce the risk of HNSCC (13).

1.1.1 Molecular pathology of HNSCC

HNSCC is a heterogeneous disease, which involves a multistep process starting from normal epithelium progressing through hyperplasia to dysplasia to carcinoma in situ and invasive carcinoma (Fig. 1.3). A plethora of studies has been published on the identification of cancer-related genes and frequently found genetic changes in HNSCC, most importantly on chromosomal arms 3p, 17p and 9p (14-16). Thus progressive accumulation of these alterations in oncogenes, proto-oncogenes and tumor suppressors can lead to the formation of a malignancy often precedes to acquire a characteristic phenotype that includes, limitless replicative potential, changes in growth factor signaling, ability to evade apoptosis, invasion, metastasis and angiogenesis (17, 18).

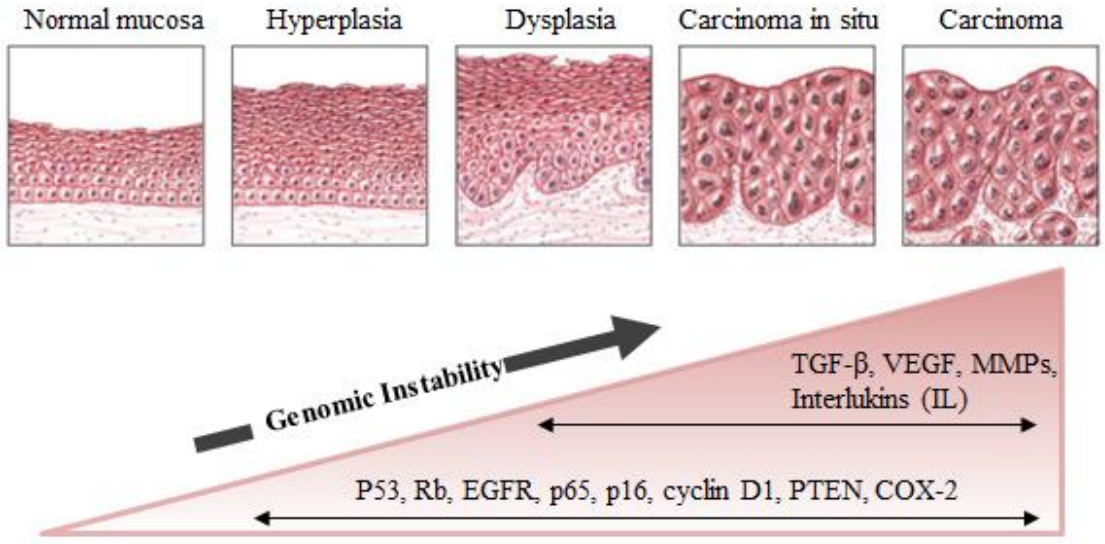

Figure 1.3: Genetic progression model for HNSCC. Head and neck cancer is progressed through a multistep processes from normal mucosa through the advancing stages of squamous dysplasia to invasive carcinoma and is driven by the progressive accumulation of genetic alterations. Genes and pathways involved are depicted. Modified from Pai et al. 2009 (15).

Cellular proliferation: p53/Rb/CDKN2A/CCND1

The TP53 and retinoblastoma (Rb) pathways are disrupted in almost all HNSCC patients, result in limitless replicative potential and immortalization. Mutations in the TP53 tumor suppressor gene are one of the earliest identified genetic alterations in HNSCC, reported in 60-80% of cases (19). In HNSCC, an increased *TP53* mutation rate is associated with tobacco and alcohol use, further contributes to the clinical behavior of tumors (20, 21). Most notably, in p53 wild-type tumors the abrogation of p53 function may be mediated by other mechanisms. These include expression of the HPV viral oncoprotein E6, overexpression/amplification of *MDM2* and deletion of *CDKN2A*, which eliminates the p14/ARF gene (22-25).

pRb is targeted early in the carcinogenesis of HNSCC by the inactivation of *CDKN2A*, encoding the cell cycle regulators p16/INK4A and p14/Arf/INK4B. *CDKN2A* mutations were found in approximately 7-9% of tumors, with copy number losses in further 20-30% cases (26, 27). In HPV-positive HNSCC, the Rb pathway is inactivated by the viral E7 protein, which binds to RB1 and abrogates the requirement for p16/INK4A silencing (28). Furthermore, amplification of *CCND1* gene, which encodes cyclin D1 on chromosomes 11q13 occurs in over 80% HNSCC, more frequently in HPV-negative tumors (29). Thus, abrogation of p53, *CDKN2A* and overexpression of cyclin D1 are associated with decreased survival and used as an independent predictors of poor prognosis to genotoxic therapy (30).

Terminal differentiation: Notch/p63 axis

One of the novel findings emerged from whole-exome sequencing studies of HNSCC was the discovery of inactivating mutations of *NOTCH1* gene in 14-15% of the HNSCC tumors, making *NOTCH1* the second most common mutation after *TP53* (26, 27). *NOTCH* pathway has been linked to multiple biological functions, including regulation of self-renewal capacity, cell cycle exit, cell survival and promoting terminal differentiation (31, 32). In haematological malignancies, NOTCH1 signaling has been reported to be protumorigenic by activating mutations (33), whereas in HNSCC, the majority were nonsense mutations, suggesting a tumor-suppressor function for this pathway (31). Additionally, Notch activity has been linked to the downmodulation of HPV-driven transcription of the E6 and E7 viral genes (34). NOTCH1 has also been found to be involved in squamous epithelial differentiation, and this is controlled by

p53-related transcription factor p63 (35). Overexpression and/or genomic amplification of the *TP63* locus have been observed in majority of invasive HNSCC (36).

Cell survival: EGFR/Ras/PIK3CA/PTEN/CASP8

EGFR overexpression is detected in many cases of HNSCC and often considered to be among the most important therapeutic targets (37). Approximately 10-30% of HNSCC display *EGFR* gene amplification, which has been suggested to correlate with poor prognosis (38). However, *EGFR* mutations are rare in HNSCC, reported in only 1-7% of patients (39). Activation of EGFR acts as an upstream signaling to both Ras-MAPK and PI3K-PTEN-AKT pathways (40). Ras mutations are less common in HNSCC and often observed in relationship to tobacco history among the Indian population but less frequently in the western world (41). One of the nuclear targets of EGFR is *CCND1* that encodes cyclin D1 protein, which involved in cell cycle progression (42).

Another important commonly activated pathway in HNSCC is PI3K signaling, which is one of the major downstream targets of EGFR. Phosphoinositide 3-kinases (PI3Ks) are a family of enzymes capable of phosphorylating the 3'-OH position of phosphoinositide lipids (PIs) and have important roles in promoting cell growth, differentiation, survival, proliferation and migration (Fig. 1.4) (43, 44). PI3Ks are activated by RTKs and catalytic subunit phosphorylates phosphatidylinositol 1,4-biphosphate (PIP_2) to form phosphatidylinositol 1,4,5-triphosphate (PIP_3), which further recruits phosphoinositide-dependent protein-kinase 1 (PDK1) and AKT to the plasma membrane, where it binds by its pleckstrin-homolgy (PH)-domain (31). At the membrane, AKT is phosphorylated at Thr308 by PDK1 (45). Full activation of AKT requires additional phosphorylation at Ser473 by the mTOR complex 2 (mTORC2) (46). AKT can also be phosphorylated at Ser477 and Thr479 by mTORC2 and DNAPK under growth factor stimulation and DNA damage, respectively (47, 48). Activation of PI3K/AKT pathway can occur by many other mechanism, including: mutation or amplification of PI3K; amplification of AKT; activation of upstream oncogenes like *RAS*; or mutation of the tumor- suppressor protein PTEN (Phosphatase and tensin homology). *PTEN*, encoding a negative regulator, mediates the conversion of PIP3 to PIP2 and subject to frequent loss of heterozygosity in approximately 40% of HNSCCs (32). Besides inactivating mutations of *PTEN*, somatic mutations of *PIK3CA*,

encoding a positive regulator of this pathway have also been described in approximately 10-20% of HNSCCs (14). 80-90% of HNSCC lesions present activation of the PI3K-AKT-mTOR axis, whereas the MAPK and JAK/STAT pathways were mutated in less than 10% of the cases (49). Thus, aberrant activation of the pathway tightly associated with tumorogenesis, poor prognosis as well as chemotherapeutic and radio-therapeutic resistance in cancer patients (50, 51). Several constituents of the apoptotic signaling cascade like caspase-8 (*CASP8*) and *BCL2*, encoding a key anti-apoptotic regulator reported to have also an important role in HNSCC (32).

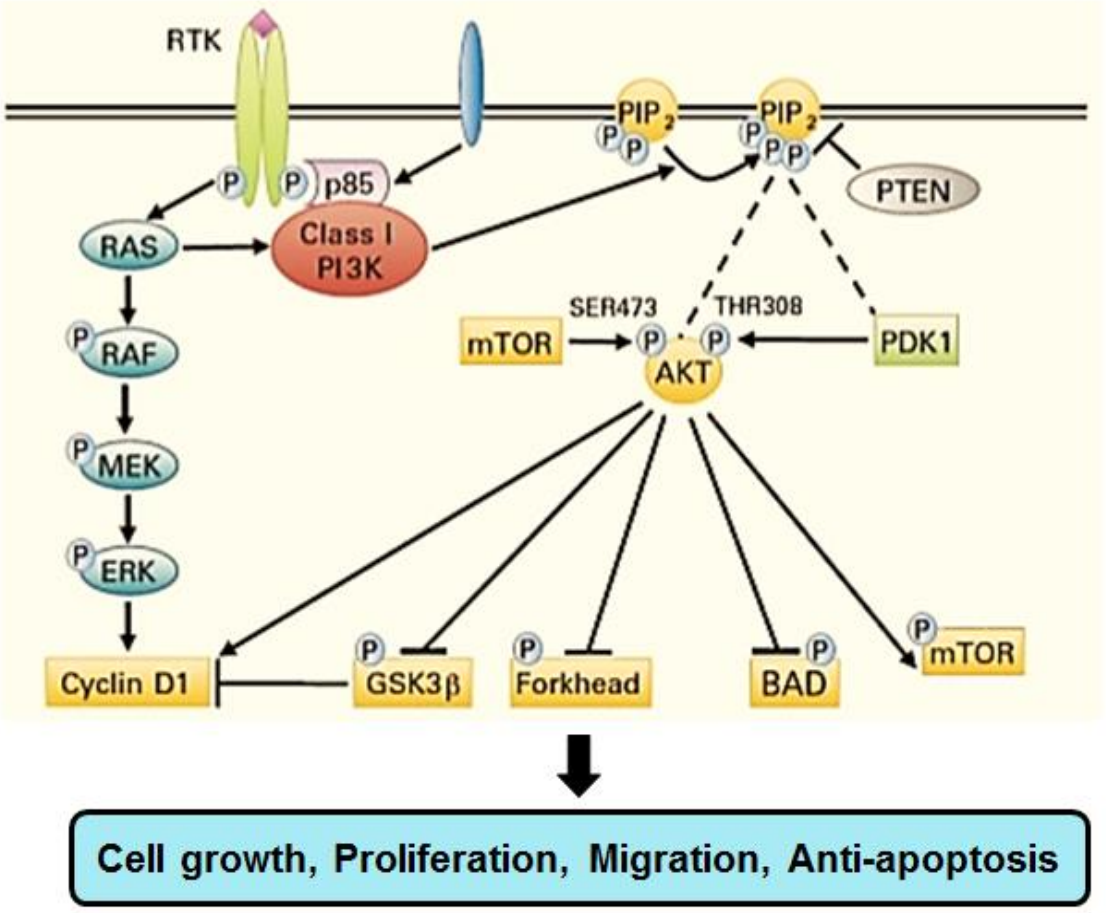

Figure 1.4: PI3K pathway. Overview of PI3K/AKT signaling and downstream effects. Modified from Psyrri et al. 2011 (52).

Additional genes/ Pathways

TGF-β receptor deletion (53), overexpression of cyclooxigenase-2 (COX-2) (54), vascular endothelial growth factor (VEGF) (55), and matrix metalloproteinases (MMPs) (56), are known to promote invasion, metastasis and angiogenesis in HNSCC. Various pro-inflammatory cytokines are also deregulated in HNSCC, including Interleukin (IL) 1-α, IL-6, IL-8, IL-10 and granulocyte-macrophage colony-stimulating factor (GM-CSF). Cross-talk between transcription factors downstream of inflammatory processes like NFκB and STAT3 have been shown to drive the unrestricted growth of HNSCC cells (57).

1.1.2 Treatment and outcome

At present, treatment options for HNSCC are selected in a multidisciplinary setting including stage, grade, patient fitness and location of the tumor. Approximately one third of patients with HNSCC come to clinical attention with early-stage disease and is treated with surgery, radiation, and /or chemotherapy, with cure rates of 70-90% (58). However, the majority of patients presents with advanced cancer and requires aggressive multimodality therapy. In the past two decades, the quality of life of patients has increased as a results of the use of more advanced surgical, radiotherapy delivery techniques and most notably the application of target drugs (such as the EGFR-specific antibody Cetuximab) combined with radiotherapy (14). Disappointingly, survival as a whole has not markedly improved because patients still frequently develop distant metastases, second primary tumors and most importantly locoregional recurrences, with limited options for effective treatment (59, 60). Therefore, finding biomarkers that predict response to chemoradiation protocols, so as to optimize personalized treatment is paramount.

1.1.3 Mouse model for recurrence

Locoregional recurrent disease is correlated with poor prognosis and is considered being the sole site failure in patients who die from HNSCC (61). Already a half century ago the term field cancerization was proposed to explain the high rate of recurrences after treatment in patients with HNSCC (62). Comparison of the genetic profiles of carcinomas and their surrounding field often indicates the presence of areas consisting of epithelial cells with dysplastic changes (63). Importantly, these macroscopically normal appearing fields are often retains in the surgical margin when the tumor is excised and acquired additional genetic changes to give rise to a local recurrence or second primary tumors. Furthermore, experimental and clinical data strongly suggest the presence of these disseminated tumor islands with high invasive potential for the development of an invasive carcinoma (64). Accordingly, the cooperative effect of molecular alterations in cancer cells and compensatory micro-environmental changes plays a critical role in tumor recurrences. Thus, a preclinical animal model is required to better understand the underlying molecular mechanism of the disease and the consecutive design of new treatment strategies.

Behren et al. (65) have already developed an orthotropic floor-of-mouth squamous cell carcinoma model in mice to study the local recurrence after surgery (Fig. 1.5). In this animal model, primary tumors were generated by trans-cervical injection of eGFP-expressing murine SCC-7 cells into the floor-of-mouth of BALB/c-nu mice. Local recurrences were obtained after microsurgical removal of primary tumors. Global gene expression analysis was conducted on whole genome arrays with samples of this mouse model and revealed 49 differentially expressed transcripts between primary and recurrent tumors (66). One candidate gene encoded the transcriptional co-regulator Myb-binding protein 1A (MYBBP1A).

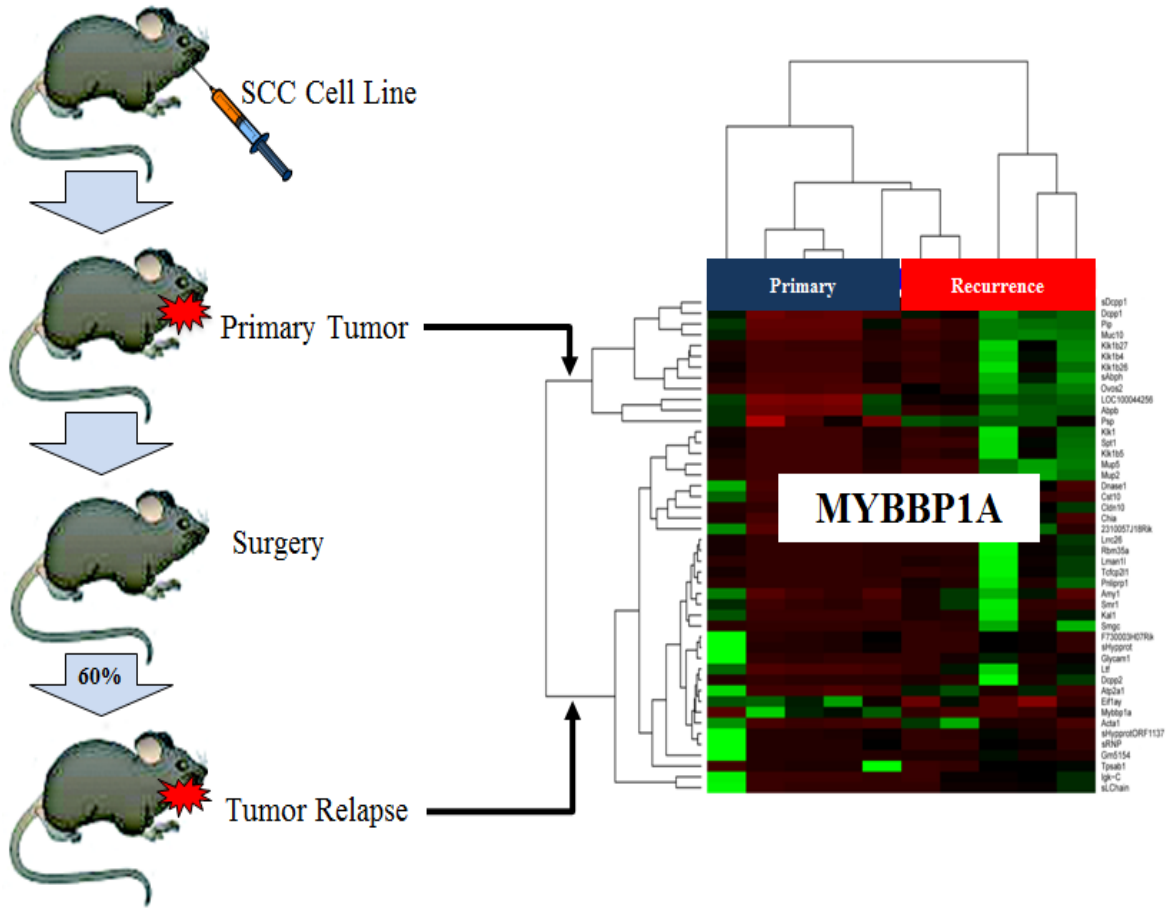

Figure 1.5: Mouse model for recurrence. The mice were injected with SCC-7 cells to develop primary tumors. 60% of the mice developed local recurrence after microsurgical removal of primary tumors. Global gene expression profiling of samples from primary and the corresponding recurrent tumors revealed a list of differentially expressed genes, represented in the heat map. One of the candidate genes encoded MYBBP1A. Modified from Sanhueza et al. 2012 (66).

1.2 Myb-binding protein 1A (MYBBP1A)

1.2.1 Localization and function of MYBBP1A

Human MYBBP1A is a 1328 aa long protein and was originally identified as an interacting partner of the proto-oncogene *c-myb* (67). The 160-kDa MYBBP1A is a nuclear protein, which is expressed ubiquitously and predominantly localized in the nucleolus by binding to nucleolar

RNA (68). MYBBP1A is post-transcriptionally processed under pathological conditions of nucleolar disruption, post-mitotic cell cycle arrest and shortage of intracellular energy, which induce its translocation from the nucleolus to the nucleoplasm (Fig. 1.6) (69-71). The carboxyl terminus of full length MYBBP1A, which contains nuclear and nucleolar localization sequences (NLS) are necessary for its subcellular localization. Unlike the full-length protein, its shorter N-terminal 140 kDa and 67 kDa post-transcriptional cleavage products are mainly localized in the nucleoplasm due to the processing of NLS (72).

Nucleolar large MYBBP1A implies an essential role in ribosome biogenesis (70). In addition, MYBBP1A interacts with several transcription factors, such as the PGC-1α, Prep1, c-Jun and CRY1 and in most cases function as co-repressor (73-76). However, it can also stimulate the transcriptional activity of aryl hydrocarbon receptor (AhR) (77). Recent evidences also established a critical function for MYBBP1A as an important regulator of NFκB and p53, implicated in cell cycle control, inflammation and carcinogenesis. MYBBP1A interacts directly with the RelA/p65 subunit of NFκB and inhibits its transcriptional activity (78). In addition, MYBBP1A located in the nucleoplasm specifically recognizes non-acetylated lysine residues of p53 to promote p53-p300 association, resulting in p53 acetylation and activation. Activated p53 binds to the target gene promoters and regulates gene expression, resulting in apoptosis or cell cycle arrest (69, 79, 80). In this context MYBBP1A act as a sensor in the nucleolus that connects intracellular energy status with the cell cycle machinery. MYBBP1A has also been linked to mitosis and DNA damage responses, since it was identified as a novel substrate for Aurora-B kinase (81) and cell-cycle checkpoint kinase 1 (CHK1) (82). Recent report also unraveled an essential role of MYBBP1A in early embryonic development (75). Thus, MYBBP1A has been shown to play an important role in essential biological functions such as cell division, cell proliferation, development and apoptosis. However detailed mechanisms underlying these activities have not been determined.

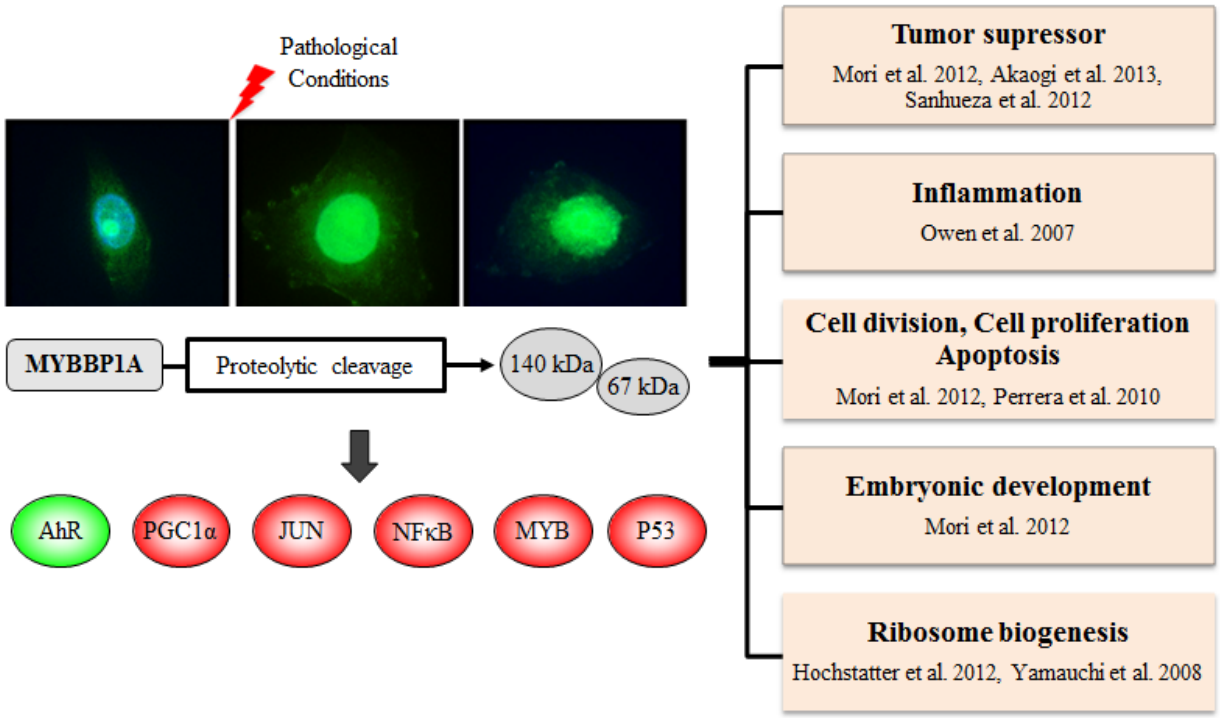

Figure 1.6: Expression and diverse roles of MYBBP1A. MYBBP1A post-transcriptionally processed by stress signal to induce its translocation from nucleolus to the nucleoplasm. MYBBP1A interact with several transcription factors to inhibit (shown in red) or stimulate (shown in green) its activity and plays an important role in essential biological functions.

1.2.2 Regulation of MYBBP1A in cancer

Recent studies unraveled a potential tumor suppressive role for MYBBP1A in RAS-mediated transformation and breast carcinogenesis. Down-regulation of MYBBP1A not only affects the expression of several genes which are involved in cell cycle control, DNA damage and cell death, it could also enhance the tumorigenicity of Ras-transformed NIH3T3 cells (75). Furthermore, *in vitro* and *in vivo* experiments using breast cancer cell lines, which express wild type p53, revealed that loss of MYBBP1A expression is associated with carcinogenesis, colony formation and anoikis resistance (83). In a preclinical mouse model of oral carcinogenesis and in HNSCC patients, MYBBP1A expression was reduced in recurrent as compared to matched primary tumors, suggesting that loss of MYBBP1A expression promotes malignant progression and treatment failure (66). Gain-of-function and loss-of-function studies in head and neck cancer

cell lines further highlighted a dual role for MYBBP1A as a key regulator in the cellular decision between cell proliferation and migration. Silencing of MYBBP1A expression by siRNA technology, results in a significant decrease in tumor cell proliferation and a strong increase in tumor cell migration (66). Thus, tumor cells with reduced MYBBP1A expression may represent a sub-population of slow-cycling but mobile cells implicated in tumor recurrence and metastasis.

1.3 Senescence

Cellular senescence is a state of permanent cell-cycle arrest, despite continued viability and metabolic activity of affected cells. It limits the propagation of damaged and stressed cells in response to a variety of detrimental stimuli. More than a decade ago, cellular senescence was originally identified by Heyflick and Moorhead to describe a state of irreversible growth arrest of human diploid cells after serious of passaging in culture and they speculated that it could be an underlying reason for ageing (84). Later, this particular type of senescence (replicative senescence) was linked to telomere attrition, a process that is implicated in chromosome instability and considered to be one of the first reported molecular triggers of senescence (85). Senescence induction also occurs in response to the activation of oncogenes such as *RAS* (86) and *RAF* (87), referred to as oncogene-induced senescence (OIS). Similarly, loss of tumor suppressors such as PTEN (88), NF1 (89) or von Hippel-Lindau (VHL) (90) can trigger senescence. In addition, oxidative stress and DNA-damage induced by ionizing radiation, UV light, chemotherapeutic drugs and pathological increases ROS have been identified as potential initiators of senescence (91-93). This type of senescence referred to as stress-induced premature senescence (SIPS) (94).

1.3.1 Molecular pathways of cell senescence

Initial growth arrest and multiple-step progression of cellular senescence are induced by a variety of stress conditions, which mainly trigger excessive DNA damage (91, 93) (Fig. 1.7). Three prevalent features, which define cellular senescence includes irreversible growth arrest and

activation of molecular pathways, secretion of SASP, and promiscuous gene expression. The initial step of cellular senescence involves the recognition of DNA damage and the activation of DNA damage responsive (DDR) pathway (95). Amplification of the DDR signal mediated by the activation of DNA damage kinases ATM, ATR, CHK1 and CHK2, which further activate several cell cycle proteins, including p53. Phosphorylated p53 protein activates the expression of p21, while activation of pRb-p16^{INK4A} occurs through p38-MAPK-mediated mitochondrial dysfunction and ROS production. Together, these changes halt cell-cycle progression, allowing cells to repair DNA damage. But if the DNA damage exceeds a certain threshold, cells undergo apoptosis or senescence (93, 95, 96).

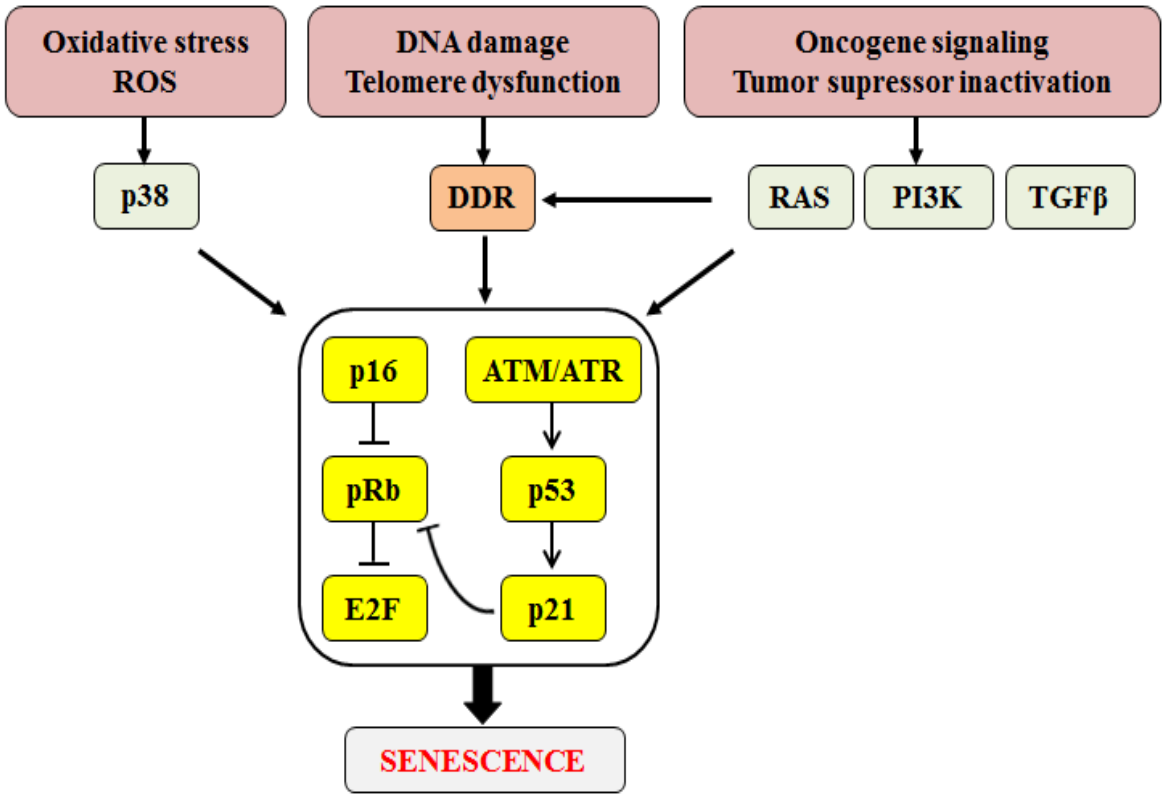

Figure 1.7: Molecular pathways of senescence. Multiple stresses trigger the activation of DDR and signaling cascades that converge on the activation of cell cycle inhibitors and the tumor suppressor RB. ROS activate p16 and p53 through their downstream effector p38. Oncogenic signaling and loss of tumor suppressors activate p16 and p53 with the participation of DDR. PI3K and TGFβ pathways are also involved to induce senescence through p21.

Thus, a sustained DDR is crucial for robust expression of the SASP and chromatin remodeling. Several studies subsequently confirmed the critical roles of p53-p21 and pRb-$p16^{INK4A}$ in the induction and maintenance of cellular senescence (95, 97, 98). The relative contribution of these pathways varies between cell types and activation of only one of these pathways may be sufficient to induce senescence (99, 100). Mutant oncogenes and loss of the PTEN tumor suppressor have the potential to activate molecular pathways of cellular senescence independent of DNA damage (88, 101). PI3K and TGFβ pathways have also been shown to induce senescence through p21 in developmental cues (102, 103).

1.3.2 Hallmarks of senescence

Senescent cells differ from other non-dividing cells such as quiescent or terminally differentiated cells by several markers and morphological changes, which in combination define the senescent state (Fig. 1.8). Senescent cells frequently display a large flattened morphology and induction of senescence-associated β-galactosidase (SA-β-gal) activity (104). The SA-β-gal reflects the increased lysosomal biogenesis that often occurs in senescent cells (91). Expression of tumor suppressors p53, p21 and p16 often serve as biomarkers to represent the arrest of the cell cycle. Another obvious marker for senescent cells is the lack of DNA replication, which is detected by the absence of proliferative markers, such as Ki67, PCNA or BrdU incorporation. Some senescent cells also display condensed heterochromatic regions, known as senescence-associated heterochromatic foci (SAHF). These foci are detected by DAPI staining, and enriched with certain histone modifications (H3 Ly9 methylation) and heterochromatin protein-1 (HP-1). Senescent cells also express proteins that are associated with DNA damage (e.g. phosphorylated H2AX (γH2AX) or p53-binding protein-1 (p53BP1)). Other markers, which represent the characteristics of senescent cells include the activation of immune surveillance-related genes and possible regulators for their pro-survival response (decoy receptor 2 (DCR2), p-Akt, p-Erk) (101, 102, 105, 106). Recent studies also identified the down regulation of Lamin B1 in senescent cells (107). Metabolically active senescent cells communicate with neighboring cells and modify the extracellular matrix through a plethora of secretory factors, including cytokines and chemokines with proinflammatory properties, as well as various growth factors and proteases collectively known as senescence-associated secretory phenotype (SASP) (108). The activation of pathways

that mediate the regulation of these secretory phenotype appears to be NFκB and p38 (109). SA-β-gal along with the presence of several such markers clearly indicates the presence of senescent cells.

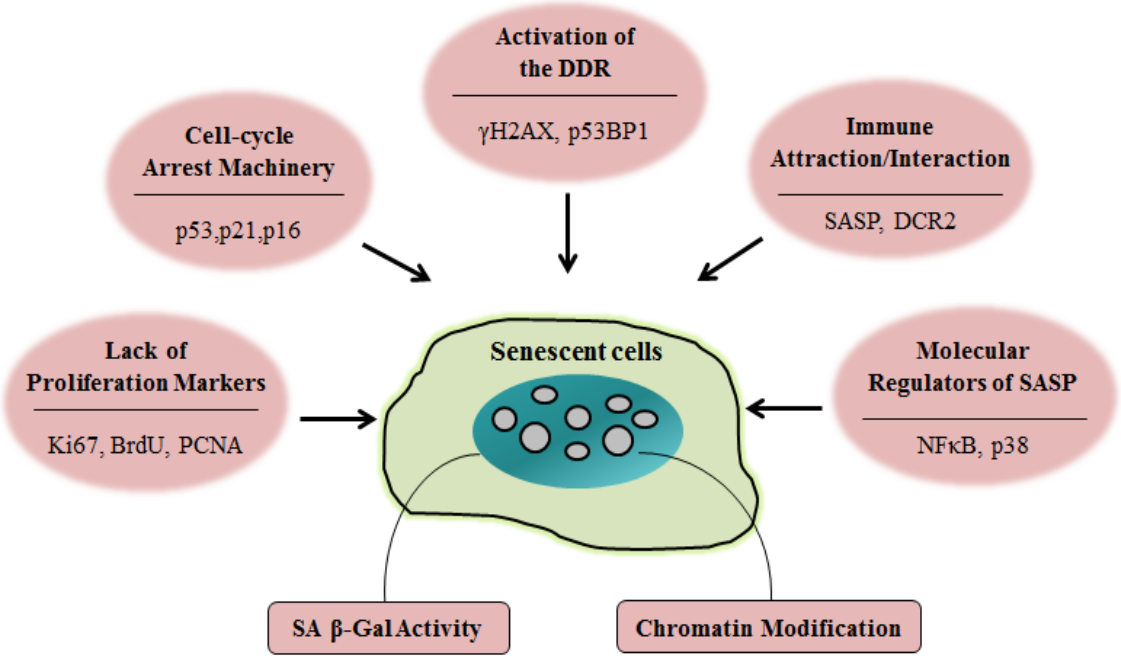

Figure 1.8: Hallmarks of senescence. A combination of markers representing different categories is necessary for the identification of senescent cells.

1.3.3 Physiological impact of cellular senescence

Senescent cells have been associated with diverse functions and impinge on fundamental biological processes that can have both beneficial and detrimental effects (Fig. 1.9).

Tumor suppression: Over the past decade, studies of human tissues and cancer-prone mice clearly demonstrate that cellular senescence prevents tumorogenesis (110-112). In response to various transforming stimuli such as activated oncogenes, cancer cells must acquire a greatly expanded growth potential, a trait that is suppressed by senescence (17). Further, the senescent program activates two powerful tumor suppressor pathways (p53 and pRb-p16^{INK4A}), which limit tumorigenesis in a cell autonomous manner (91, 92). Accordingly, in premalignant human nevi

and colon adenoma the detection of senescent cells is accompanied with markedly diminished malignant progression (113). Likewise, in mouse models with oncogenic Ras expression or Pten deletion, senescent cells were detectable in the premalignant tissues (110, 111, 114). In addition, there is evidence for the induction of senescence in response to chemotherapy or after reactivation of p53 (115, 116). In these cases, senescent response elicits an inflammatory response through SASP factors, which eliminates the senescent cells and confers tumor regression (117, 118).

Limiting tissue damage: Senescence has also been shown to limits tissue damage following short-term injury and facilitates its repair through SASP expression. This comprehensive role was demonstrated in two recent studies. In a mouse model for liver damage, upon acute liver injury, hepatic stellate cells proliferate and secrete extracellular matrix (ECM) components, which produce a fibrotic scar (119). In this model, senescent cells limit fibrosis due to the enhanced secretion of ECM degrading proteins. In another mouse model, cellular senescence limits tissue damage at sites of cutaneous wound healing (120).

Promoting embryonic development: Senescent cells are essential in mammalian embryonic development. Embryonic senescent cells share several features of OIS, including expression of p21 and SASP, which is necessary for the normal placental function. However, these senescent cells do not display a DDR but exhibit activation of TGFβ and PI3K pathways (103, 121). This developmentally programmed senescence is followed by macrophage mediated clearance and tissue remodeling.

1.3.4 Pathological impact of cellular senescence

Recent studies have shown that the accumulation of senescent cells is related to age-associated diseases and tumor promotion. Thus, senescence can be viewed as a double edged sword with both beneficial and deleterious effects (122, 123).

Impairment of tissue integrity and function: *In vivo* as well as *in vitro* studies have provided convincing evidence that accumulation of senescent cells contributes to the overall decline in tissue regenerative potential that occurs with ageing and is associated with reduced stem-cell

proliferation capacity (124, 125). Recently, a seminal study by Baker et al. in transgenic mice, which lack $p16^{INK4A}$ expressing cells provides further evidence that senescent cells are important drivers of multiple age-related pathologies (126). In addition, SASP factors secreted by senescence cells could act to disrupt the local stem-cell niche in a non-autonomous manner (127). SASP factors have the potential to negatively impact their surrounding microenvironment by cleaving membrane-bound receptors, signaling ligands, extracellular matrix and inducing EMT (96, 128). However, recent evidences demonstrate that activation of EMT is linked to the suppression of senescence (129). Taking together, promiscuous gene expression in senescent cells contributes to impairment in the cellular function and critically contributes to common pathologies such as, Alzheimer's disease, diabetes, obesity, atherosclerosis and liver cirrhosis (98).

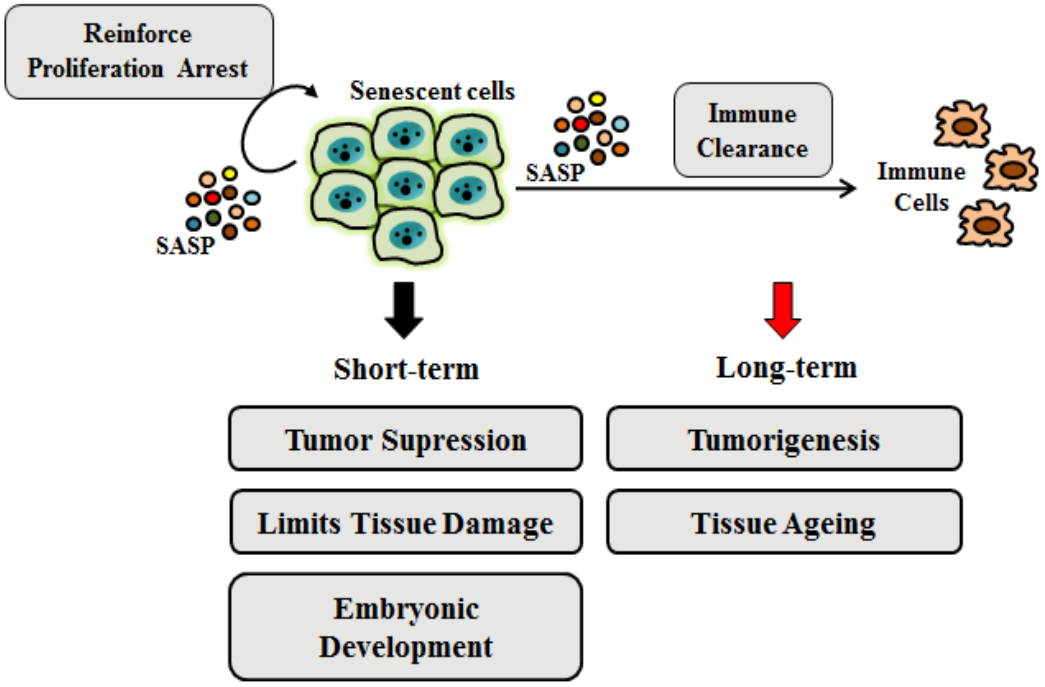

Figure 1.9: Biological impact of cellular senescence. Metabolically active senescent cells secrete soluble and insoluble proteins as well as other factors collectively termed the SASP. These secretory factors reinforce the senescence proliferation arrest and also involved in the initiation of immune surveillance and clearance of senescent cells. Thus, short-term presence of senescent cells noted to be beneficial for tumor suppression, wound healing and embryonic development. However, long-term persistence of senescent cells is increasingly thought to play a role in tumor progression and age-related diseases. Modified from Burton et al. 2014 (101).

Tumor promotion: Senescence-inducing (p53-p21 or pRb-p16^{INK4A} pathways) stimuli are potentially oncogenic, and cancer cells acquire mutations in these pathways that allow them to bypass senescence, a crucial step in the development of cancer (91). Seemingly paradoxical, tumor-promoting role of senescence can be explained by the fact the senescent cells are able to promote malignancy in the cells around them. Accordingly, senescent cells co-cultured with tumor cells secrete SASP factors, which strikingly affect the behavior of neighboring cells to facilitate tumor growth (108). Furthermore, xenotransplantation of senescent cells with fully malignant cancer cells have shown to accelerate the tumor formation in mice (115, 130, 131). Thus, paracrine activities of many SASP proteins create a tissue microenvironment, which induce EMT and the invasiveness of premalignant cells (128).

1.4 Aims of the study

An increasing body of experimental evidence indicates a critical role of MYBBP1A in cellular senescence. First, MYBBP1A has been shown to regulate the activity of two key players in cellular senescence, namely p53 and RelA/p65 a subunit of NFκB, by direct physical interaction (78, 132). Second, Mori and colleagues demonstrated that loss of MYBBP1A affects expression of genes involved in cell cycle control and DNA damage, some of which are also implicated in cellular senescence (75). However, the regulation and function of MYBBP1A in the development and maintenance of cellular senescence as well as the clinical relevance of senescent tumor cells in HNSCC patients have not been addressed so far. Therefore, aim to investigate whether MYBBP1A function is implicated in cellular senescence using cell culture model of genotoxic senescence as a functional screening system.

For this purpose, following questions were addressed:

- What is the functional contribution of MYBBP1A in initiation and maintenance of genotoxic-induced senescence?
- What is the clinical relevance of senescent tumor cells in a retrospective cohort of HNSCC patients?

Materails and Methods

2 Materials

2.1 Equipment's and Consumables

EQUIPMENTS AND CONSUMABLES	COMPANY
1.5 ml, 2 ml Reaction Tubes	Eppendorf, Hamburg
2 ml Cryotubes	Nunc
Adhesion slides Super Frost® Plus	Menzel-Gläser, Braunschweig
AEC+ Substrate-Chromogen, Ready-to-Use	Dako Cytomation, Hamburg
AlphaMetrix tissue punch	AlphaMetrix Biotech, Rodgau
Autoclave	VX95 Systec GmbH, Wettenberg
Binocular Plan APO 1.0x	Leica, Wetzlar
Casy cell counter	Roche, Mannheim
Cell culture sterile hood Hera Safe	Thermo Fisher Scientific, USA
Cell incubator	Binder, Tuttlingen
Cell scraper	TPP, Switzerland
Centrifuge 5417R	Eppendorf, Hamburg
Centrifuge Biofuge 13	Hereaus Instruments, Hanau
Centrifuge Varifuge 3.0R	Hereaus Instruments, Hanau
Cooling centrifuge 5403, 5415R	Eppendorf, Hamburg
Compact Mini-Centrifuge	Hecht, Sondheim
Cover slips (24x36 mm and 24x50 mm)	Knittel, Bielefeld
Cryo freezing container	Thermo Fisher Scientific, USA
Cryo vials (1.8 ml)	Steinbrenner, Wiesenbach
DAKO Pen Dako A/S	Glostrup, Denmark
Developer Classic E.O.S	Agfa, USA
Disposable scalpel	Feather, Osaka (Japan)
Dumont forceps	Fine Science Tools, Heidelberg
Electrophoresis chamber for agarose gels	Buddenberg, Mannheim
Electrophoresis chamber for SDS-PAGE	Bio-Rad Laboratories, Munich
Epi Chem II Darkroom (Gel documentation)	UVP, Upland (CA, USA)
Eppendorf research pipettes	Eppendorf, Hamburg
Filtertips	Biozym Scientific, Oldendorf
Fluoreszenzmikroskope BX50F	Olympus Microscopy, Hamburg
Freezer	Liebherr, Ochsenhausen

Freezer -80°C	Harris/Theromo Scientific
Fridge 4°	Liebherr, Ochsenhausen
Gel documentation system	Peqlab Biotechnology, Erlangen
Glass beakers	Fisherbrand, Schwerte
Hamamatsu NanoZoomer Scanner	Hamamatsu Photonics GmbH
Ice-machine	AF20, Scotsman
Kryostat/Microtome blades C35	Feather, Osaka (Japan)
Kryotome 2800 Frigocut	Leica, Nussloch
Magnetic stirrer/heat plate Ika® RH basic	Sigma-Aldrich, USA
Magnetic stirrer/heat plate Variomag Monotherm	H+P Labortechnik, München
Magnetic stirrer/heat plate MR 3001K	Heidolph, Schwabach
MicroAmp® 96-well optical adhesive film	Applied Biosystems, Foster City, CA
MicroAmp® fast optical 96-well reaction plate	Applied Biosystems, Foster City, CA
Microplate Reader 680	Bio-Rad Laboratories, Munich
Microscope BX-50F	Olympus, Hamburg
Microscope IX51	Olympus, Hamburg
Microwave	Robert Bosch GmbH, Stuttgart
Milli-Q	Millipore, Bedford (MA, USA)
MJ Mini Gradient Thermal Cycler	Bio-Rad Laboratories, München
Nanodrop Spectrophotometer, ND-1000	PeqLab, Erlangen
Needles (25G, 26G, 27G)	Braun, Melsungen; TERUMO, Belgium
Nuclease free reaction caps (safe-lock)	Eppendorf, Hamburg
PCR Cycler MJ Mini™	Bio-Rad Laboratories, Munich
PCR stripes (8x0,2ml)	NerbePlus, Wiensen/Luhe
PCR-Thermocycler (Gene Amp System 2400)	Perkin Elmer, Wellesley (MA, USA)
pH-meter	WTW, Weilheim
Pipettes	Gilson-Abimed, Düsseldorf
Pipettips	Micro-Bio-Tec Brand, Giessen
Pipettor Pipetboy acu	Brand, Wertheim
Platform shaker Polymax 1040	Heidolph, Schwabach
Power supply Power Pac 300/3000	Bio-Rad Laboratories, München
Precision scales	Sartorius, Göttingen
Reaction caps (1,5 ml and 2 ml)	Eppendorf, Hamburg
Rotator Rotoshake Genie®	Scientific industries, USA
Scales	Sartorius, Göttingen
SC30 (BF camera)	Olympus, Hamburg
Steam-cooker	Braun, Kronberg
StepOnePlus™ Real-Time PCR System	Applied Biosystems, Foster City, CA
Thermomixer	Eppendorf, Hamburg
Tissue Tek VIP 5 Jr	Sakura, USA
Trucount 15 ml, 50 ml Tubes	Falcon, Greiner, Nunc

Vortex “Reax 2000”	Heidolph, Kehlheim
Water baths	GFL M&S Laborgeräte
Western blot imaging system FluorChem Q	Biozym, Hessisch Oldendorf
Western blot membrane Optitran BA-S83	Whatman, Dassel
Wet blotting transfer system	Bio-Rad Laboratories, Munich
Whatman 3MM paper	GE Healthcare, Dassel
X-ray films	Fuji, Düsseldorf
XM10 (black/white camera)	Olympus, Hamburg

2.2 Chemicals

COMPONENT	COMPANY
10x PCR buffer	Genaxxon, Biberach
Acetic acid	Merck, Darmstadt
Acetone	Fisher Scientific, UK; Sigma, Taufkirchen
Acrylamid/Bisacrylamid (30:0.8)	Roth, Karlsruhe
Agarose	Roth, Karlsruhe
Ammonium peroxodisulfate (APS)	Sigma, Taufkirchen
β-Mercaptoethanol	Merck, Darmstadt
BCA reagents	Thermo Scientific, USA
Biotyinylated secondary antibody	Vector Laboratories, Burlingame, USA
Boric acid	Roth, Karlsruhe
Bovine serum albumine, fraction V	PAA, Pasching, Austria
Bromphenol Blue	Sigma Aldrich, München
Calcium chloride ($CaCl_2$)	Merck, Darmstadt
Dimethylsulfoxide (DMSO)	Merck, Darmstadt
Disodium hydrogen phosphate ($Na_2HPO_4x2H_2O$)	Merck, Darmstadt
Dithiothreitol (DTT)	AppliChem, Darmstadt
ECL reagent solutions	AppliChem, Darmstadt
EDTA	AppliChem, Darmstadt
Eosin	Roth, Karlsruhe
Ethanol p.a.	Merck, Darmstadt
Ethanol, denaturated 99,7%	Roth, Karlsruhe
Ethanolamine	Merck, Darmstadt
Ethidiumbromide	AppliChem, Darmstadt
Ethylenediamine-tetraacetate (EDTA)	Roth, Karlsruhe
Eukitt	Kindler, Freiburg
Formaldehyde 37%	Sigma Aldrich, München
GelRed	Biotium, Hayward, CA
Glycerol	AppliChem, Darmstadt
Haematoxylin	AppliChem, Darmstadt

Hematoxylin according to Gill II	Roth, Karlsruhe
Hoechst 33342	Biomol, Hamburg
Hydrochloric Acid	Merck, Darmstadt
Hydrogen peroxide	Merck, Darmstadt
Isopentan	Roth, Karlsruhe
Isopropanol	Roth, Karlsruhe
Methanol	Merck, Darmstadt
$MgCl_2$	Genaxxon, Biberach
Microplate Reader Model 680	Bio-Rad Laboratories, München
Milk powder	Roth, Karlsruhe
$MnCl_2$	Roth, Karlsruhe
N, N, N‘, N‘, Tetramethyl ethylenediamine (TEMED)	Roth, Karlsruhe
$NaH_2PO_4xH_2O$	Merck, Darmstadt
Natrium chloride	Roth, Karlsruhe
Natrium-deoxycholat	AppliChem, Darmstadt
NP-40	Sigma Aldrich, München
Oligo-dT primers	Fermentas, St. Leon-Rot
Paraffin	Vogel, Giessen
Potassium Chloride	Roth, Karlsruhe
RNase-free water	Ambion, Life Technologies, Frankfurt
Sodium Chloride	Roth, Karlsruhe
Sodium Citrate	Roth, Karlsruhe
Sodium hydroxide	Merck, Darmstadt
Sodiumdodecylsulfate (SDS)	Gerbu Biotechnik, Gaiberg; Roth, KA
Tris HCl	Roth, Karlsruhe
Tris-base	Roth, Karlsruhe
Triton X-100	AppliChem, Darmstadt
Tween 20	AppliChem, Darmstadt
Xylol	AppliChem, Darmstadt

2.3 Molecular biology reagents

COMPONENT	COMPANY
Agilent RNA 6000 Nano Kit	Agilent Technologies, Böblingen
AKT Inhibitor V, Triciribine	Calbiochem (EMD Millipore)
BCA protein assay reagent	Thermo Scientific, USA
BrdU (5-bromo-2-deoxyuridine)	BD Pharmingen, Germany
Cell lysis buffer	NEB, UK
DAB kit	Vector Laboratories, Burlingame, USA
DNaseI Digest Kit	Qiagen, Hilden
dNTPs	GeneOn, Ludwigshafen
GelRed® DNA stain	Genaxxon, Biberach
GeneRuler 100bp DNA ladder	Fermentas, St. Leon-Rot
GeneRuler DNA ladder mix	Fermentas St. Leon-Rot
ImmPRESS Anti-Rabbit	Vector Laboratories, Burlingame, USA
Lipofectamine™ 2000	Invitrogen, Karlsruhe
miRNeasy Mini Kit	Qiagen, Hilden
MG132	Sigma Aldrich, USA
MultiScribe™ reverse transcriptase	Applied Biosystems, Foster City, CA
Oligo-dT primers	Fermentas, St. Leon-Rot
PCR buffer S	Genaxxon, Biberach
PeqGOLD protein marker IV, pre-stained	PeqLab, Erlangen
Phosphatase inhibitor 1 + 2	Sigma, Taufkirchen
PI3 Kinase Inhibitor (LY294002)	Cell signaling, Germany
Power SYBR® Green PCR master mix	Biosystems, Foster City, CA
Proteinase K	Applied Gerbu, Heidelberg
dNTPs	Fermentas, St Leon Roth
RNeasy Mini Kit	Qiagen, Hilden
RNase-free DNase Set	Qiagen, Hilden
Riboblock RNase inhibitor	Fermentas, St. Leon-Rot
Revertaid M-MuLV Buffer	Fermentas, St. Leon-Rot
Revertaid M-MuLV Reverse Transcriptase	Fermentas, St. Leon-Rot
Senescence β-Galactosidase Staining Kit	Cell signaling Technology, Germany
Taq polymerase	Genaxxon, Biberach
Vectastain Elite-ABC-Peroxidase	Vector Laboratories, Burlingame, USA

All kits and reagents were used according to the manufacturer's protocol unless otherwise stated.

2.4 Buffers and solutions

Blocking reagent for histology	0.1 % BSA, 5 % host serum in PBS
10x Citrat Buffer	1.8 mM citric acid, 8.2 mM sodium citrate
6x DNA loading buffer	0.25 % (v/v) Bromphenol blue, 0.25 % (v/v) Xylene Cyanol, 30 % (v/v) glycerol
4 % formaldehyde	4 % (v/v) formaldehyde in PBS
4x Laemmli buffer	250 mM Tris-HCl pH 6.8, 8 % (v/v) SDS, 40 % (v/v) glycerol, 500 mM DTT, bromphenolblue
NP-40 lysis buffer	150 mM NaCl, 50 mM Tris-HCl, pH 7.4, 1 % NP-40, 10 mM EDTA, 10 % glycerol, freshly added 1:100 v/v protease inhibitors
Mowiol	6 g glycerol, 2.4g Mowiol 4-88, 6 ml H_2O
Separation gel	10-15 % acrylamide/bisacrylamide, 375 mM Tris-HCl pH 8.8, 0.1 % SDS, 0.1 % APS, 0.1 % TEMED
Stacking gel	4 % acrylamide/bisacrylamide, 125 mM Tris-HCl pH 6.8, 0.1 % SDS, 0.1 % APS, 0.1 % TEMED
Stripping solution	15 g glycine, 1 % SDS, 10 ml Tween-20, adjusted to pH 2.2 with 37 % HCl, add 1l H_2O
10 x PBS	1.37 M NaCl, 27 mM KCl, 82 mM Na_2HPO_4 x 2 H_2O, 17 mM NaH_2PO_4 x H_2O
10x SDS running buffer	250 mM Tris-base, 1.92 M glycine, 1 % (v/v) SDS
10x TBE	1 M Tris, 1 M boric acid, 20 mM EDTA
10x TBS	61 g Tris base, 160 g NaCl, ad 1 l H_2O, adjusted to pH 7.6
PCR reaction mix	1.1x PCR buffer S, 1.7 mM $MgCl_2$, 220 µM dNTPs
Western blot transfer buffer	25 mM glycine, 0.15 % (v/v) ethanolamine, 20 % (v/v) methanol

2.5 Antibodies

Primary Antibodies

ANTIGEN	HOST	DILUTION	SORUCE
β-Actin	Mouse	1:10000	Sigma-Aldrich/A5441
AKT	Rabbit	1:1000	Cell Signaling/CS-9272
phospho- AKT (Ser473)	Rabbit	1:1000	Cell Signaling/CS-4060
phospho- AKT (Thr308)	Rabbit	1:1000	Cell Signaling/CS-4056
Caspase-3	Rabbit	1:1000	Cell Signaling/CS-9665
γ-H2AX	Rabbit	1:400 (IF)	Cell Signaling/CS-9718
MYBBP1A	Rabbit	1:1000	Abcam/Ab-54160
MYBBP1A	Rabbit	1:100 (IF)	Abcam/Ab-99361
p21(CDKN1A)	Mouse	1:1000(WB) 1:50(IF)	BD Pharmingen/556431

Secondary Antibodies

ANTIGEN	HOST	DILUTION	LABEL	SORUCE
Mouse	goat	1:5000	HRP	Cell Signaling/CS-7076
Rabbit	goat	1:5000	HRP	Cell Signaling/CS-7074
Mouse	donkey	1:200	Cy3	Dianova
Rabbit	donkey	1:200	Alex488	Dianova
Rabbit	goat	1:500	biotin	Vector, (BA-100)

2.6 Oligonucleotides

PRIMER		SEQUENCE	T_A
β-Actin	for	CCAACCGCGAGAAGATGA	60˚C
	rev	CCAGAGGCGTAGAGGGATAG	
MYBBP1A	for	CGCACCACCTGTGCCGTGCCCGGCG	60˚C
	rev	CTTGGTCAGGAAGGAGCTCAGTGCT	
IL-6	for	GAAAGCAGCAAAGAGGCACT	60˚C
	rev	TTTCACCAGGCAAGTCTCCT	
IL-8	for	TTGGCAGCCTTCCTGATTTC	60˚C
	rev	TCTTTAGCACTCCTTGGCAAAAC	
IL-1β	for	CCACAGACCTTCCAGGAGAATG	60˚C
	rev	GTGCAGTTCAGTGATCGTACAGG	
TGF-β1	for	TGGTGGAAACCCACAACGAA	60˚C
	rev	GAGCAACACGGGTTCAGGTA	

2.7 siRNA and Plasmids

NAME	COMPANY
Control siRNA	Santa Cruz/sc-37007
MYBBP1A siRNA(h)	Santa Cruz/sc-396003
pcDNA3.1	Invitrogen, Germany

2.8 Cell culture

Cell culture media and supplements

Dulbecco‘s Modified Eagles Medium (DMEM)	PAA Laboratories, Austria
Fetal calf serum (FCS)	Sigma Taufkirchen
L-Glutamine	PAA Laboratories, Austria
Penicillin/Strptomycin	PAA Laboratories, Austria
Trypan blue	Fluka, Neu-Ulm
Trypsin	PAA Laboratories, Austria
Opti-MEM® I Reduced Serum Medium	Gibco, Life Technologies

Cell lines

NAME	DESCRIPTION	SOURCE
FaDu	Human hypopharyngeal carcinoma	ATCC
Cal-27	Human oral adenosquamous carcinoma	ATCC
HeLa	Human cervix adenocarcinoma	ATCC
SCC-25	Human oral squamous carcinoma of the tongue	ATCC

2.9 Human tissue blocks

Tumor specimens for tissue micro array analysis were obtained from OPSCC patients treated at the University Hospital Heidelberg between 1990 and 2008. Paraffin-embedded tissue specimens from OPSCC patients were provided by the tissue bank of the National Center for Tumor Disease (Institute of Pathology, University Hospital Heidelberg) after approval by the local institutional review board (ethic vote 206/2005). Clinical and follow-up data for all patients were provided by the Department of Otolaryngology, Head and Neck surgery, at the University Hospital Heidelberg. Only tissue samples of primary tumors were included in the present study.

2.10 Software

PROGRAME	DISTRIBUTOR
Adobe Acrobat 9.0; Photoshop CS5; Illustrator CS5	Adobe, San Jose, USA
CellSens Dimension 1.5	Olympus, Hamburg
EasyControl 2.04 for Epi Chem II darkroom	UVP, Upland (CA, USA)
Endnote v. X7	Adept Scientific GmbH, Frankfurt
Mendeley Desktop 1.7.1	Mendeley Ltd., London, UK
Hamamatsu NanoZoomer (NDP-Viewer)	Hamamatsu Photonics, Herrsching
Image J	W. Rasband, National Institutes of Health, Maryland, USA
IBM SPSS Statistics 20	IBM Corporation, Somers NY, USA
Microsoft Office 2007	Microsoft Corporation
Microsoft Windows XP	Microsoft Corporation
Nikon NIS-Elements 3.20.02	Nikon
Sigma Plot v. 12.5	Systat Software Inc. Washington, USA
StepOne Software v. 2.2.2	Life Technologies, Darmstadt

3 Methods

3.1 Protein biochemistry methods

3.1.1 Preparation of protein extracts

Protein extraction was performed on cultured cells. Pelleted cultured cells were lysed by ice-cold RIPA buffer (50 mM Tris-HCl pH 8.0, 150 mM NaCl, 0.1% SDS, 0.5% (v/v) deoxylacid Na^+-salt, 1% (v/v) NP-40) with freshly added protease inhibitor and phosphatase inhibitor cocktail (1:100) (Sigma-Aldrich, Germany). Then samples were incubated for 10 min on ice and centrifuged for 10 min at 13000 rpm at 4 ˚C (Centrifuge 5403, Eppendorf). The supernatant was collected and stored at -80 ˚C. One aliquot was taken for determination of protein concentration in the lysate.

3.1.2 Determination of protein concentration

Protein concentration in RIPA lysates was determined using the BCA protein assay kit (Thermo Scientific) according to the user's manual.

3.1.3 SDS polyacrylamide gel electrophoresis (SDS-PAGE)

Sodiumdodecylsulfate-polyacrylamide gel electrophoresis (SDS-PAGE) was performed to separate proteins according to their molecular weight. The SDS-PAGE is composed of a stacking (4% Acrylamide/Bisacrylamide, 125 mM Tris-HCl pH 6.8, 0.1% SDS, 0.1% APS, 0.1% TEMED) and a separation gel (10-15% Acrylamide/Bisacrylamide, 375 mM Tris-HCl pH 8.8,

0.1% SDS, 0.1% APS, 0.1% TEMED). The percentage of the separation gel was adapted according to the size of the target proteins. Equal amounts of protein samples (20 µg) were mixed with 4xLaemmli buffer containing 4% β-Mercaptoethanol and incubated at 95 ˚C for 5 min until loaded onto the gel. The gel run was performed in 1x SDS running buffer at 25-35 mA. For protein size estimation, a pre-stained protein marker (PeqGOLD protein marker IV, PeqLab) was run on parallel to the samples.

3.1.4 Transfer of proteins to nitrocellulose membranes (Western blot)

Denatured proteins separated by the SDS-PAGE were transferred onto nitrocellulose membranes (Optitran BA-S83) using a wet-blotting system from Bio-Rad. The pre-assembled blot comprised of separation gel and nitrocellulose membrane embedded in three sheets of Whatman 3MM paper on either side was pre-incubated in Western blot transfer buffer (25 mM glycine, 0.15% ethanolamine, 25% (v/v) methanol). The transfer was carried out for 1 - 1.5 h in Western blot transfer buffer at a constant voltage of 100 V. Following transfer, the membrane was incubated in 5 % BSA or milk in PBS-T (PBS-0.5% Tween) for 30 min at RT while shaking in order to block unspecific binding of the antibodies. The membrane was incubated with the diluted primary antibody (in blocking buffer) o/n at 4°C. The membrane was washed at least three times with PBS-T for 10 min while shaking. Finally, the membrane was incubated with the diluted secondary antibody coupled to horse radish peroxidase (HRP) (in blocking buffer) for 1 h at RT. Subsequently, the membrane was washed as before and incubated for 1 min with the enhanced chemiluminescence solution (Thermo Scientific). The signals were detected by exposing the membrane to a X-ray film in the dark followed by incubation in the Classic E.O.S developer (Agfa). All antibodies used for Western blot analysis are listed in section 2.5.

3.2 Molecular biology methods

3.2.1 Isolation of total RNA

Total RNA was isolated from cultured cells using RNeasy Mini Kit (Qiagen) according to the manufacturer's instructions.

3.2.2 Measurement of RNA quantity and quality

Quality and quantity of isolated RNA were assessed using a Nanodrop Spectrophotometer (ND-1000 UV-VIS, PeqLab) according to the manufacturer's instructions. Purity of extracted RNA and contamination by proteins and aromatic compound was determined using the OD 260/280 and the OD 260/230 ratio. The ratio of the sample of absorbance with OD 260/280 of 1.8-2.0 and OD 260/230 absorbance ratio greater than 2.0 were accepted and used for further analysis.

3.2.3 cDNA synthesis

5 µg total RNA was reverse transcribed into cDNA using reverse transcriptase. Therefore, RNA was diluted in 35 µl nuclease-free H_2O and 0.5 µl of Oligo (dT) 18 primer (100 µM, Fermentas). RNA was denatured at 70 ˚C for 5 min followed by 5 min at 4 ˚C. Subsequently, a reaction mix containing 10 µl 5x RevertAid buffer, 2 µl 25 mM dNTP mix, 2 µl RiboLock^{TM} RNase Inhibitor (40 U/µl, Fermentas) and 0.5 µl RevertAidTM M-MuLV reverse transcriptase (200 U/µl, Fermentas) were added to reach a final volume of 50 µl. The reaction was incubated for 1 h at 42 ˚C. Obtained cDNA was stored at -20 ˚C.

3.2.4 Amplification of DNA by polymerase chain reaction (PCR)

Polymerase chain reaction (PCR) amplification was routinely performed for semi-quantitative analyses of gene expression or the detection of specific genomic loci. For this, 15 ng cDNA or 3 µl of genomic DNA (10-500 ng) was mixed with 45 µl of PCR reaction mix (10 x PCR buffer S, 1.7 mM $MgCl_2$ (Genaxxon), 220 µM dNTPs (Fermentas), 0.2 µl of each primer (50 pmol/µl), 0.3 µl Taq-plymerase S (Genaxxon) and ddH_2O was added to a final volume of 50 µl). The PCR reaction was performed according to the following protocol:

Initial Denaturation	94 ˚C	5 min	
Denaturation	94 ˚C	30 sec	
Primer hybridization	T_A ˚C	30 sec	25-40 cycles
Elongation	72 ˚C	45 sec	
Final elongation	72 ˚C	5 min	
Hold	4 ˚C	∞	

Afterwards, the PCR reaction was analyzed by agarose gel electrophoresis (3.2.6). The specific annealing temperatures (T_A) for the respective primers are listed in section 2.6.

3.2.5 Quantitative real-time PCR (RQ-PCR)

For relative quantification of target gene expression analysis, SYBR green-based real-time PCR was performed on the StepOnePlus™ real-time PCR system (Applied Biosystems). Every PCR reaction was carried out in triplicates on a 96 well plate with 5 ng of cDNA in a final volume of 20 µl containing 10 µl of Power SYBR® Green PCR Master Mix (Applied Biosystem) and 0.1 µl forward and reverse primers (50 pmol/µl each). Since AmpliTaq polymerase (present in Power SYBR® Green PCR Master Mix) has an efficient elongation capacity already at 60 ˚C, a two-step cycling stage was generally sufficient (Stage 2). An additional elongation phase was only included when the amplified fragment was longer than 300 bp. Primer sequences and corresponding annealing temperatures are provided in Table 1.6. The following PCR program was used:

Stage 1	Cycle 1	94 ˚C	5 min
Stage 2 (40x)	Cycle 2	94 ˚C	30 sec
		T_A ˚C	30 sec
		72 ˚C	30 sec
Stage 3	Cycle 3	95 ˚C	15 sec
	Cycle 4	60 ˚C	1 min
	Cycle 5	+0.5 ˚C	15 sec (up to 95 ˚C)

Data obtained from real-time PCR were analyzed using the StepOne™ software v2.2 (Applied Biosystems). Target gene (GOI, gene of interest) cycle of threshold (CT) values was normalized to the corresponding CT values of housekeeping genes (HKG), i.e. β-Actin using the ΔCT method. Primer specificity was determined by melt curve analysis and amplicon size verification by agarose gel electrophoresis (2.2.6). Primer efficiency was measured by analyzing consecutive dilution series of reference cDNAs ranging from 25 ng to 0.1 ng and was included into the calculation of fold induction.

$$\frac{Eff_{GOI}^{\,Ref(GOI)-Sample(GOI)}}{Eff_{HKG}^{\,Ref(HKG)-Sample(HKG)}} = \text{Fold Induction}$$

3.2.6 Agarose gel electrophoresis

DNA fragments generated by conventional or semi-quantitative PCR reactions were separated according to their molecular size by agarose gel electrophoresis. For fragments between 100 bps and 400 bps a 2 % agarose gel in 1x TBE buffer by boiling in a microwave was prepared and intercalating DNA dye GelRed® DNA stain (Genaxxon) was added in a 1:20,000 ratio. Prior to loading, DNA samples were mixed with 6x loading buffer and the liquid gel was poured into the gel chamber. GeneRuler™ DNA Ladder Mix (0.1 - 10.0 kbp, Fermentas) or 100 bp DNA Ladder (100 - 1000 bp, Fermentas) were used as a reference to define the size of the specific fragments and separation was performed in 1xTBE buffer at constant voltage (120 V). Bands were visualized under UV light and photographed.

3.3 Cell culture

3.3.1 Cultivation of cell lines and treatment

Human HNSCC cell lines and HeLa were purchased from ATCC. Cells were maintained in Dulbecco's modified Eagle's medium (DMEM) supplemented with 10% fetal bovine serum (Invitrogen, Germany), 2 mM L-Glutamine (Invitrogen, Germany) and Antibiotics (50 µg/ml Pencillin-Streptomycin, Invitrogen, Germany) in a humidified incubator of 6% CO_2 at 37º C. To avoid mycoplasm contamination, mycoplasm tests were performed routinely by PCR analysis using the PromoKine Mycoplasma PCR detection Kit. For passaging, cells were trypsinized with 1 ml Trypsin/EDTA (0.2% Trypsin in PBS/EDTA) after reaching a confluency of 80-90%. Trypsin reaction was stopped with medium and trypsinized cells transferred to a Falcon tube. Following centrifugation for 3 min at 1000 rpm (Megafuge 1.0, Heraeus), the cell pellet was resuspended in the appropriate amount of media and counted in a cell counter. The cell number needed was plated on new cell culture dishes. To freeze cells, $1x10^6$ cells were frozen in 1.5 ml freezing medium (10% DMSO in FCS). For long-term storage, cells were stored in liquid nitrogen.

Unless otherwise indicated, cells were challenged in the absence or presence of 10 µM of etoposide (Sigma-Aldrich, Germany) for the indicated time period to induce DNA damage.

3.3.2 Transient transfection of cell lines

In all cases cells were trypsinized 24 hours before transfection and seeded on a 6-well cell culture plate ($3x10^5$/ well). The transfection of FaDu and HeLa cell lines was performed using Lipofectamine™ 2000 (Invitrogen, Germany) according to manufacturer´s instructions. Prior to transfection, cell media was changed with Opti-MEM® I reduced Serum Media (Invitrogen), which was again replaced with normal growth media 4-6 hours after transfection. Analyses of MYBBP1A silencing and ectopic overexpression were done 48 hours after transfection.

3.3.3 BrdU incorporation assay

Cell proliferation was analyzed using the BrdU (5-bromo-2-deoxyuridine) Flow Kit (BD pharmingen, Germany) according the manufacturer's instructions. BrdU quantification was performed using ImageJ software. Total cells were quantified by counterstaining with Hoechst 33342 (Sigma-Aldrich, Germany).

3.3.4 Senescence-associated β-galactosidase (SA-β-gal staining)

Cells were fixed in fixation buffer and SA-β-galactosidase assay was performed using a Senescence β-Galactosidase Staining Kit (Cell Signaling Technology, Germany) in accordance with the manufacturer´s instructions. Senescence induction was quantified by ImageJ software upon staining of the nuclei with Hoechst 33342 (Sigma-Aldrich, Germany) and is given as relative amount of positive cells.

3.3.5 Clonogenic survival assay

Radioresistance was measured by a colony formation assay following exposure to irradiation. FaDu cells were transfected with scramble or MYBBP1A specific siRNAs and 48 hours post-transfection, 1000 cells were seeded in 6 well plates. Cells were exposed to a radiation dose of 5 Gy. Irradiated cultures and non-treated controls were incubated for 10 days, fixed with methanol and stained with 1% crystal violet. Stained clones were rinsed twice with water, dried and counted. The survival fraction was calculated according to the number of colonies divided by the number of cells seeded.

3.3.6 Immunofluorescence (IF)

Cells were grown on sterile coverslips and fixed with phosphate-buffered saline (PBS) - 4% paraformaldehyde for 15 min at room temperature. After being washed with PBS, the cells were permeabilized with 0.5%Triton X-100 buffer in PBS and blocked with PBS-1% bovine serum albumin-0.2% Tween 20 for 30 min at room temperature. Coverslips were incubated with

primary antibody in blocking buffer (PBS-1% bovine serum albumin-0.2% Tween 20) for 2h. The coverslips were rinsed with PBS and then incubated with fluorochrome-conjugated secondary antibody. Cells were washed again with PBS, counterstained with Hoechst 33342 (Sigma-Aldrich, Germany) and visualized by fluorescence microscopy. All antibodies used for the analysis are listed in section 2.5.

3.4 Histology methods

3.4.1 Preparation of paraffin-tissue sections

Sections from paraffin-embedded tissue were prepared by cutting the paraffin blocks in 6 µm slices with the microtome RM2155. The sections were then dried at 42 ˚C o/n and stored at room temperature.

3.4.2 Immunohistochemistry (IHC)

Immunohistochemistry analysis enables the detection of specific proteins on tissue sections with antibodies. First, the 5 µm tissue paraffin sections were deparaffinized in xylene for ten minutes and then rehydrated in a descending ethanol series (100%, 95%, 90%, 80%, 70%, 50%, 30% (v/v) ethanol in ddH_2O, 2 min each). Endogenous peroxidase was blocked with 3 % H_2O_2 for 10 min and heat-mediated antigen retrieval was performed in citrate buffer (pH 6) for 30 min in a steam-cooker, then cooled down for additional 10 min, and rinsed in tap water. Sections were washed with PBS and blocked in horse serum (ImmPress, VectorLaboratories, Burlingame, CA, USA) for 30 min to block unspecific binding sites. Subsequently, primary antibody was incubated in blocking buffer o/n at 4 °C in a wet chamber. Afterwards, sections were washed trice in PBS under agitation for 5 minutes and incubated with the corresponding, peroxidase coupled secondary antibody (ImmPress) for 30 min at RT. Subsequently, sections were washed once with PBS and incubated (1-5 min) with the DAB peroxidase substrate (brown staining

signal) (Vector Laboratries Inc., CA 94010, USA). Samples were counterstained with hematoxylin and washed with tap water for 10 min. The tissue sections were dehydrated in increasing percentage of ethanol for 10 seconds each (70%, 90%, 100%) and 2 min each in xylol. The sections were the mounted with Evanolor Eukitt (Kindler GmbH, Freiburg, Germany). All antibodies which were used IHC are listed in section 2.5.

3.5 Human patient samples

3.5.1 Tissue microarray (TMA) production

Tissue microarrays containing multiple spots from primary OPSCC patients as well as healthy mucosa were generated as previously described (133). Tissue microarrays included a collection of 188 tumor biopsies of patients as well as healthy mucosa. Briefly, these biopsies were stained by hematoxyline and eosin (H&E) and stained sections were cut from each donor block to define representative tumor regions. Small tissue cylinders with a diameter of 0.6 mm were taken from selected areas of each donor block using a tissue chip microarrayer (Beecher Instruments) and transferred to a recipient paraffin block. The recipient block was subsequently incubated at 37 ˚C for 1 h. This block was cut in 5 μm paraffin sections with a cryostat at 20 ºC.

3.5.2 TMA scoring

TMAs were scanned using the Nanozoomer HT Scan system (Hamamatsu Photonics, Japan) following immunohistochemistry as described in 2.4.2. Three experienced observers analyzed scanned slides by using the NDP Viewer software (version 1.1.27). The semi-quantitative analysis was performed according to the number of stained tumor cells (score A: 1 = no positive cells, 2 = less than 33% positive cells, 3 = between 34% and 66%, 4 = more than 66% positive cells) and according to the staining intensity (score B: 1 = no staining, 2 = weak staining, 3 = moderate staining, 4 = high staining). Only primary tumors were included in the analysis and

scores from spots of the same patients were combined using the median value. Subsequently, the number of stained tumor cells (score A) and staining intensity (score B) were multiplied resulting in the final expression score (range 1–16). To determine the final activity score, a ratio (pAKT(Ser473) or pAKT(Thr308)/total AKT) was calculated. Patients were further divided in to two subgroups with $MYBBP1A^{low}pAKT^{high}$ (n=7) and all other combinations (n=54).

3.5.3 Statistical analysis

Statistical analysis was done using SPSS (Version 19) and SAS (Version 9.2) statistics software. Differences between the groups were assessed using Chi square test or Fisher's exact test. Patient and tumor characteristics were obtained from clinical data. Clinical data were extracted from the electronic patient files of the university hospital Heidelberg and transferred to the laboratory database. The included data mainly refer to general information (yes/no) without quantitative data. The HPV status and viral transcript were determined as described previously (134). Pearson and Spearman's correlation between score A and B were tested.

Overall survival (OS) was calculated from registration date until date of OPSCC-related death, censoring patients alive at last follow-up and non–OPSCC-related deaths. Progression-free survival (PFS) was calculated from the date of primary tumor diagnosis to the date of the first local recurrence, lymph node or distant metastasis, second primary carcinoma or date of OPSCC-related death within the follow-up period (events), or to the date of OPSCC-unrelated death or without progression (censored). Estimation of OS and PFS distributions were performed by the Kaplan-Meier method and differences between the groups were determined by log-rank tests (135). Multivariate Cox proportional hazard models were used to analyze the association between $MYBBP1A^{low}AKT^{high}$ expression scores and overall survival of OPSCC, together with covariates age (continuous variable), gender (female vs. male), clinical stage (IV vs. I-III), alcohol and tobacco consumption (never vs. former/current) and human papillomavirus (HPV) status (HPV active vs. inactive). No imputation methods for replacing missing values of the covariates were used. For all covariates, the validity of the proportional hazards assumption was tested with Schoenfeld residuals.

The results are expressed as means ± standard deviations (SD) of three independent experiments, each performed in triplicate. Statistical significance was determined using the Student´s *t* test; $p<0.05$ was considered significant. Statistical evaluation of obtained data was performed with SigmaPlot 11.0 (Systat Software Inc.).

Results

4 Results

An increasing body of experimental evidence indicates a critical role of MYBBP1A in cellular senescence. In order to investigate the regulation and function of MYBBP1A in the development and maintenance of cellular senescence the following topics were addressed: (a) expression of MYBBP1A in an established cell culture model of genotoxic senescence, (b) functional contribution of MYBBP1A in the initiation and maintenance of senescence by loss-of-function and gain-of function approaches, and (c) combinatorial analysis in a retrospective cohort of oropharyngeal SCC (OPSCC) patients by immunohistochemical staining to elucidate the clinical relevance of senescent tumor cells.

4.1 Regulation and function of MYBBP1A during DNA damage-induced senescence *in vitro*

To elucidate the role of MYBBP1A under conditions of DNA damage-induced senescence in tumor cells, an *in vitro* model for cellular senescence was established using the topoisomerase inhibitor etoposide (VP16), a commonly used anticancer drug (136).

4.1.1 Etoposide induced morphological and biochemical features of senescence *in vitro*

Recent publications have shown that low-dose etoposide-treatment induces irreversible DNA strand breaks accompanied by a senescent-like phenotype (119, 137-139). Accordingly, FaDu cells, a human HNSCC cell line, were treated with the clinically relevant concentration of etoposide (10 μM) for 24h and induction of senescence markers in addition to the enlarged morphology was investigated. Immunofluorescence microscopy revealed an accumulation of

DNA double strand breaks, which was monitored by persistent nuclear γH2AX staining at day 3 after treatment (Fig. 4.1A). Cells also exhibited a significant decrease in cell proliferation as assessed by BrdU incorporation (Fig. 4.1B). Furthermore, a peak in cell death as determined by Caspase-3 processing was seen 2 days after etoposide treatment, but was absent at later time points (Fig. 4.1C). Western blot analysis also demonstrated a strong induction of the CDK inhibitor $p21^{CDKN1A}$ following treatment, an early marker of cellular senescence (105). These observations strongly indicated that in response to DNA damage, a senescent-like state was induced.

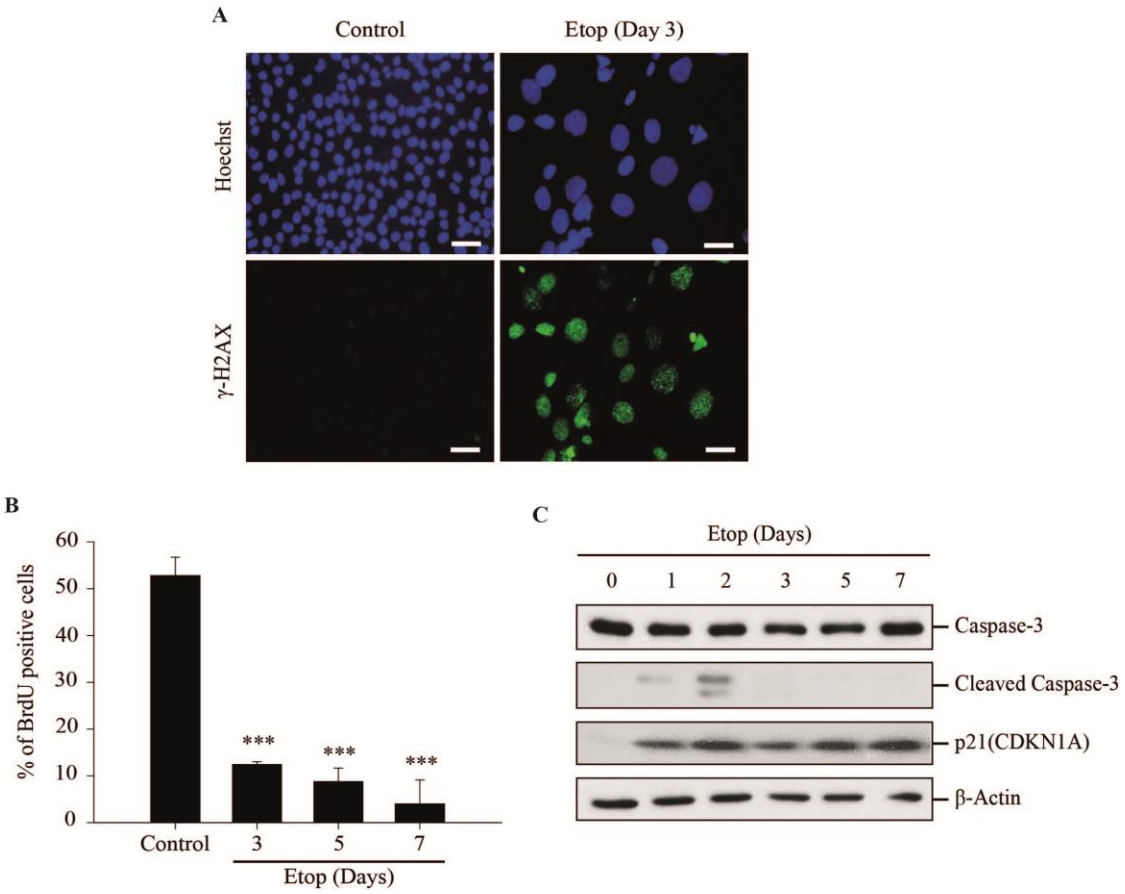

Figure 4.1: Etoposide induces DNA damage in FaDu cells. Cells were cultured in the absence or presence of 10 µM etoposide for 24 h to induce DNA damage. (A) 3 days post-treatment, persistent DNA damage was determined by immunofluorescence staining for γ-H2AX. (B) Decreased cell proliferation was assayed by BrdU incorporation and the relative percentage of BrdU-positive cells is given as mean value ± SD (n=3) of control and etoposide-treated cells at the indicated time points. (C) Whole cell lysate was extracted at the indicated time points and activation of apoptosis was determined by Caspase-3 processing using Western blot analysis. The extracts were also immunoblotted for the senescence marker $p21^{CDKN1A}$ using β-Actin as loading control for protein quality and quantity. White scale bar represents 50 µm.

It is well established that senescent, but not pre-senescent or terminally differentiated cells stain positive for SA-β-gal (104). To investigate whether the previously observed irreversible cell cycle arrest was accompanied by senescence induction, cells were assayed for SA-β-gal activity. FaDu cells exhibited a significant increase in SA-β-gal activity relative to controls, 3 days post treatment, and the percentage of SA-β-gal positive cells continued to increase up to 65% at day 7 (Fig. 4.2).

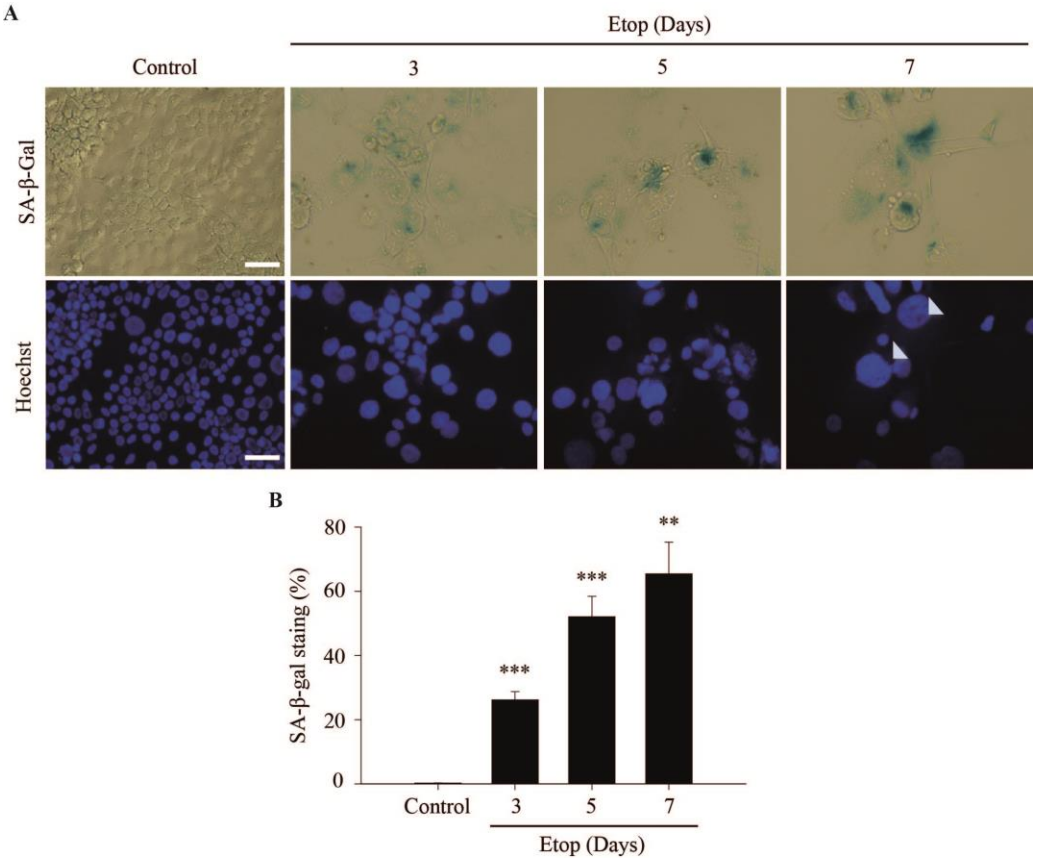

Figure 4.2: DNA damage induces senescence in FaDu cells. Cells were cultured in the absence or presence of 10 µM etoposide for 24 h to induce DNA damage. (A) Efficient induction of senescence was analyzed by SA-β-Gal staining of control and etoposide-treated cells at the indicated time points post-treatment. (B) Senescence induction was quantified and is given as relative amount of SA-β-Gal positive cells. Data are represented as mean ± SD (n=3). White scale bar represents 50 µm. Statistical analysis was performed using unpaired two-tailed t-test; ** $p<0.01$; *** $p<0.001$.

To further characterize the DNA damage-induced senescence phenotype, etoposide treated cells were examined for the induction of a ‘senescence–associated secretory phenotype’ or ‘SASP’. SASP is associated with the upregulation of distinct cytokines such as IL-6, IL-8, and most importantly IL-1β, which can mediate a positive feedback loop to maintain or amplify the effect of SASP (140). Quantitative RT-PCR analyses confirmed that expression of IL-6, IL-8 as well as IL-1β was upregulated after exposure to etoposide (Fig. 4.3). Thus, etoposide per se was able to induce senescence in FaDu cells, which was characterized by SASP and increased secretion of various cytokines.

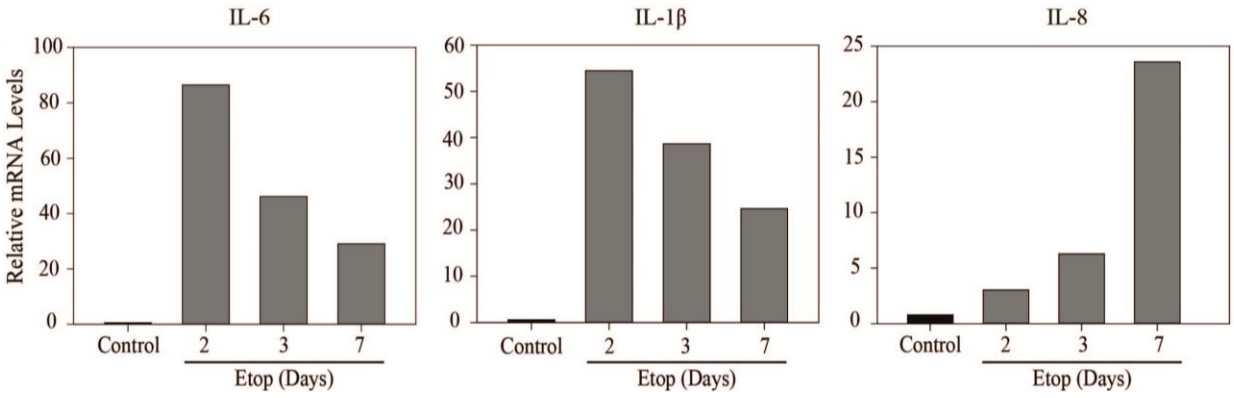

Figure 4.3: DNA damage-induced senescence initiates SASP. Cells were pre-treated with etoposide for 24h to induce DNA damage. At the indicated time points post-treatment, total RNA was extracted, reverse transcribed and transcript levels of IL-6, IL-8 and IL-1b as markers for SASP were monitored by quantitative RT-PCR. Bars represent the mean of three technical replicates.

4.1.2 Translocation and loss of MYBBP1A during DNA damage-induced senescence

To address the regulation of MYBBP1A in the setting of stress-induced senescence, MYBBP1A protein levels were investigated following treatment. Interestingly, etoposide-treated FaDu cells showed a gradual decrease in MYBBP1A protein expression, while $p21^{CDKN1A}$ as a marker of early cellular senescence was strongly induced (Fig. 4.4A). Co-immunofluorescence staining confirmed predominant localization of MYBBP1A in the nucleolus of $p21^{CDKN1A}$ negative cells, and its translocation into the nucleoplasm or loss in $p21^{CDKN1A}$ positive cells in response to DNA damage (Fig. 4.4B). Dissociation of MYBBP1A from the nucleolus to the nucleoplasm has been

reported to be associated with ribosomal stress induced by DNA damaging agents (69). Taken together, these results demonstrated that in response to DNA damage, MYBBP1A first translocated from the nucleolus to the nucleoplasm and subsequently, its protein levels decreased in senescent cells.

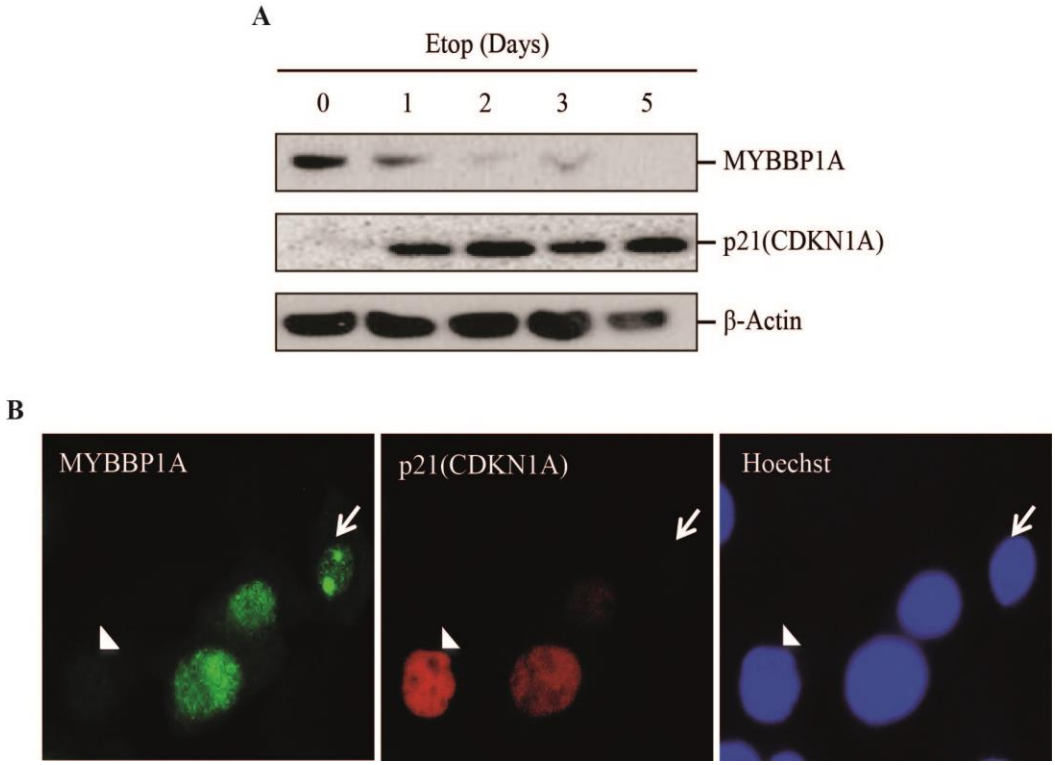

Figure 4.4: DNA damage-induced senescence involves the translocation and loss of MYBBP1A expression in FaDu cells. Cells were pre-treated with etoposide for 24h to induce DNA damage. (A) Western blot analysis demonstrates decreased MYBBP1A but increased of $p21^{CDKN1A}$ protein levels after the indicated time points after etoposide treatment. Detection of β-Actin served as loading control for protein quantity and quality. (B) Representative pictures of co-immunofluorescence staining for MYBBP1A (left panel) and $p21^{CDKN1A}$ at day 3 post-treatment with etoposide. Arrow indicates a cell with nucleolar MYBBP1A but no $p21^{CDKN1A}$ staining, and arrowhead indicates a cell with $p21^{CDKN1A}$ but no MYBBP1A staining.

In order to determine whether MYBBP1A protein down-regulation is a common feature during genotoxic-induced senescence, its expression was further examined in the cervical cancer cell line HeLa following etoposide treatment. Similar to FaDu cells, etoposide treatment in HeLa cells induced the typical senescence alterations including an enlarged morphology, strong nuclear accumulation of γH2AX as well as significant increase in SA-β-gal activity (Fig. 4.5).

Quantitative analysis showed that 92% of cells stained positive for SA-β-gal seven days post treatment, indicating a severe senescent phenotype (Fig. 4.5B).

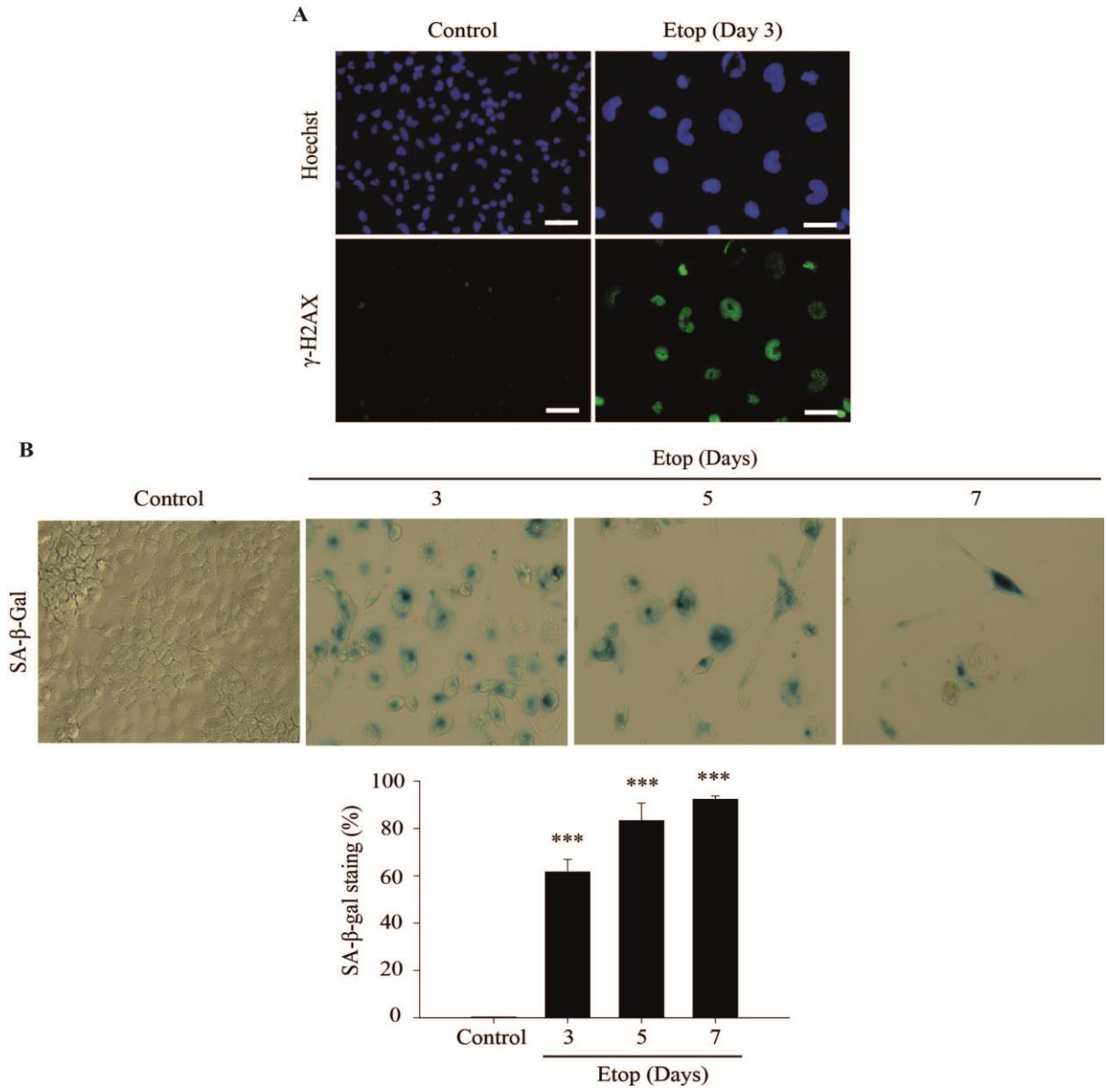

Figure 4.5: Etoposide induces DNA damage and senescence in HeLa cells. Cells were pre-treated with etoposide for 24h to induce DNA damage. (A) 3 days post-treatment, persistent DNA damage was determined by immunofluorescence staining for γ-H2AX. (B) The presence of senescent cells was determined by SA-β-gal staining at the indicated time points. Data are represented as percentage total of β-gal positive cells ± SD (n=3). Statistical analysis was performed using unpaired two tailed Student's t-test; *** $p<0.001$. White scale bar represents 50 μm.

Consistent with the observations in FaDu cells, a gradual decrease in MYBBP1A protein levels was observed following treatment (Fig. 4.6A). Moreover, immunofluorescence studies confirmed the translocation and loss of MYBBP1A in senescent HeLa cells (Fig. 4.6B).

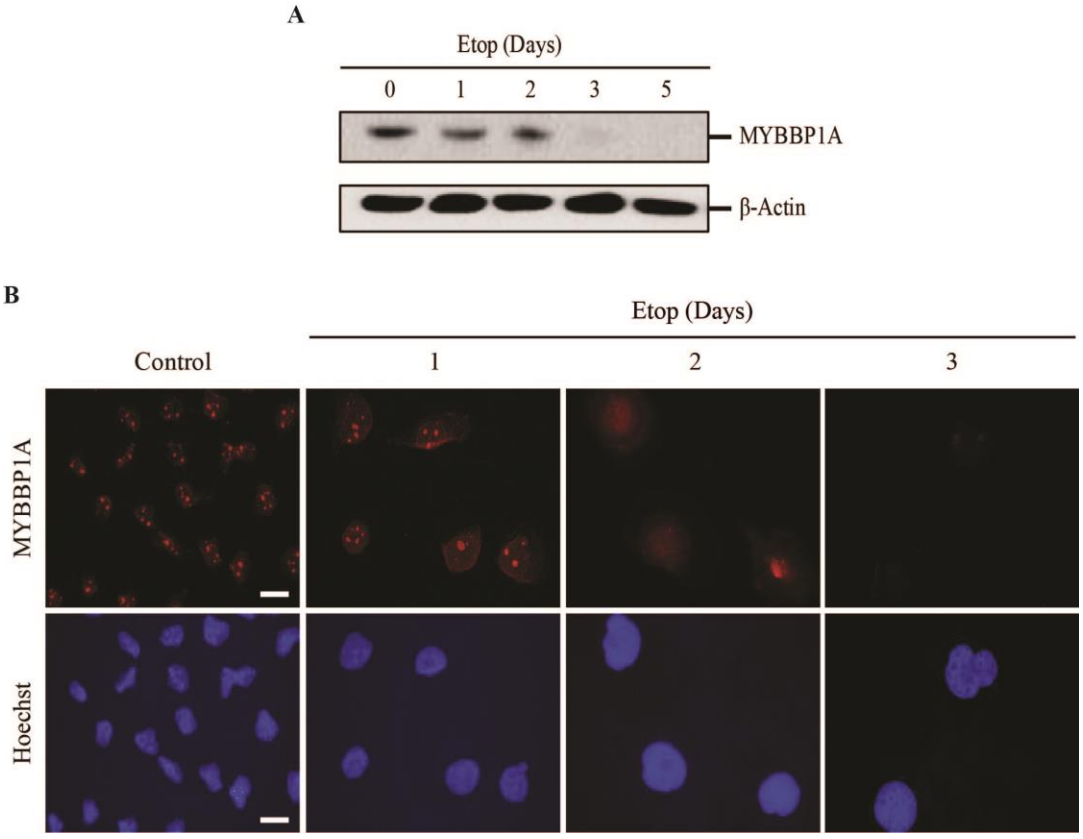

Figure 4.6: DNA damage-induced senescence involves the translocation and loss of MYBBP1A protein in HeLa cells. Following 24hours treatment with DNA damaging agent (10 µM etoposide), MYBBP1A expression was analyzed. Western blot (A) and immunofluorescence staining (B) revealed MYBBP1A translocation and loss of protein following treatment. Detection of β-Actin served as loading control for protein quantity and quality. Nuclear staining with Hoechst 33324. White scale bar represents 50 µm.

4.1.3 Silencing of MYBBP1A is not sufficient to induce senescence *in vitro*

In the past, it was proposed that down-regulation of *Mybbp1a* in mouse embryonic fibroblasts reveals a rapid entry into senescence (75). To investigate whether loss of MYBBP1A is sufficient to induce senescence in tumor cells, gene silencing was conducted by transient

transfection of FaDu cells with control (scramble) or MYBBP1A-specific siRNAs (siMYBBP1A). Silencing efficiency was confirmed three days post-transfection by Western blot analysis (Fig. 4.7A). Previously, several studies demonstrated that deletion or down-regulation of MYBBP1A has a profound effect on the cellular growth rate by affecting the expression of several genes involved in cell cycle control, DNA damage and cell death (75, 83). Consistent with this reports, MYBBP1A-depleted FaDu cells displayed a slight but significant decrease in BrdU incorporation as compared to the scramble-controls (36% v. 42%, Fig. 4.7B). However, silencing of MYBBP1A did not induce any marker of senescence tested, including cell or nuclear morphology (data not shown), $p21^{CDKN1A}$ expression (Fig. 4.7A) and SA-β-gal staining (Fig. 4.7C), indicating that loss of MYBBP1A expression is not sufficient to trigger senescence in FaDu cells.

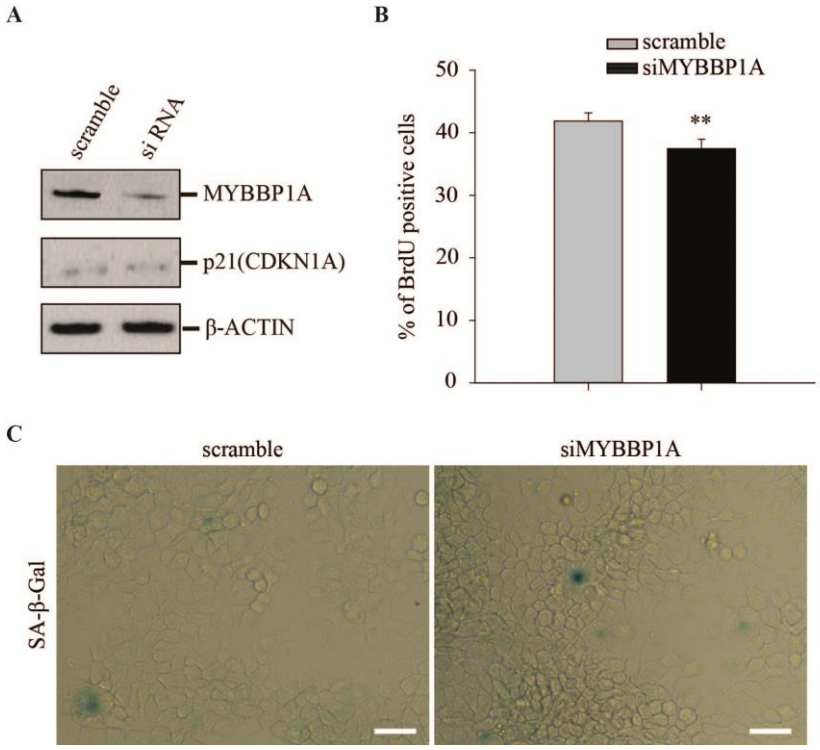

Figure 4.7: Silencing of MYBBP1A is not sufficient to induce senescence in FaDu cells. (A) Efficient silencing of MYBBP1A 72 hours after transient transfection was demonstrated with whole cell lysate of FaDu-siMYBBP1A and FaDu-scramble cells by Western blot analysis. The extracts were also immunoblotted for the senescence marker $p21^{CDKN1A}$ and detection of β-Actin was used as loading control. (B) Samples were analyzed for BrdU incorporation 3 days post-transfection. Data are represented as mean ± SD (n=6) (unpaired ratio two-tailed t-test; ** $p<0.01$). (c) Representative pictures of SA-β-gal staining (blue staining) at day 5 post transfection. White scale bar represents 50 μm.

4.1.4 Silencing of MYBBP1A accelerates DNA damage-induced senescence

To determine whether MYBBP1A modulates the efficacy of DNA damage-induced senescence, FaDu cells were first transfected with control or MYBBP1A-specific siRNAs and subsequently subjected to etoposide. Although silencing of MYBBP1A had no major impact on basal or etoposide-induced $p21^{CDKN1A}$ expression (Fig. 4.8A), it resulted in a slight but significantly decreased amount of BrdU positive cells after etoposide treatment (Fig. 4.8B). MYBBP1A depleted cells exhibited a significant increase in the relative number of senescent tumor cells at day 5 post-treatment (2-3 fold) as determined by SA-β-gal-positive staining (Fig. 4.8C). This result suggests that, in the context of DNA damage-induced senescence, inactivation of MYBBP1A plays a critical role in modulating the efficacy of the senescence program.

Similar results were obtained upon analysis of HeLa cells with MYBBP1A silencing after etoposide treatment as compared to scramble-controls. Although $p21^{CDKN1A}$ expression was induced by etoposide, it maintained at the same level independent of silencing of MYBBP1A expression (Fig. 4.9A). In addition, active replication measured by BrdU incorporation revealed a significant decrease in the percentage of BrdU positive cells in the MYBBP1A-delpleted cells compared to scramble-controls following treatment (Fig. 4.9B). After 5 days of treatment, SA-β-gal activity was evaluated and found to be enhanced in MYBBP1A depleted cells, consistent with the previous results (Fig. 4.9C). Taken together, these data confirmed that loss of MYBBP1A is not sufficient to trigger senescence in tumor cells, but modulates the efficacy of genotoxic-induced senescence.

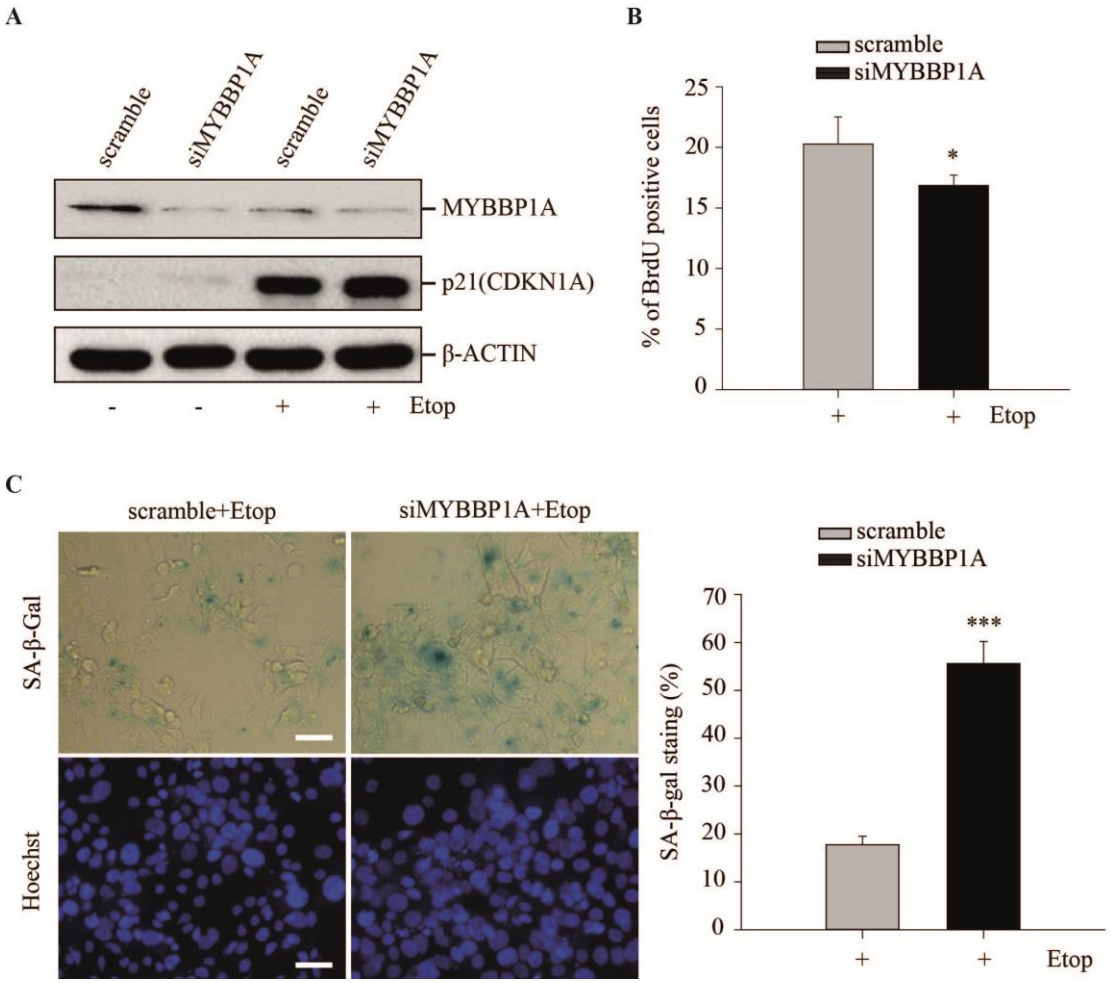

Figure 4.8: Silencing of MYBBP1A accelerates DNA damage-induced senescence. FaDu cells were transiently transfected with scramble or siRNAs directed against MYBBP1A. After 48 hours of transfection, cells were incubated in the presence or absence of 10 µM etoposide for 24 hours and subsequently cultured for 5days. (A) Cell lysates were subjected to Western blot analysis for indicated proteins 5 days post-treatment. β-Actin served as a loading control. (B) Samples were analyzed for BrdU incorporation 5 days post-etoposide treatment. Data are represented as percentage total of cells ± SD (n=6) (unpaired ratio two-tailed t-test; * $p<0.05$). (C) Samples were fixed and analyzed for SA-β-gal activity 5 days post treatment. Quantification of SA-β-Gal-positive cells revealed increased relative amounts of positive cells for siMYBBP1A transfected cells as compared to scramble controls. Data are expressed as percentage total of cells ± SD (n=3) (unpaired ratio two-tailed t-test; *** $p<0.001$). White scale bar represents 50 µm.

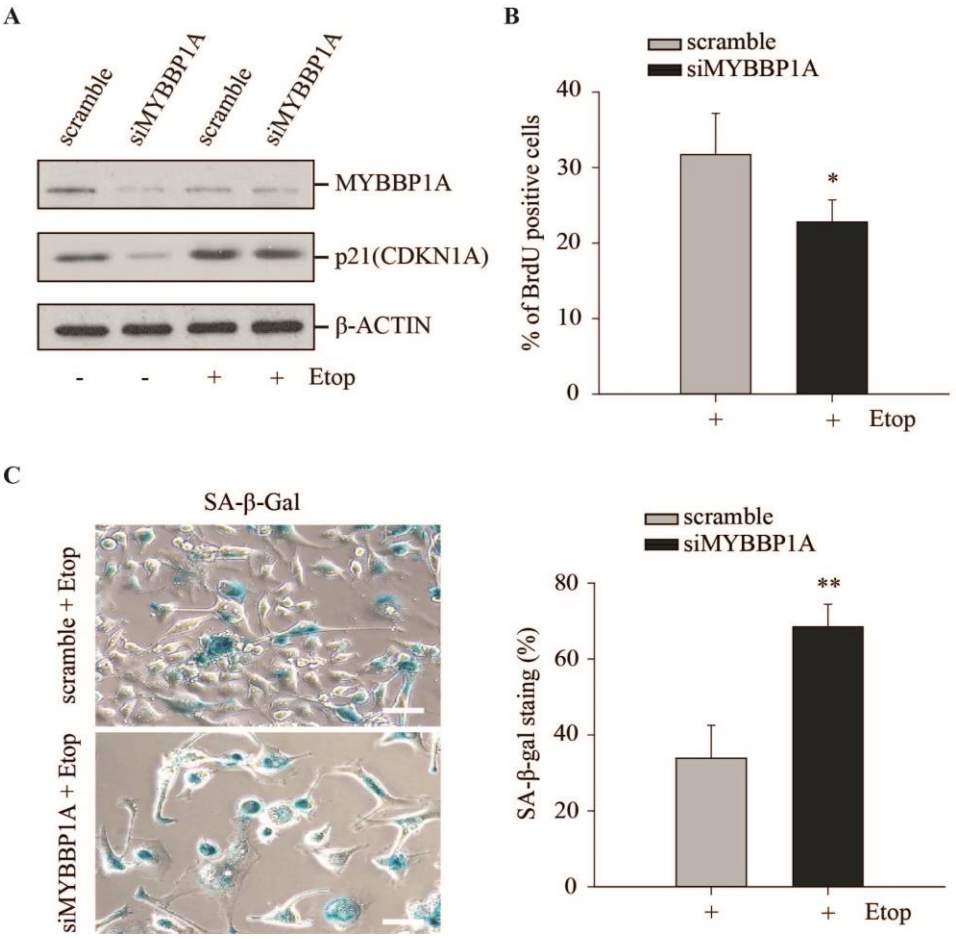

Figure 4.9: Silencing of MYBBP1A expression accelerates DNA damage-induced senescence in HeLa cells. HeLa cells were transiently transfected with scramble and siMYBBP1A. At day 2, transfected cells were treated with 10 µM etoposide for 24 hours. (A) Cell lysates were subjected to Western blot analysis for indicated proteins 5 days post-treatment. Detection of β-Actin served as loading control for protein quantity and quality. (B) Samples were analyzed for BrdU incorporation 5d post-treatment. Data are represented as mean ± SD (n=3) (unpaired ratio two-tailed t-test; * $p \leq 0.05$). (C) Samples were fixed and analyzed for SA-β-Gal activity 5d post-treatment. Data are represented as percentage total of cells ± SD (n=3) (unpaired ratio two-tailed t-test; ** $p < 0.01$). White scale bar represents 50 µm.

4.1.5 Ectopic overexpression of MYBBP1A attenuates DNA damage-induced senescence

To dissect the functional role of MYBBP1A in cellular senescence, HeLa cells were transiently transfected with control (Mock) or FLAG-tagged amino-terminal region of MYBBP1A ($MYBBP1A^{p67}$) and subjected to etoposide treatment. Unlike the full length MYBBP1A (also

known as p160), its shorter N-terminal 67 kDa fragment has been shown to be more stable (72). Western blot analysis with Anti-FLAG antibodies reveled prominent ectopic protein expression, which was also detectable after etoposide treatment (Fig. 4.10A). Furthermore, the expression of markers of senescence and proliferation was analyzed in these cells. Despite the expression of MYBBP1A, no difference was observed in γH2AX staining and $p21^{CDKN1A}$ induction post treatment (Fig. 4.10B). Although no obvious difference in early markers of senescence was found, $MYBBP1A^{p67}$ cells displayed increased BrdU incorporation (Fig. 4.10C) and decreased SA-β-gal activity as compared to control after treatment (Fig. 4.11). These results demonstrate that overexpression of MYBBP1A could bypass genotoxic-induced senescence.

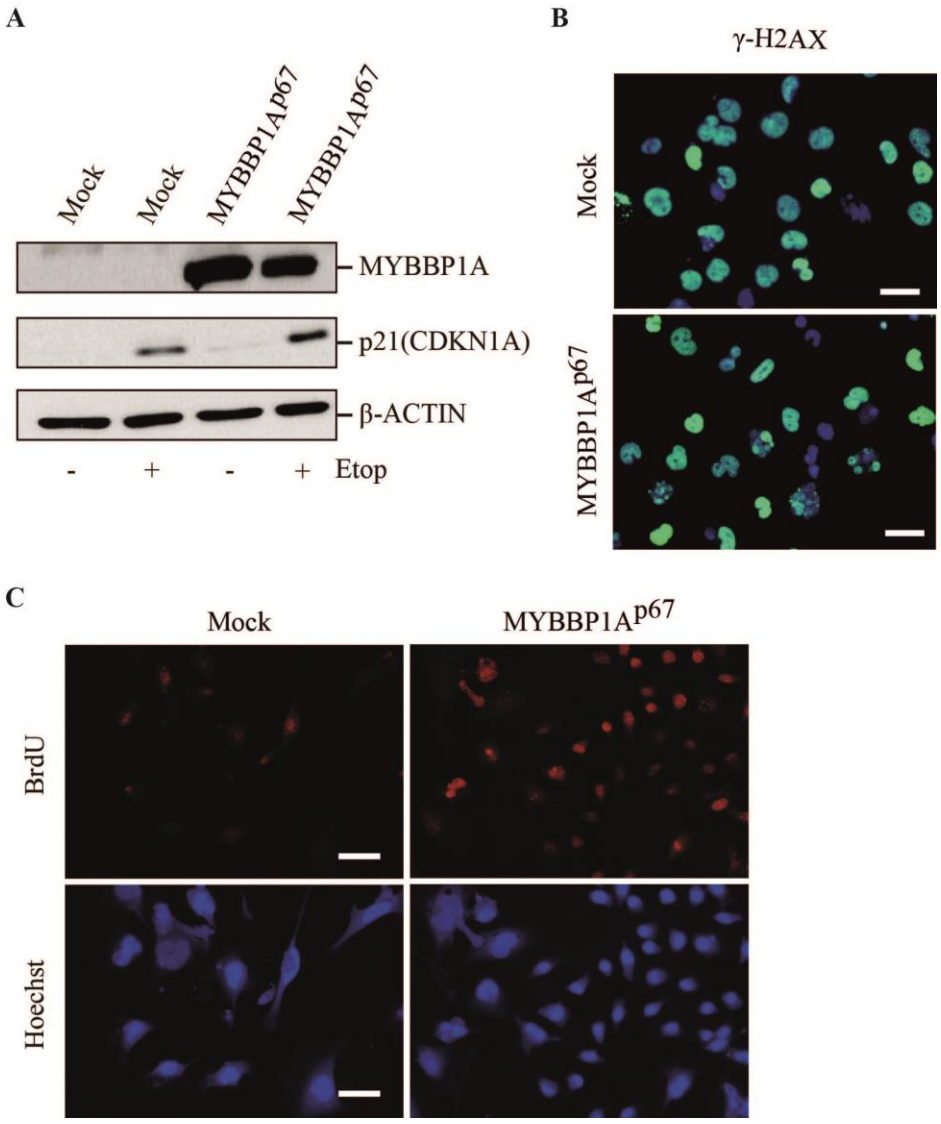

Figure 4.10: Ectopic overexpression of MYBBP1A^{p67} in HeLa cells. HeLa cells were transiently transfected with control (mock) and a MYBBP1A^{p67} expression plasmid. At day 2, transfected cells were treated with 10 µM etoposide for 24 hours. (A) Cell lysates were subjected to Western blot analysis for indicated proteins 5 days post-treatment. Detection of β-Actin served as loading control for protein quantity and quality. (B) 5 days post-treatment, persistent DNA damage was determined by immunofluorescence staining for γ-H2AX (green fluorescence). (C) Samples were analyzed for BrdU incorporation (red fluorescence) 5 d post-treatment. Nuclear staining with Hoechst 33324. White scale bar represents 50 µm.

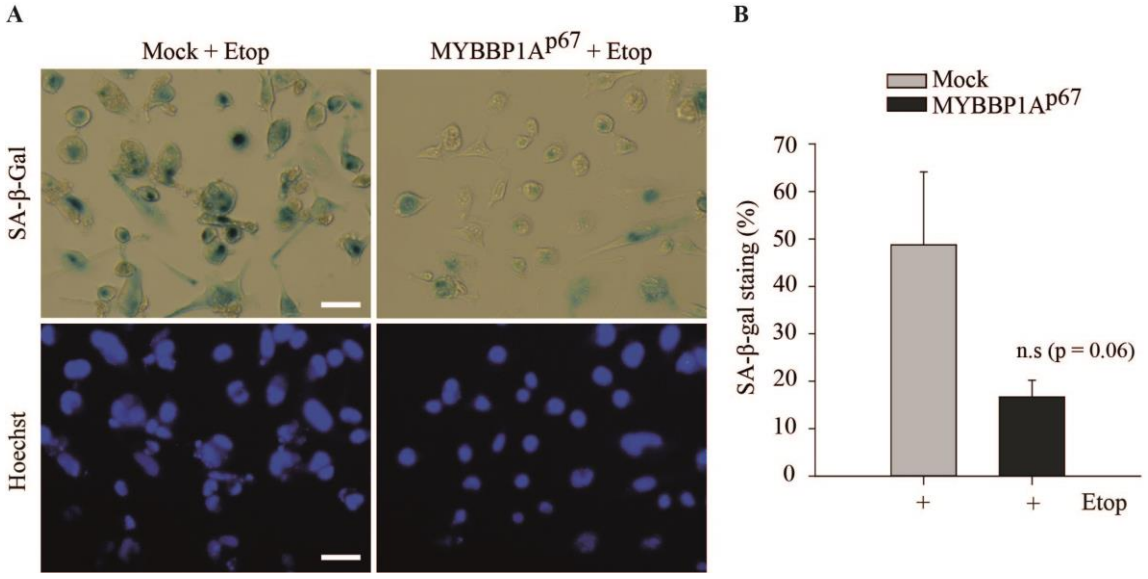

Figure 4.11: Ectopic overexpression MYBBP1A^{p67} attenuates DNA damage-induced senescence in HeLa cells. HeLa cells were transiently transfected with Mock and MYBBP1A^{p67}. At day 2, transfected cells were treated with 10 µM etoposide for 24 hours. (A) Samples were fixed and analyzed for SA-β-Gal activity 5d post-treatment. (B) Quantification of SA-β-Gal-positive cells revealed decreased relative amounts of positive cells for MYBBP1A^{p67} transfected cells as compared to Mock controls. Data are expressed as percentage total of cells ± SD (n=3). Nuclear staining with Hoechst 33324. White scale bar represents 50 µm.

4.1.6 Knockdown of MYBBP1A expression modulates the expression of SASP factors and confers radio-resistance

MYBBP1A was demonstrated as an important repressor of NFκB-dependent transcription (78), and in response to DNA damage activated NFκB conferred induction of SASP (141). Consequently, MYBBP1A-dependent alterations in the transcription of SASP related cytokines

were analyzed in DNA damage-induced senescent cells. Upon etoposide treatment FaDu-siMYBBP1A cells exhibited slightly increased expression of IL-6, IL-1β and TGF-β as compared to scramble controls, which did not reach statistical significance (Fig. 4.12). These results support the assumption that MYBBP1A might represent a key player towards maintenance rather than the initiation of senescence.

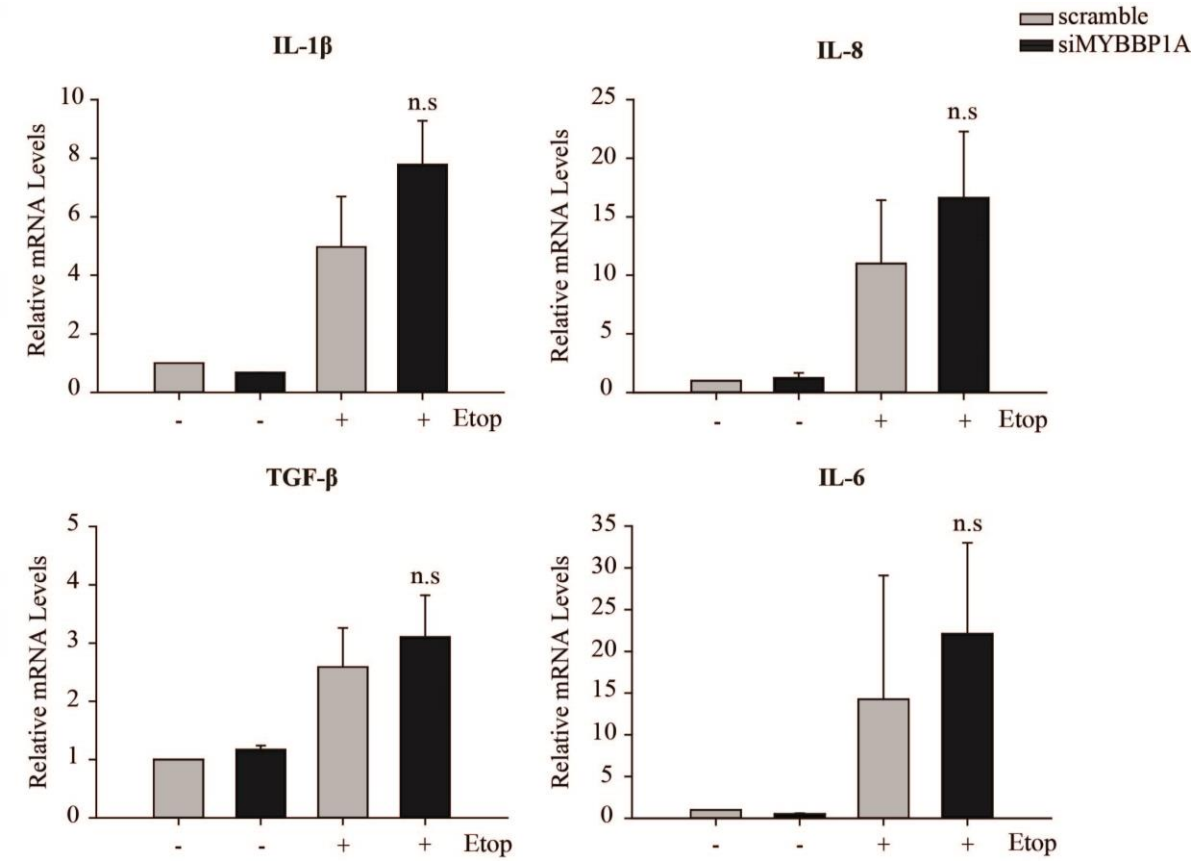

Figure 4.12: Silencing of MYBBP1A accelerates expression of SASP components following DNA damage. FaDu-Mock and FaDu-siMYBBP1A cells were treated in the presence (+) or absence (-) of etoposide for 24h after transient transfection. At day 5 post-treatment total RNA was extracted for quantitative RT-PCR. Relative transcript levels of the SASP-related cytokines IL-1β, IL-8, IL-6 and TGF-β are given as mean value ± SD (n=3). Unpaired ratio two-tailed t-test; n.s. = not significant.

Results so far indicated that silencing of MYBBP1A accelerates the DNA damage-induced senescence and modulates the expression of SASP components. Next, the impact of MYBBP1A silencing on the sensitivity of FaDu cells to irradiation was determined. FaDu cells were transfected with MYBBP1A specific siRNA or scramble controls and 48h post-transfection cells were exposed to a single dose of 5 Gy. Radiosensitivity was determined by a colony-forming

assay (CFA) and revealed an almost 2-fold increase in clonogenic survival for siMYBBP1A transfected cells as compared to the scramble controls (Fig. 4.13). To our knowledge, these result shows for the first time that loss of MYBBP1A expression is associated with radio-resistance.

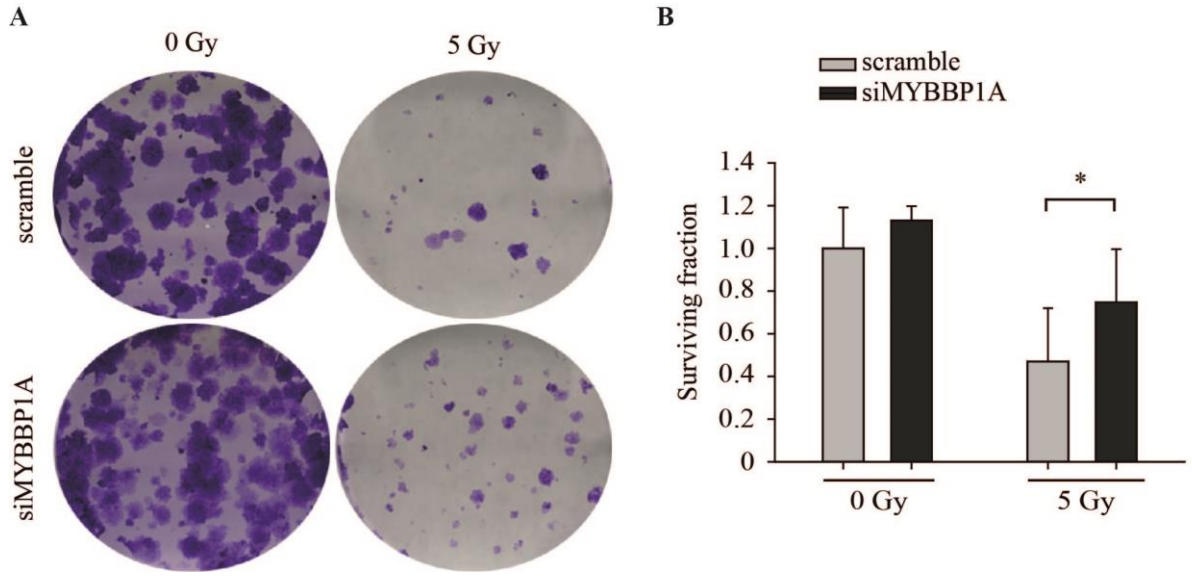

Figure 4.13: Knockdown of MYBBP1A expression confers radioresistance. FaDu cells were transiently transfected with control and MYBBP1A specific siRNAs. 48h post-transfection, cells were irradiated with a single dose (5 Gy). Following treatment, cells were cultured for 10 days and colonies were stained with crystal violet. (A) Representative images demonstrate increased numbers of colonies for MYBBP1A depleted cells after irradiation compared with scramble controls. (B) Results are represented as the mean surviving fraction (± SD), which was determined for three independent experiments (unpaired ratio two-tailed t-test; * $p<0.05$).

4.2 MYBBP1A-PI3K/AKT signaling cascade in stress-induced senescence *in vitro*

Protein kinase B is the major effector of the phosphoinositide 3-kinase (PI3K) pro-survival pathway (142). In the context, activation of the PI3K/AKT pathway (Fig. 1.4) was regarded as an essential survival signal to counteract the pro-apoptotic effects under stress conditions or presence of DNA damaging agents, which might also promote tumorogenesis (143, 144). Accordingly, PI3K/AKT pathway activation might act as a pivotal survival signal during DNA damage-induced senescence.

4.2.1 Activation of the PI3K/AKT pathway in stress-induced senescence

To investigate activation of PI3K/AKT pathway as a function of DNA damage-induced senescence, phosphorylation of AKT on Ser473 was analyzed in FaDu and HeLa cells following etoposide treatment. As shown in Fig. 4.14A, FaDu cells showed loss of MYBBP1A expression and a strong increase in AKT phosphorylation (pAKT(Ser473)) in response to etoposide by Western blot analysis, which was consistent with previous observations (143, 145). Similar data concerning inverse regulation of MYBBP1A protein and pAKT(Ser473) were also detected in HeLa cells after etoposide treatment (Fig. 4.14B). It is worth noting that the response kinetics was heterogeneous and slightly different in FaDu and HeLa cells. Collectively, these data strongly suggest that low MYBBP1A expression and parallel rise in pAKT(Ser473) may indicate tumor cells in a pre-senescent stage.

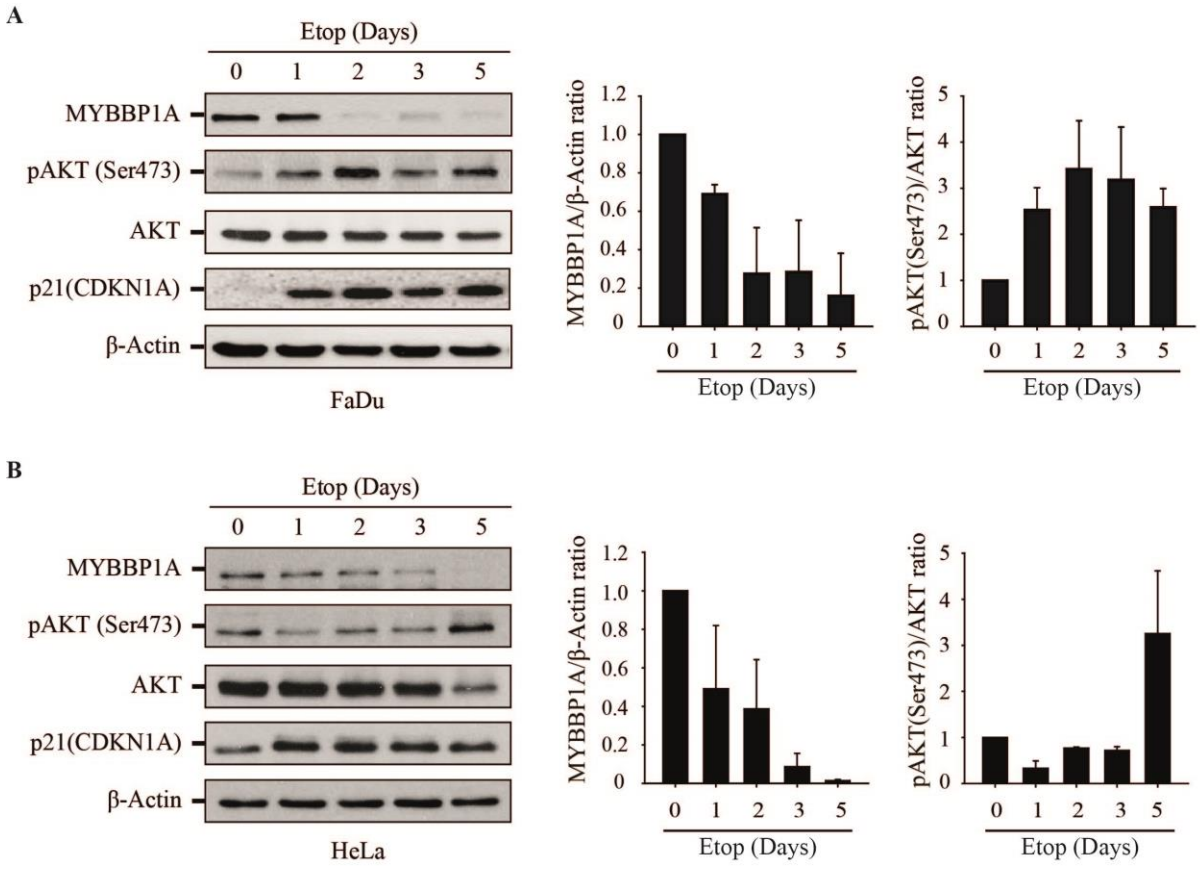

Figure 4.14: Inverse regulation of MYBBP1A and pAKT(Ser473) protein levels after DNA damage. (A) Inverse regulation of MYBBP1A and pAKT(Ser473) protein levels were determined by Western blot analysis with whole cell lysate of control (0 day) and etoposide-treated FaDu cells. Detection of total AKT and β-Actin served as a loading control for protein quality and quantity. Signals were quantified by ImageJ and bar graphs show changes in MYBBP1A/β-Actin and pAKT(Ser473)/AKT ratios normalized to control at day 0 are shown beside the blots. Data represent mean ± SD of three independent experiments. (B) Western blot analysis and quantification of MYBBP1A and pAKT(Ser473) protein levels post treatment in HeLa cells.

4.2.2 Loss of MYBBP1A during DNA damage induced senescence is independent of AKT signaling

To investigate whether the activation of AKT signaling is causally linked to loss of MYBBP1A expression, level of pAKT(Ser473) was analyzed in FaDu and HeLa cells following silencing of MYBBP1A expression. Similar to previous result, efficient silencing of MYBBP1A was observed 72h after transfection in both cell lines. However, no difference in pAKT(Ser473) levels were seen between cells transfected with either control or MYBBP1A-specific siRNA (Fig. 4.15), suggesting that activation of AKT signaling is not related to the loss of MYBBP1A expression.

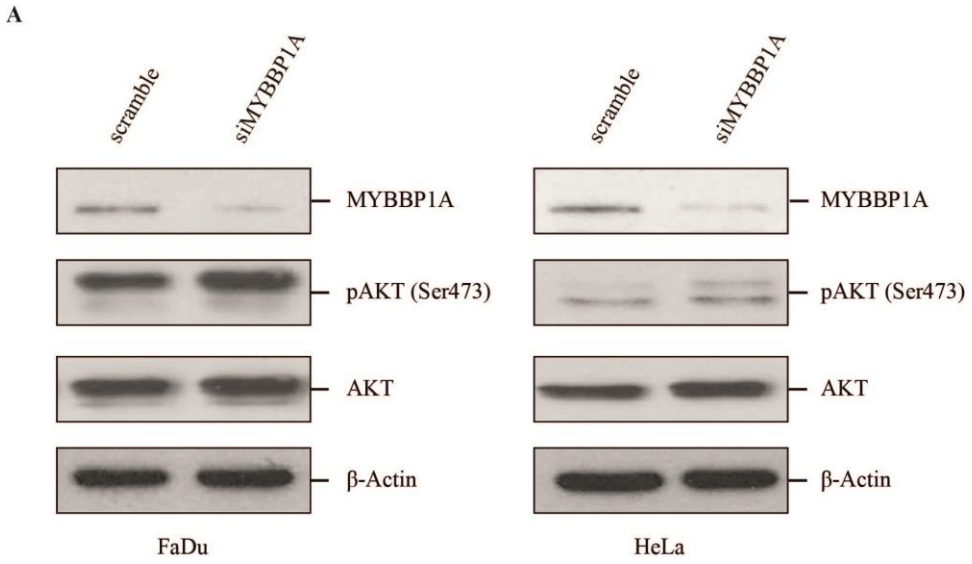

Figure 4.15: Loss of MYBBP1A expression does not induce AKT phosphorylation. (A) Efficient silencing of MYBBP1A 72 hours after transient transfection was demonstrated with whole cell lysate of FaDu and HeLa cells by Western blot analysis. The extracts were also immunoblotted for pAKT(Ser473). Detection of total AKT and β-Actin served as a loading control for protein quality and quantity.

To further address the question whether genotoxic-induced down-regulation of MYBBP1A is under the influence of activation of PI3K/AKT pathway, FaDu cells were treated with etoposide in the presence or absence of potent inhibitors. LY294002 (20 μM) was used to inhibit PI3K and Triciribine (20 μM) to inhibit AKT, the downstream effector of PI3K (Fig. 4.16). However, inhibition of AKT had no major impact on MYBBP1A protein levels upon etoposide treatment. In contrast to a previous report (143), LY294002 treatment did not provoke inhibition of AKT phosphorylation as detected by Western blot analysis. Interestingly, LY294002 stabilizes the expression of MYBBP1A post treatment. These results suggest that, although inhibition of PI3K mediated stabilization of MYBBP1A protein post etoposide treatment, AKT was not essential to transduce the signal and may potentially be regulated via other pathways.

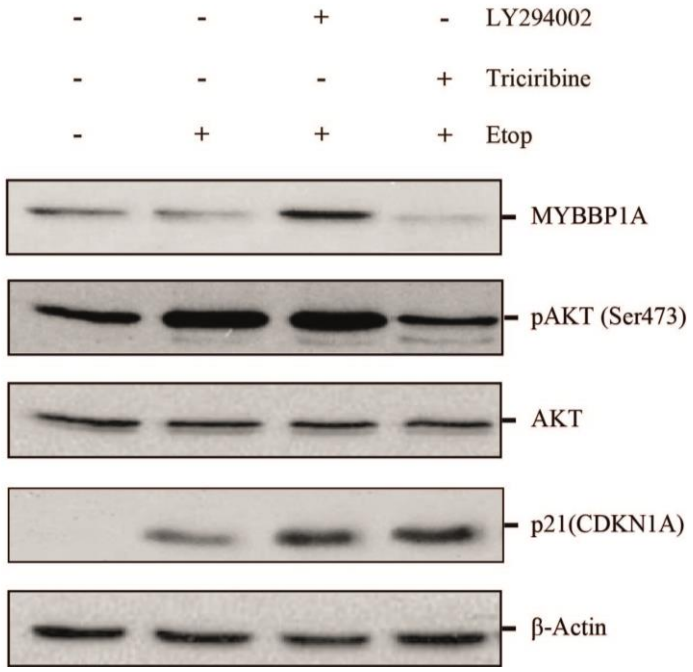

Figure 4.16: Increased MYBBP1A protein stability by LY294002 treatment in the presence of genotoxic stimuli. Cells were treated with (+) or without (-) etoposide (10 μM), LY294002 (20 μM) or Triciribine (10 μM) as indicated. After 72h the cells were lysed and the expression of MYBBP1A and pAKT(Ser473) was determined by Western blot. Detection of total AKT and β-Actin served as a loading control for protein quality and quantity.

4.2.3 Post transcriptional modifications for MYBBP1A protein stability

In the past, it has been suggested that MYBBP1A protein stability was regulated by post-transcriptional modifications, including ubiquitination and proteasomal degradation (71). Accordingly, MYBBP1A transcript and protein levels were analyzed in a panel of HNSCC cell lines and HeLa cells. Accordingly, SCC-25 cell line showed comparable transcript levels with Cal-27, but difference in the protein levels (Fig. 4.17A-B). However, FaDu and HeLa cell lines showed prominent expression at the transcript and protein level. This finding suggested a post-translational mechanism for the regulation of MYBBP1A protein levels. In line with this assumption, preliminary data demonstrated that treatment of SCC-25 cells that exhibit MYBBP1A transcripts but only low protein levels with the proteasome inhibitor MG-132 resulted in increased protein stability when compared to untreated controls (Fig. 4.17C). To further investigate the regulation of MYBBP1A protein stability by ubiquitination during DNA damage-induced senescence, SCC-25 cells were pre-treated with MG-132 followed by incubation with etoposide. As depicted in Fig. 4.17D, cells did not survive following MG-132 treatment in the presence of etoposide, mostly due to strong induction of apoptosis (146). Even though, MYBBP1A protein levels are at least in part regulated by posttranslational modifications, the molecular mechanism resulting in the loss of MYBBP1A expression in the presence of genotoxic stimuli remains elusive and will be a major challenge for the future.

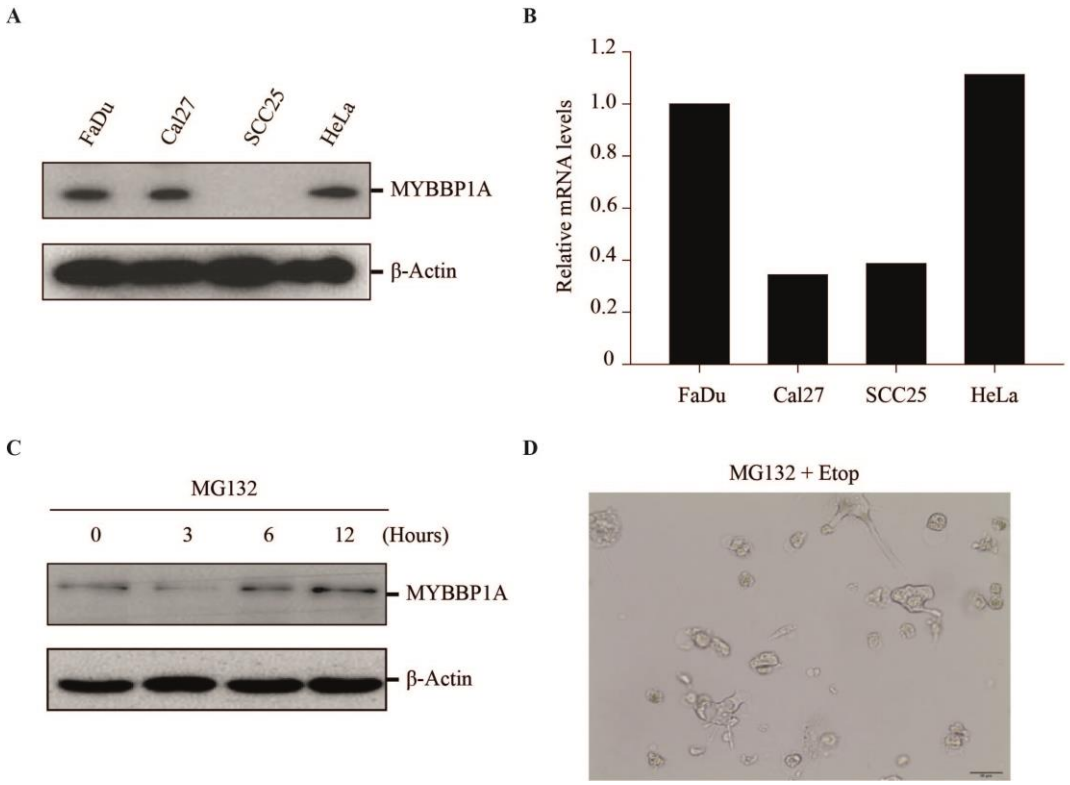

Figure 4.17: MYBBP1A protein stability by ubiquitination and toxicity of MG-132 in the presence of genotoxic stimuli. MYBBP1A expression in a panel of HNSCC cell lines and HeLa cells was determined at protein level by Western immunoblot (A), while transcript levels were analyzed by quantitative RT-PCR (B). (C) Western blot analysis demonstrates stabilization of MYBBP1A protein after the indicated time of MG-132 (10 μM) treatment in SCC-25 cells. β-Actin served as a loading control. (D) Microscopic analysis revealed dramatic decrease in the cell survival following treatment of FaDu cells with MG-132 (10 μM) and etoposide (10 μM).

4.2.4 SCC-25 an *in vitro* model for post-senescent tumor cells

As loss of MYBBP1A expression was associated with DNA damage-induced senescence, the presence of additional markers for senescence was investigated in parental SCC-25 cells. In line with a previous publication (53), SCC-25 cells exhibited high pAKT(Ser473) levels. In addition, SCC-25 cells under normal culture conditions were characterized by enlarged cell morphology, increased $p21^{CDKN1A}$ expression and nuclear γH2AX staining as compared with other HNSCC cell lines (Fig. 4.18A-B). Quantitative RT-PCR also demonstrated increased transcript levels of SASP-related cytokine IL-1β in SCC-25 cells (Fig. 4.18C). Even though, SCC-25 showed

several features of senescence, SA-β-gal activity was not detectable (Fig. 4.19A), suggesting that these cells might represent a post-senescent cells that regained the capacity to proliferate.

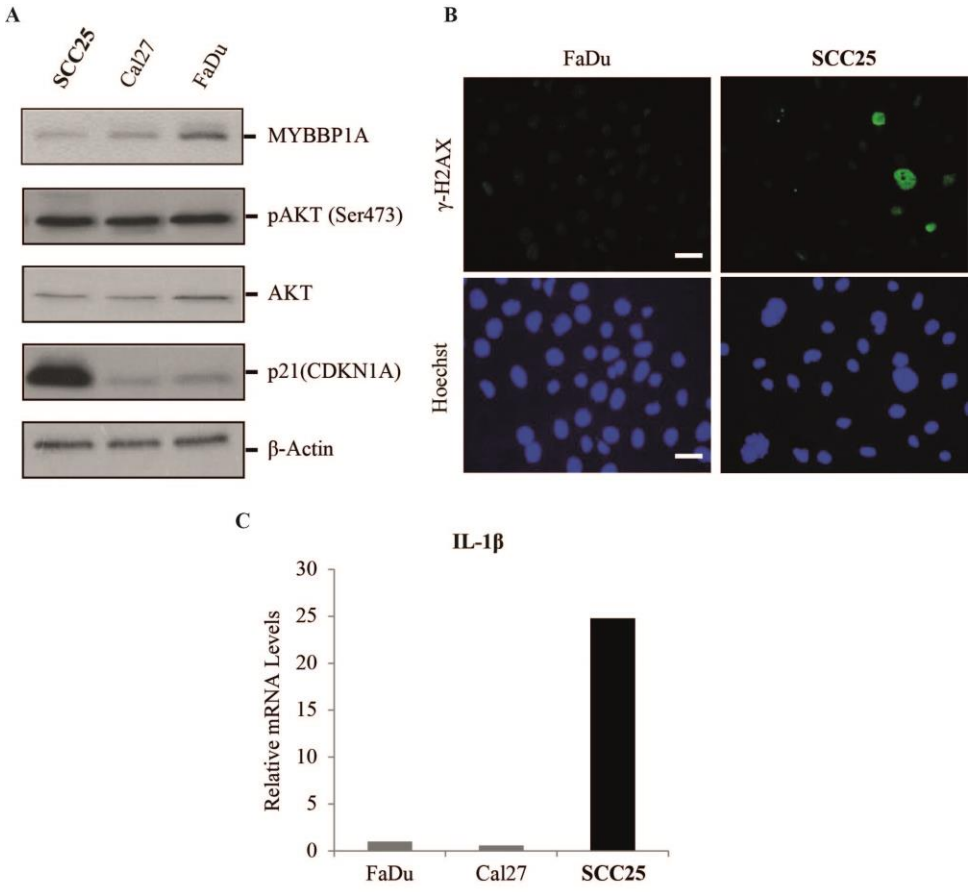

Figure 4.18: SCC-25 an *in vitro* model for post-senescent tumor cells. (A) In a panel of HNSCC cell lines, the levels of MYBBP1A, pAKT(Ser473) and the senescence marker $p21^{CDNK1A}$ were investigated by Western blotting. β-Actin served as a loading control. (B) SCC-25 cells were cultured, fixed and analyzed by immunofluorescence with the γ-H2AX antibody. Nuclear staining with Hoechst 33324. White scale bar represents 50 μm. (C) Total RNA was extracted; reverse transcribed and transcript level of IL-1β was monitored by quantitative RT-PCR in a panel of HNSCC cell lines. Bars represent mean value of three technical replicates.

To further characterize the DNA damage-induced senescence phenotype, SA-β-gal activity was determined in SCC-25 cells following etoposide treatment. Interestingly, no obvious increase in SA-β-gal activity was found in SCC-25 cells at day 5 post-treatment, while most FaDu cells that served as positive control were SA-β-gal positive (Fig. 4.19B). Taken together, these results suggest that SCC-25 represents a bona fide *in vitro* model for post-senescence with

MYBBP1A^{low}pAKT^{high} expression and some features of senescence except SA-β-gal activity. Moreover, SCC-25 showed treatment resistance towards genotoxic stimuli.

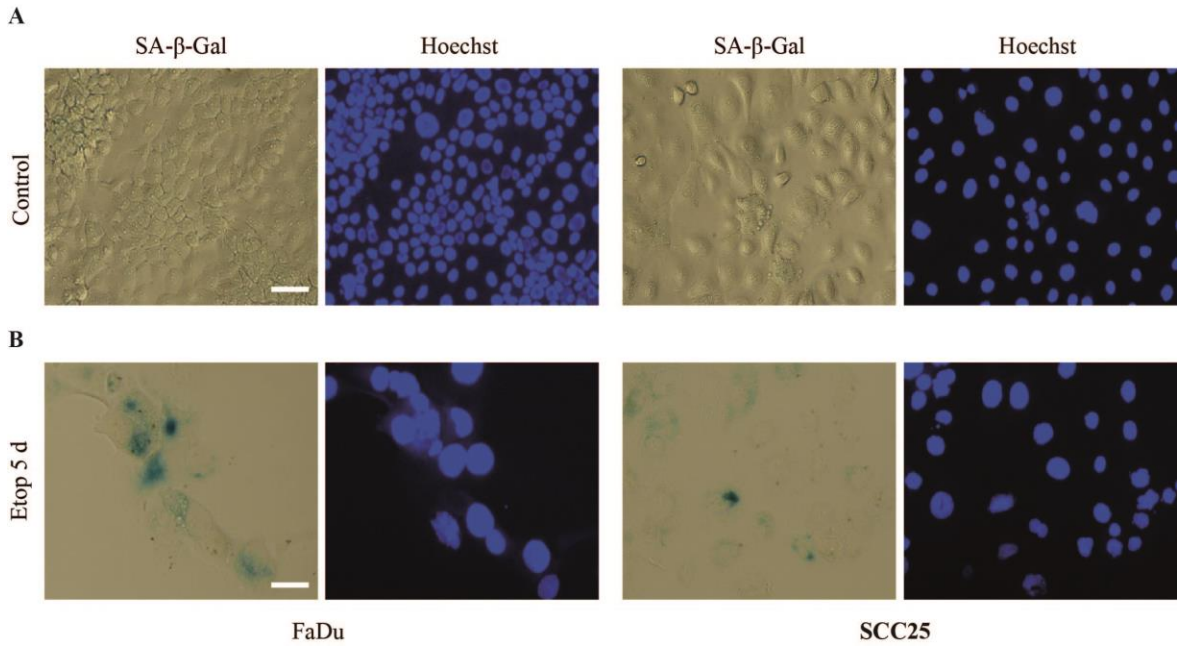

Figure 4.19: Response of SCC-25 cells towards exposure to etoposide. FaDu and SCC-25 cells were assessed for SA-β-gal activity in the presence (B) and absence (A) of etoposide. Hoechst staining was used to visualize DNA. White scale bar represents 50 µm.

4.3 Clinical relevance of senescent tumors cells in OPSCC patients

Even though senescence is often described in the context of therapeutic benefits in HNSCC (147, 148), our knowledge concerning its correlation with clinical and histopathological characteristics as well as the clinic outcome remains limited. In the past, several clinical and experimental studies demonstrated a paracrine cross talk between senescent cells and adjacent tumor cells during malignant progression and conditions of treatment failure (108, 149). To gain further insight into the clinical relevance of our findings, protein levels of MYBBP1A, total AKT and pAKT(Ser473) were analyzed in tissue samples from human primary OPSCC patients (n=61) (Fig. 4.20).

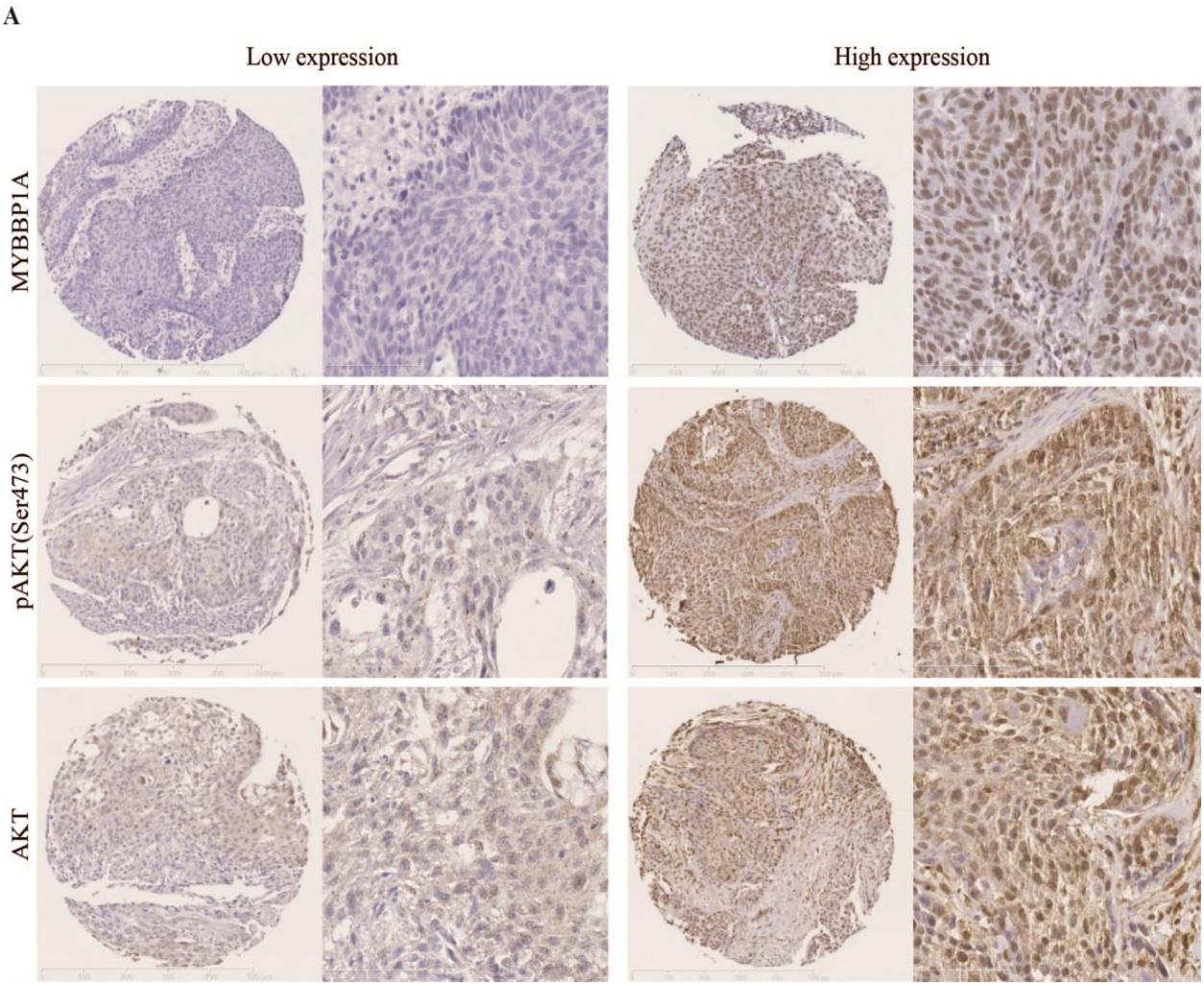

Figure 4.20: Heterogeneous pattern of MYBBP1A and pAKT(S473) **protein levels in primary tumors of OPSCC patients. (A) R**epresentative images of immunohistochemical (IHC) staining for low (left panel) and high expression (right panel) of MYBBP1A, pAKT(S473) and AKT on tissue sections of primary OPSCCs (brown signal). Counterstaining was performed with Hematoxyline.

4.3.1 Correlation analysis of MYBBP1A^{low}pAKT^{high} expression score with clinical and histopathological features

The relative amount of positively stained cells and the staining intensity for MYBBP1A, pAKT and AKT proteins were determined by three independent observers (Kindly provided by Gustavo A Sanhueza and Dominik Horn). A combinatorial analysis revealed a subgroup of seven patients with MYBBP1A^{low}pAKT(Ser473)^{high} staining pattern relative to combination of all other patterns (n=54). Subsequently, the expression pattern was compared with several clinico-pathological patient parameters (Table 4.1). Patients with an age group<58, current alcohol and tobacco consumption, HPV non-driven tumors, large tumor size, lymph node metastasis, and advanced clinical stages tended to show a MYBBP1A^{low}pAKT(Ser473)^{high} staining pattern, but the associations were not statistically significant. Moreover, two patients with distant metastasis showed a significant correlation with in the primary tumor (p=0.012), but the relevance of this finding was hampered by the small amount of patients with distant metastasis in our study cohort. In summary, the MYBBP1A^{low}pAKT(Ser473)^{high} staining pattern confirmed the presence of pre-senescent or senescent tumor cells in a subpopulation of OPSCC patients, which was not significantly correlation with any clinico-pathological feature tested.

Table 4.1: Correlation analysis of MYBBP1A^{low}pAKT(Ser473)^{high} expression score and clinico-pathological features

Characteristics	**Total** (N=61)	**MYBBP1A^{low}/AKT(Ser473)^{high}** (N=7)	Others (N=54)	p-value[1]
Age(years)				
< 58	32	6	26	0.068
≥ 58	29	1	28	
Gender				
Male	46	5	41	0.555
Female	15	2	13	
Tumor size				
T1-T2	27	1	26	0.096
T3-T4	34	6	28	
Lymph nodes				
N0	16	0	16	0.104
N+	45	7	38	
Distant metastasis				
M0	58	5	53	0.012
M+	2	2	0	
Missing	1		1	
Clinical stage				
I-II	8	0	8	0.353
III-IV	53	7	46	
Grade				
G1-G2	32	3	29	0.44
G3-G4	23	1	22	
Missing	6	3	3	
Alcohol				
Never-Former	10	0	10	0.265
Current	51	7	44	
Tobacco				
Never-Former	14	2	12	0.511
Current	47	5	42	
HPV				
Driven	11	1	10	0.602
Non-driven	47	6	41	
Missing	3		3	

[1] χ2test.

4.3.2 MYBBP1A^{low}pAKT(Ser473)^{high} staining pattern in primary tumors of OPSCC patients confers a poor prognosis

Next, the possibility was analyzed whether MYBBP1A^{low}pAKT(Ser473)^{high} expression could serve as a prognostic biomarker for OPSCC patients. The MYBBP1A^{low}pAKT(Ser473)^{high} expression score was compared with progression free survival (PFS) as well as overall survival (OS). Univariate Kaplan-Meier analysis revealed a significantly higher probability for patients with a MYBBP1A^{low}pAKT(Ser473)^{high} staining pattern to have shorter PFS (p=0.007) (Fig. 4.21A). Moreover, a significant correlation was found between the MYBBP1A^{low}pAKT(Ser473)^{high} expression score and a poor OS ($p<0.001$) as compared to patients with all other combination scores. In summary, this data suggested an inverse regulation of MYBBP1A and pAKT(Ser473) protein levels in the pathogenesis of OPSCC and that patients with MYBBP1A^{low}pAKT(Ser473)^{high} expression are at high risk for unfavorable clinical outcome.

4.3.3 MYBBP1A^{low}pAKT(Thr308)^{high} staining pattern was not associated with poor prognosis in OPSCC patients

It is worth mentioning that full activation of AKT requires phosphorylation at Thr308 and Ser473 by PDK1 and mTORC2, respectively (48). Therefore, primary OPSCC tumor samples were analyzed for pAKT Thr308 expression and scored as described above. PFS was calculated according to the stratification of patients with MYBBP1A^{low}pAKT(Thr308)^{high} staining (n=7) and all other combination patterns (n=47). No significant impact on patient outcome was observed (Fig. 4.22A). Also, the presence of MYBBP1A^{low}pAKT(Thr308)^{high} tumor cells within the tumor mass did not influence overall survival (Fig. 4.22B). Remarkably, significant correlations were only found considering AKT phosphorylation at Ser473 but not at Thr308, suggesting a more critical role of mTOR/AKT signaling for the clinical behavior of OPSCC patients with low MYBBP1A expression.

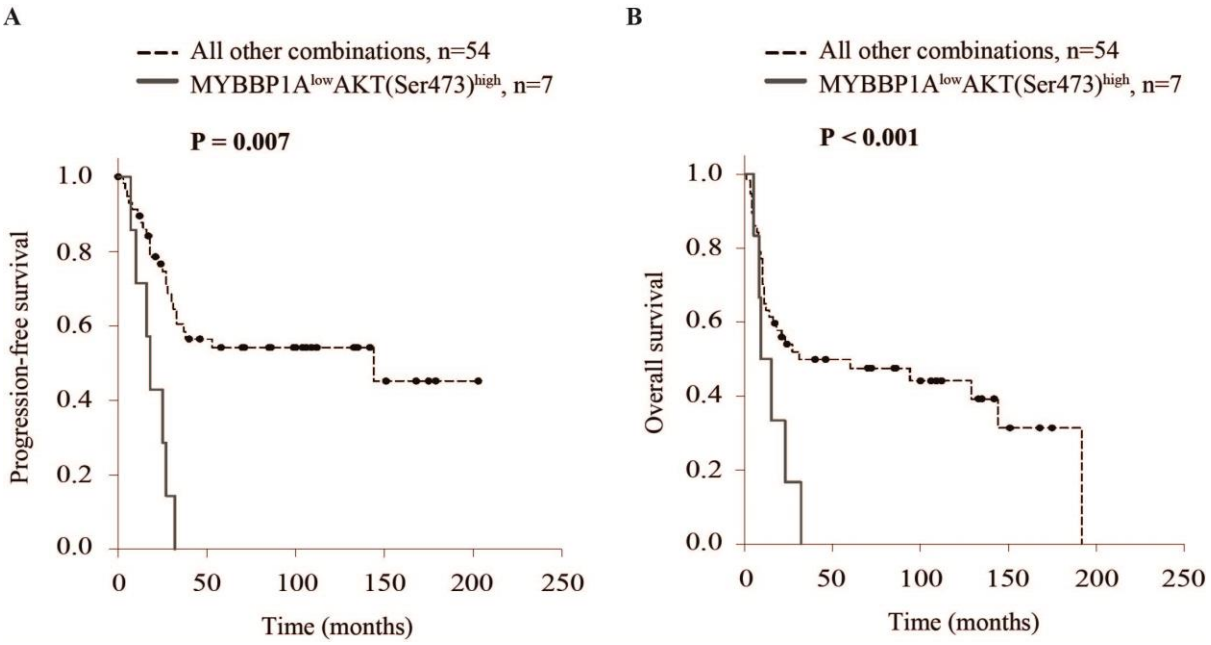

Figure 4.21: Inverse MYBBP1A expression and AKT (Ser473) phosphorylation is associated with unfavorable clinical outcome. Kaplan-Meier plot for progression-free (A) and overall survival (B) revealed that patients with low MYBBP1A expression but high levels of pAKT(Ser473) had a significantly reduced survival as compared to others.

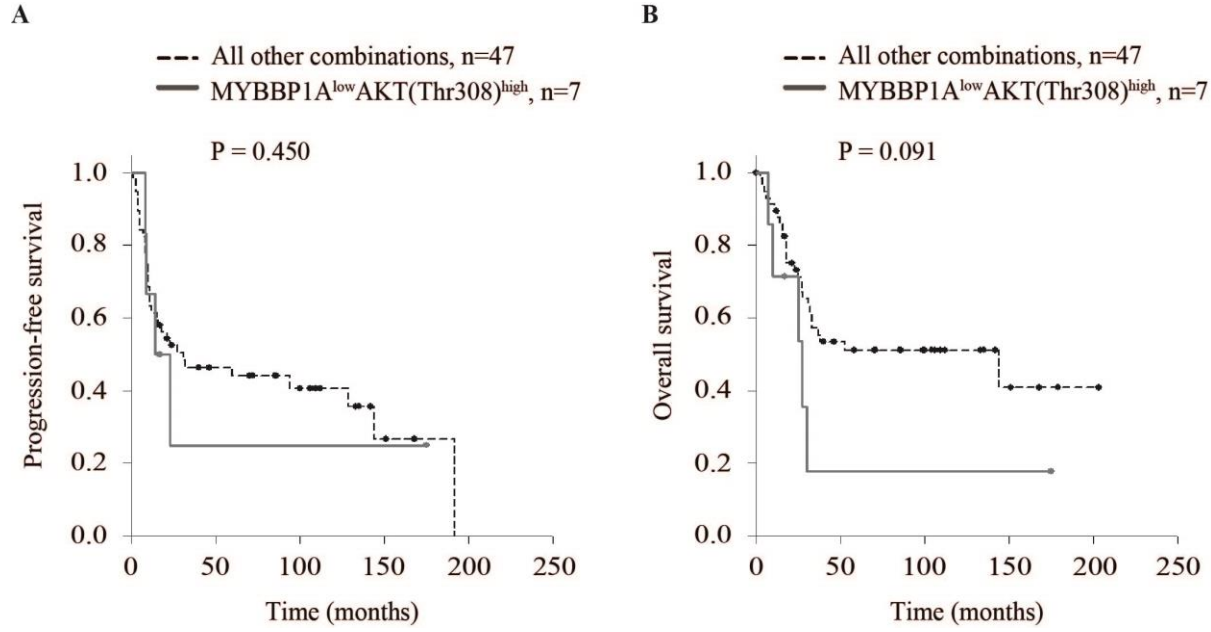

Figure 4.22: MYBBP1A^{low}pAKT(Thr308)^{high} does not serve as unfavorable risk factor in primary OPSCC patients. Kaplan-Meier plot for progression-free (A) and overall survival (B) according to low or high MYBBP1A and pAKT(Thr308) protein levels in primary tumors of OPSCC patients revealed no significant correlation with survival.

4.3.4 MYBBP1A^{low}pAKT(Ser473)^{high} staining pattern served as an independent risk factor for unfavorable clinical outcome of OPSCC patients

Prognostic significance was further evaluated by a multivariate Cox proportional hazard analysis (Table 4.2). Multivariate Cox regression including putative prognostic factors and the HPV status revealed a statistically significant association only for MYBBP1A^{low}pAKT(Ser473)^{high} with a higher risk for OPSCC related death (HR=7.10; 95% CI=1.85-27.24; p=0.03). These results demonstrated that a MYBBP1A^{low}pAKT^{high} staining pattern served as an independent risk factor for unfavorable clinical outcome of OPSCC patients.

Table 4.2: Multivariate analysis of overall survival for OPSCC patients according to the Cox proportional hazards model

Parameter	HR (95% CI)	p-value
Age		
<58 vs. >58	1.96(0.76-5.05)	0.16
Gender		
Female vs. Male	1.90(0.62-5.86)	0.26
Grade		
G3-G4 vs. G1-G2	0.65(0.23-1.81)	0.41
Clinical stage		
III-IV vs. I-II	2.91(0.52-16.24)	0.22
Alcohol		
Current vs. Never-Former	0.40(0.08-1.88)	0.25
Tobacco		
Current vs. Never-Former	1.40(0.40-4.90)	0.61
Tumor size		
T3/4 vs. T1/2	1.36(0.48-3.84)	0.56
Distant metastasis		
M+ vs. M0	4.32(0.24-77.11)	0.32
HPV status		
HPV Inactive vs. active	1.69(0.39-7.29)	0.49
MYBBP1A/AKT immunohistochemistry [a]		
MYBBP1A ^{low}/AKT(Ser473) ^{high} vs. Others	**7.10(1.85-27.24)**	**0.03**

Statistical analysis was done using SAS (9.2) software. Significant values are represented in bold
HR hazard ratio, CI confidence intervals

[a] Adjusted by age, gender, grade, clinical stage, tobacco/alcohol consumption, tumor size, distant-metastasis and HPV status. For all covariates, the validity of the proportional hazards assumption was tested with Schoenfeld residuals.

Discussion

5 Discussion

5.1 Loss of MYBBP1A expression is a common feature during DNA damage-induced senescence

MYBBP1A has been implicated in distinct biological functions such as cell proliferation, DNA damage and cell death. As such, research efforts have been focused on understanding the critical role of MYBBP1A in adult tissue function or homeostasis. However, the physiological function of MYBBP1A during senescence and the detailed mechanisms underlying these activities have yet to be elucidated. The goal and the scope of the present study were to identify the novel function of MYBBP1A in DNA damage-induced senescence.

Topoisomerase inhibitors such as etoposide are commonly used in anti-neoplastic therapy to induce DNA damage in tumor cells and to limit the propagation of damaged and stressed cells by cell cycle arrest or apoptosis (150, 151). It has also been shown that etoposide is able to induce senescence in normal human fibroblast, colon, ovarian and adenocarcinoma cell lines (136, 139). In line with this, the two human carcinoma cell lines FaDu and HeLa, which were used in this study, respond to etoposide by inducing cellular senescence. Our data are consistent with a model in which genotoxic DNA damage induces the activation of p21, which may sustain G2/M phase arrest as well as the formation of abnormally shaped giant cell and nuclei (139). In response to DNA damage, MYBBP1A first translocated from the nucleolus to the nucleoplasm and subsequently, its protein levels decreased in senescent cells (Fig. 5.1). This finding is in line with the studies by Kuroda et al. (69) and Yamauchi et al. (71), showing that stress signals which inhibit ribosomal biosynthesis induce nuclear disruption and lead to translocation of the nucleolar protein MYBBP1A into the nucleoplasm. However, this is the first study demonstrating that loss of MYBBP1A protein in the establishment of a senescent phenotype.

It is widely accepted that the p53 tumor suppressor protein is pivotal for the initiation and maintenance of senescence growth arrest (91, 152), mainly following its activation by the DNA damage response via ATM-mediated phosphorylation. Moreover, activated p53 triggers the expression of pro-senescence target genes such as p21, affecting several physiological and metabolic pathways responsible for the establishment of senescence (153). Interestingly it has been shown that MYBBP1A regulates p53 function by acetylation to induce cell cycle arrest and apoptosis (69). Several studies have shed light into this issue and have proven that under nucleolar stress MYBBP1A specifically interacts with nonacetylated lysine residues of p53 and induces its acetylation, which enables the effective p53-activating function (69, 79, 80). The fact that both FaDu and HeLa cell lines used in this study express no or only mutated p53 suggest that the regulation of MYBBP1A as well as its putative mode of action in senescence may be in a p53-independent manner. However, at the current state it cannot be ruled out that mutant p53 can also drive a senescence response to DNA damage (154). For example, a single mutation in p53, E177R, abolishes the apoptotic function of p53 while retaining control of cell cycle and senescence functions (155). Further investigation will be required to clarify this issue.

5.2 Silencing of MYBBP1A modulates the efficacy of genotoxic-induced senescence

A growing body of evidence indicates that deletion or down-regulation of MYBBP1A has a profound effect on the growth rate of cells by affecting the expression of several genes involved in cell cycle control, DNA damage and cell death (75, 83). Down-regulation of MYBBP1A was also reported to be involved in the transcriptional induction of $p21^{CDKN1A}$ by a p53-independent mechanism (75). Evidently, primary mouse embryonic fibroblast (MEFs) from MYBBP1A knockout mice showed a rapid entry into senescence (75). Therefore, the effect of MYBBP1A silencing on senescence was investigated in tumor cells. Although, a significant decrease in the number of BrdU positive cells was observed following MYBBP1A depletion, it has no direct effect on the induction of senescence markers such as $p21^{CDKN1A}$ and SA-β-gal staining tested. However, silencing of MYBBP1A under stress conditions resulted in an increase in the relative amount of SA-β-gal positive cells as well as SASP factors, although the expression of $p21^{CDKN1A}$

did not change. Based on these observations, it was tempting to hypothesize that translocation and further loss of MYBBP1A expression following DNA damage are not necessary to trigger the senescence program but modulates its efficacy.

MYBBP1A was demonstrated as an important repressor of NFκB dependent transcription, by competing with the co-activator p300 for interaction with RelA/p65 (78). Several publications also pointed to the nuclear accumulation of p65 upon etoposide treatment accompanied by the stimulation of serine-536 phosphorylation, indicating transcriptionally active RelA/NFκB (156-158). Indeed, we observed pRelA/p65 nuclear staining in tissue sections of primary OPSCC patients with low MYBBP1A protein expression (data not shown). In response to DNA damage NFκB activation conferred induction of SASP by influencing the expression of NFκB target genes (141, 159, 160). Similar results have been reported in which NFκB inhibition by either genetic depletion or a pharmacological inhibitor attenuates SASP and delays DNA damage-induced senescence (161, 162). However, we cannot rule out the possibility that the observed increase in SASP in FaDu cells with silenced MYBBP1A expression reflects the relative abundance of senescent cells post treatment rather than a direct influence on NFκB activity.

To demonstrate a causal link between MYBBP1A ablation and DNA damage-induced senescence, we aimed to revert the senescent phenotype by ectopic overexpression of a stable amino-terminal variant of MYBBP1A (p67) in HeLa cells. Compared to the full-length MYBBP1A protein (p160), p67 lacks the C-terminal region containing the nucleolar localization sequence (68). Interestingly, it has been shown that the nucleolar full-length protein stimulates ribosome biogenesis and that the translocation of MYBBP1A from the nucleolus to the nucleoplasm upon ribosome stress plays an important role to block cell cycle progression by suppressing c-Myb target genes (71). Furthermore, an increasing number of studies report the important role of the nucleolus in cell cycle regulation and senescence (163, 164). Accordingly, expression analysis of markers of senescence and proliferation following etoposide treatment revealed severely diminished SA-β-gal activity and increased proliferation in the HeLa-MYBBP1A (p67) cells, while nuclear γH2AX staining and p21 induction were unaltered compared to mock controls. These results strongly suggest that in response to stress signals, translocation and abrogation of MYBBP1A plays an important role in cellular senescence.

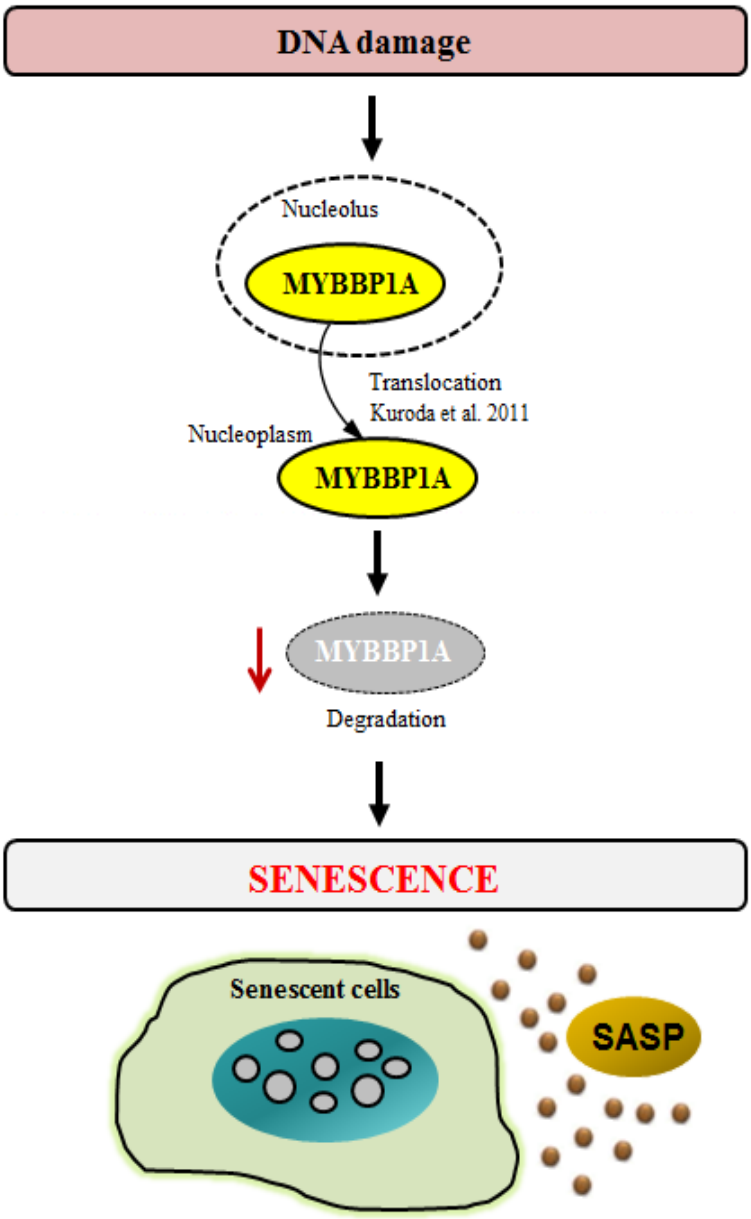

Figure 5.1: Schematic model for the critical role of MYBBP1A in the establishment of senescence induced by DNA damage. Proposed model for the regulation and function of MYBBP1A in DNA damage-induced senescence. In response to DNA damage, MYBBP1A first translocates from the nucleolus to the nucleoplasm. Loss of MYBBP1A expression was not sufficient to trigger senescence, but modulates the efficacy of a genotoxic-induced senescence. Relative abundance of senescent cells could also contribute to accelerate the availability of SASP factors.

5.3 Inverse regulation of MYBBP1A and AKT phosphorylation resembles a senescent like phenotype

The RAS-PI3K-AKT signaling pathway is one of the major mediators of cellular survival/apoptosis determinant. In the context of persistent DNA damage, sustained activation of the AKT pathway alleviates cellular stress and ultimately, promotes cellular survival by mechanisms involving the regulation of anti-apoptotic proteins such as Bcl-2 and Bcl-xl (144, 165). Multiple lines of evidence also indicate that constitutive activation of PI3K/AKT signaling leads to the accumulation of reactive oxygen species followed by an irreversible proliferation arrest (senescence) via a p53/p21-dependent pathway (166, 167). Moreover, activation of this pathway through PTEN loss, overexpression or activating mutation of PI3K (PI3KCA) and overexpression of AKT can trigger oncogene-induced senescence (OIS) in primary murine fibroblasts and multiple lines of cultured endothelial cells (88, 114, 167, 168). Together, these emerging evidences point to a pivotal role of PI3K/AKT signaling cascade during DNA damage-induced senescence. In line with these findings, our data showed that etoposide treatment induces the phosphorylation of AKT along with the loss of MYBBP1A expression.

In light of increasing evidence that posttranslational mechanisms, including ubiquitination and proteasomal degradation, regulate MYBBP1A protein stability by a not yet fully understood molecular mechanism (66, 71), it is tempting to speculate that activation AKT might encounter a critical function for MYBBP1A. To examine the role of AKT activation on the down-regulation of MYBBP1A protein levels, FaDu cells were treated with etoposide in the presence or absence of Triciribine, a potent inhibitor of AKT activity (169). However, inhibition of AKT had no major impact on the MYBBP1A protein levels upon etoposide treatment. Conversely, no difference in pAKT(Ser473) levels were seen between FaDu cells transfected with either control or MYBBP1A-specific siRNA. In summary, these data demonstrated that loss of MYBBP1A in combination with increased pAKT(Ser473) levels represents a characteristic feature of genotoxic induced senescence of tumor cells, but questioned a direct causal link. Interestingly, inhibition of PI3K pathway by LY294002 after etoposide treatment stabilizes the expression of MYBBP1A without influencing the AKT activity. This is most likely due to the fact that LY294002 is also a potent inhibitor of other kinases implicated in DNA stress response, such as DNA-PK, ATM,

and ATR (170). The finding that, inhibition of PI3K was not sufficient to repress AKT protein can be explained by a possible scenario where activation of receptor signaling in cells exposed to this inhibitor activates PI3K as well as parallel pathways by physiologic feedback inhibition of the other components of the signaling network (171, 172). Accordingly, other signaling cascades might be responsible for the loss of MYBBP1A upon DNA damage. A recent study demonstrates that Tripeptidyl-peptidase II (TPPII) interacts with MYBBP1A and the cell cycle regulator CDK2 that is involved in the regulation of cell cycle, apoptosis and senescence (173). It is worth noting that MYBBP1A has been linked to mitosis and DNA damage responses, since MYBBP1A was identified as a novel substrate for Aurora B kinase (81) and cell-cycle checkpoint kinase 1 (CHK1) (174). Interestingly, MYBBP1A is phosphorylated by Aurora B kinase (81) and inhibition of Aurora kinases is associated with senescence (175). This suggests a possible functional role of Aurora B kinase or CHK1 in the regulation of MYBBP1A stability during genotoxic induced senescence, which needs to be addressed by functional studies in the future.

OIS by aberrant activation of PI3K/AKT signaling was earlier described as a tumor-suppressing defense response that restricts the progression of benign lesion to malignancy *in vivo* (114). However, Damsky et al. (176) demonstrated that instead of mediating senescence, activation of the PI3K/AKT pathway abrogates senescence induction by $BRAF^{V600E}$ and allows resumption of proliferation. Mouse models have shown that *Cdkn2a* loss primes a subset of growth-arrested $Braf^{V600E}$ nevi is involved in melanoma development, and along with PI3K/mTOR/AKT activation, may encourage tumorogenesis (113, 177, 178). These observations are in agreement with another study, which has also shown that *Pten* inactivation and PI3K activation in senescent nevi can rapidly induce murine cancers (179). In this respect, the cell culture experiments of the present work would suggest that under conditions of DNA damage, activation of AKT signaling is critical in mediating the bypass of senescence, leading to the question of whether our results represent a pre-senescence or post-senescence phenotype. The assumption that the activation of PI3K pathway represents a post-senescent phenotype that regains the capacity to proliferate is further underscored by findings on the senescence features in SCC-25 cells. Even though, under normal condition SCC-25 showed several features of senescence in addition to $MYBBP1A^{low}pAKT^{high}$ protein levels, SA-β-gal activity was not detectable. To this point, next-generation sequencing (NGS) analysis of HNSCC cell lines revealed *TP53*, *CDKN2A* and

PIK3CA mutations in SCC-25 (180). This observation is in accordance with prior work suggesting that activation of the PI3K/AKT pathway due to *Pten* deletion and loss of TGF-β signaling pathway in HNSCC cell lines, results in cancer progression through cellular senescence evasion (53). It is worth noting that the PTEN/PI3K/AKT pathway is the most frequently altered signaling node in head and neck cancer and have critical roles in driving tumor growth and proliferation (53, 181). Together, these results suggest that SCC-25 represent a bona fide *in vitro* model for post-senescence, where loss of MYBBP1A and PI3K/AKT activation results in bypassing senescence and resumes cancer progression, presumably in the setting of additional stochastic events. Nonetheless, these findings have implications for the molecular pathogenesis of precursor to cancer progression with regard to senescence, a topic with significance for therapy.

5.4 MYBBP1A^{low}pAKT(Ser473)^{high} staining pattern serves as a promising biomarker for OPSCC patients at high risk for treatment failure

The *in vitro* experiments demonstrate a causal link between loss of MYBBP1A and the establishment of a senescent phenotype after etoposide treatment. Moreover, the data clearly shows that an inverse regulation of MYBBP1A and AKT phosphorylation on Ser473 is a characteristic feature of senescent tumor cells. To gain further insight into the clinical relevance of these findings, MYBBP1A expression and AKT phosphorylation patterns were investigated on tumor sections of primary OPSCC. The staining pattern was compared with clinical and histopathological features, but revealed no significant correlation except for distant metastasis. The relevance of this finding was hampered by the small number of patients in the cohort with distant metastasis. Additional retrospective and prospective studies using tumor samples of larger patient cohorts will be needed to support the association between MYBBP1A^{low}pAKT(Ser473)^{high} staining and clinical as well as pathological features.

Considering that Akt activation is a significant prognostic indicator for oral squamous cell carcinoma (182, 183), it is also conceivable to postulate that in the clinical setting a

MYBBP1A^{low}pAKT(S473)^{high} has a prognostic value and might stratify patients at high risk for treatment failure. The presented data that a MYBBP1A^{low}pAKT(S473)^{high} staining pattern is significantly correlated with poor PFS and OS strongly supports this assumption and suggests that the presence of cells with a senescent-like phenotype can be used as a promising biomarker for OPSCC patients. Strikingly, significant correlations were only found considering AKT phosphorylation at S473 but not at T308, suggesting a more critical role of mTOR/AKT signaling for the clinical behavior of OPSCC patients with low MYBBP1A expression. In line with this data, the clinical benefit of targeting PDK1, the upstream kinase of AKT (Thr308) phosphorylation, was limited in HNSCC (184). Indeed, there are several lines of evidence suggesting that pAkt accumulation and PTEN down-regulation detected in HNSCC contributes to malignant progression from normal epithelium to dysplasia and then to infiltrating carcinoma (181, 182, 185). Owing to the pronounced activity of mTOR/AKT signaling in surgical margins of HNSCC patients, AKT activation has been found to be an independent risk factor for recurrence and second primary tumors (186). Likewise, the activation of downstream components of PI3K signaling is associated with a worse clinical outcome as shown for patients with lung, colon and esophageal adenocarcinomas (187-189). While, most studies assign pro-tumorigenic and pro-metastatic function to PI3K/AKT/mTOR pathway by regulating cell growth, survival, angiogenesis and therapy resistance (190, 191), many recent studies also report senescence associated adverse effects (53, 167, 192).

In summary, the presented data clearly indicates that OPSCC patients with a MYBBP1A^{low}pAKT^{high} staining pattern have a poor clinical outcome, which might be due at least in part to the presence of senescent tumor cells (Fig. 5.2). In this context, it is worth noting that most of the patients in the retrospective cohort of OPSCC patients were treated with first-line or adjuvant radiotherapy. Radiation exerts its anticancer effects primarily by inducing DNA double-strand breaks and activation of DNA damage response, subsequently resulting in therapy-induced cellular senescence (TCS) (193). Several studies support the premise that a subset of tumor cells might eventually overcome senescence and regain clonogenic potential, thus drive the genesis of malignancy, leading to tumor recurrence (194-198). Tumor cells in a state of prolonged TCS will have a continuing impact on therapy outcomes because of their SASP activity, which may actually promote growth and progression of surviving tumor cells (199). Moreover, the PI3K/AKT/mTOR pathway has been implicated in therapeutic resistance and was

identified as a suitable drug target in HNSCC (51, 200, 201). In accordance with these reports, an improved clonogenic survival of MYBBP1A depleted FaDu cells after irradiation was demonstrated by a CFA assay, which could at least in part contribute to treatment failure of tumors enriched with the presence of MYBBP1A^{low}pAKT^{high} tumor cells. An equal if not greater concern is that in several studies the emergent cells from the TCS phenotype were often characterized as highly malignant and/or therapy resistant tumor cells (193, 202, 203). In support of this assumption, SCC-25 cells characterized by MYBBP1A^{low}pAKT^{high} expression showed resistance towards etoposide treatment. These data further underscore the initial assumption that loss of MYBBP1A and PI3K activation results in bypassing senescence and resume cancer progression in SCC-25 cells. It will be interesting to investigate how stabilization of MYBBP1A changes behavior of SCC-25 cells upon treatment with genotoxic stimuli and might sensitize these cells towards etoposide or irradiation.

5.5 Relevance of the senescent phenotype in cancer progression and treatment strategies

There have been many experimentally derived lines of evidence to support the concept that senescence may have evolved to initially protect humans against the formation of early onset cancers. Moreover a series of studies identified senescence markers in several paraneoplastic lesions, both in humans and in mice (110, 111, 113, 114). Furthermore, loss of tumor suppressors, such as PTEN, RB1, neurofibromin 1 (NF1) and inositol polyphosphate-4-phosphatase, typeII (INPP4B) appear to initiate senescence in premalignant tumors (89, 114, 204, 205). Thus, it is conceivable that, in premalignant cells the engagement of senescence halted further progression; the frequency of overtly malignant tumors indicates that many cells either do not have fully active senescence programs or develop bypass mechanisms to regain proliferation capabilities.

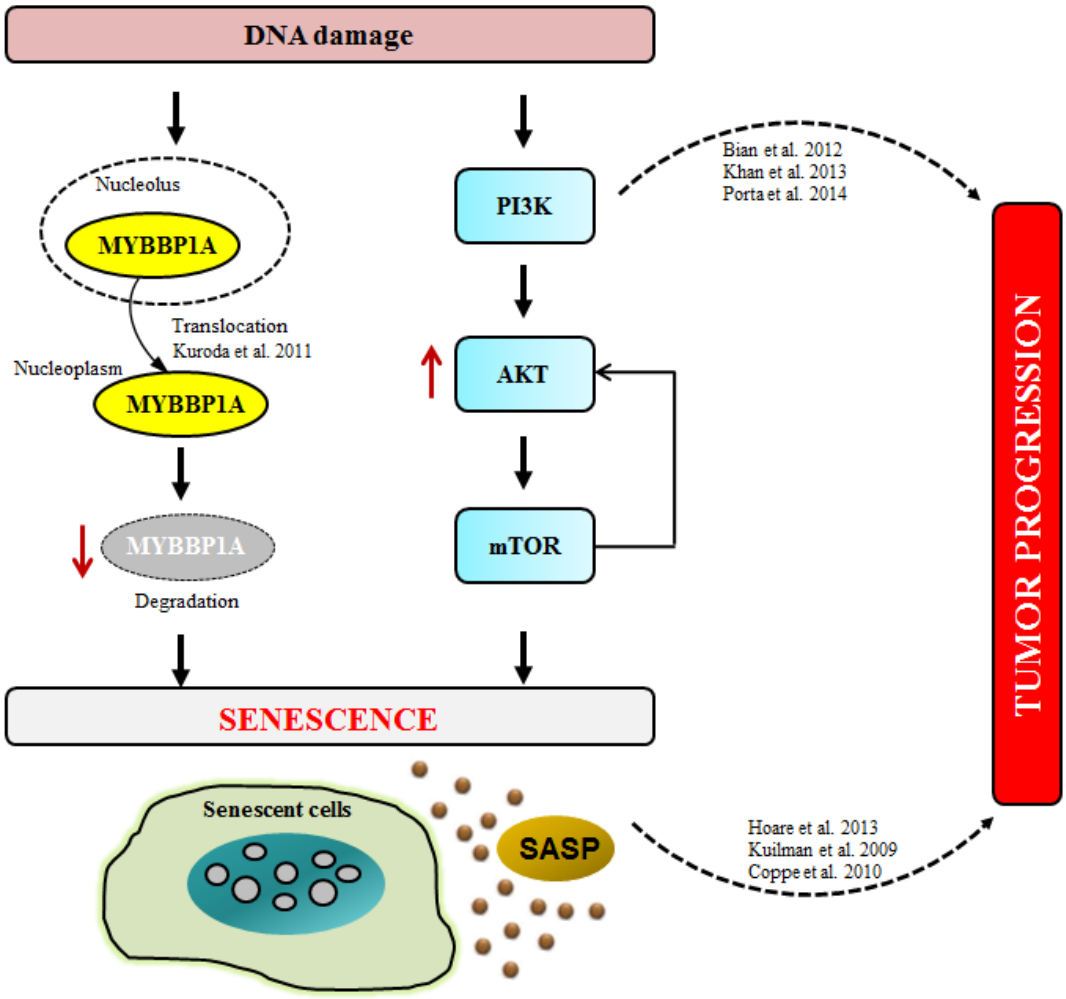

Figure 5.2: Schematic model for the inverse regulation of MYBBP1A and PI3K-mTOR-AKT signaling pathways in the establishment of senescence and tumor progression. Inverse regulation of MYBBP1A and AKT(Ser473) phosphorylation is a characteristic feature of senescent tumor cells. Moreover, the presented results suggest a more critical role of the mTOR/AKT pathway for the poor clinical outcome of patients with low MYBBP1A levels. A direct link between the induction of senescence and radioresistance has been proposed previously and is most likely due to tumor cell survival and growth by paracrine action of SASP factors.

Several of the earliest studies looked at the role of two major tumor suppressors, p53 and RB1 and found that following inactivation, cells were able to bypass senescence after being challenged with DNA damage (206, 207). Furthermore, other investigators found that the disruption of p21 and p16 expression promotes the reversal of the senescent phenotype (208, 209). Additional findings suggest that RAS and BRAF mutations acquired by the immortal cells may trigger an alternative mechanism contributing to the evasion of senescence (177, 210). The

investigators further showed that subsets of tumor cells emerge from a senescent state were more resistant to chemotherapeutics than the parental cells (211). This is further complicated by the fact that senescent cells still appear to be metabolically active retaining the potential to secrete paracrine acting factors. Thus during the course of tumorigenesis, senescence escape can be facilitated by the proinflammatory signature of the SASP factors (108). Moreover, increasing evidence, particularly from sophisticated mouse models show that in the context of a malignancy, senescent cells actively communicate with neighboring cells and the extracellular matrix through SASP factors, which can facilitate cellular proliferation and tumorigenesis (108, 212). For example, secreted pro-inflammatory factors such as VEGF, GRO1, IL-6 and IL-8 enhance invasion and induce an epithelial to mesenchymal transition in carcinoma cells, a phenotype shown to be resistant to chemotherapy and radiation (128, 140, 213, 214). Accordingly, xenotransplantation of senescent cells with pre-malignant cells was shown to facilitate the proliferation and invasiveness of mouse and human epithelial tumor cells in immunocompromised mice (130, 131, 215, 216).

In solid tumors, the treatment with chemotherapeutics and ionizing radiation has been shown to induce the senescent phenotype (217, 218). This has been verified in evaluations of lung, prostate and breast carcinoma patients receiving neoadjuvant therapy, which revealed a marked increase in the expression of senescence markers in the resected tumors (128, 139, 194). There have been an increasing number of reports across several cancer types indicating that senescence is associated with a poor therapeutic index to cancer therapeutics. The regimens currently used to apply anti-cancer therapeutics represent an ideal scenario for microenvironment damage responses-resulting in senescence to promote resistance. This observation appears consistent with a previous study using malignant pleural mesothelioma. In this study chemotherapy resistance was described in patients whose tumors showed evidence of senescence while a substantially higher apoptosis rate was observed in the subset of patients that did not exhibit a change in senescence markers (219). Furthermore, an induction of tumor cell senescence following neoadjuvant therapy was associated with a poor clinical outcome (219). In line with this data, Waldman and coworkers described increased clonogenic growth in the presence of irradiation-arrested bystander cells (220). Thus, the adverse consequences of senescence during the malignant progression appears to be consistent with the presented results, demonstrating that DNA damaging agents induce senescence phenotypes marked by a $MYBBP1A^{low}pAKT^{high}$

staining pattern critically contributing to poor clinical outcomes, most likely due to the treatment failure and growth by paracrine action of SASP factors. Our current knowledge firmly centered on the concept that the presence of senescent cells in malignant tumors may have adverse consequences in a clinical setting and careful individualized medical indications need to be considered when targeting senescence effectors for cancer therapy.

In the future new therapeutic strategies to enhance senescent cell clearance in malignant tumors should be tested to improve the clinical outcome. Therefore, it is worth speculating that interference with MYBBP1A and PI3K/mTOR/AKT pathways will be beneficial for improving the clinical outcome of HNSCC patients. Currently, inhibitors specifically targeting PI3K/mTOR/AKT pathways are in clinical trials against a variety of different advanced cancers (51, 200, 221). However, it is still uncertain which tumors are more likely to respond to this kind of targeted therapy. Nevertheless, a follow-up study will be required to determine the impact of restoration of MYBBP1A on the potential of reverting senescent cells back to their normal functioning state. In light of the present data in which PI3K inhibitor (LY294002) has been found to restore MYBBP1A expression by an unknown mechanism, the use of PI3K inhibitors are already in the clinical trials for treating HNSCC patients in conjunction with chemotherapy or cetuximab (31). The clinical benefit of these drugs might be due to the rescue of pre-/post-senescent cells from their fate. Accordingly, AKT inhibitors and the mTOR inhibitors rapamycin, everolimus and temsirolimus are being assessed for HNSCC at the phase II stage in neoadjuvant and recurrent/metastatic settings (31).

As such, there are a number of other therapeutic avenues of research that have the potential to eliminate senescent cells or prevent their accumulation, and reconstitution of effective senescence surveillance is one of them. In support of this concept, a recent study found that injection of PolyI:C, was able to facilitate the elimination of senescent cells in fibrotic liver (119). However, robust stimulation of the immune system in aged individuals should be taken with caution, since it might be able to refuel the already existing systemic inflammation. Of note, apart from the elimination of senescent cells, drugs which can modulate SASP or the upstream regulators such as p38 MAP kinase and NFκB to reduce inflammation could also be beneficial to eliminate the adverse activities of senescent cells. For example, inhibiting NFκB signaling was resulted in suppression of the SASP phenotype and enhancement of tumor response to

chemotherapy in a mouse model of lymphoma (161). Alternative strategies could be the design of pharmacological compounds that can specially induce programmed cell death in senescent cells or block the road to senescence following neoadjuvant therapy. This will provide an effective means for elimination of senescent cells regardless of the reason for their presence. However, such a drug is not yet available; still some existing compounds like mTOR inhibitors and Sirt6 activators might produce a similar outcome and might be of-high-interest to purse in the following years (222, 223). Several reports have suggested that restoring the activity of tumor suppressor protein p53 by low-molecular-weight compounds to promote the immune mediated clearance and targeted interference of $p16^{Ink4a}$ gene to selectively remove the senescent cells via drug induced apoptosis could also be used as an attractive and powerful approach (108, 224, 225). In addition senescence immunotherapy using senescence associated antigens, which would be specific enough to allow efficient recognition of senescent cells could be much more effective preventing its deleterious effects. However, it would also be necessary to investigate how each of these strategies affects the beneficial role of senescent cells in wound healing or pathological as well as physiological conditions. Interestingly, change in life style including avoidance of damaging agents like cigarettes and UV-light, caloric restriction and physical exercise were reported to affect prevalence of senescent cells in tissues (226). Accordingly, the outcome of anticancer therapy is not only determined by the quantitative effect on cancer cells forced to irreversibly exit the cell cycle but may also depend on novel capabilities acquired by senescence cells. Thus, understanding the circumstances under which these responses are triggered will be important for the development of personalized medicine.

5.6 Conclusion and Perspectives

In summary, the present work provides experimental evidence for the existence of a MYBBP1A^{low}pAKT(Ser473)^{high} phenotype in the onset and maintenance of senescence induced by genotoxic stress. In accordance with published reports, our data confirmed intracellular translocation and subsequent degradation of MYBBP1A in response to DNA damage. But for the first time we demonstrated a causal link between the loss of MYBBP1A and the establishment of a senescent phenotype after etoposide treatment. It is worth noting that silencing of MYBBP1A was not sufficient to trigger senescence in tumor cell lines, but it modulated the efficacy of genotoxic-induced senescence and augmented resistance to irradiation. Interestingly a direct link between the induction of senescence and radioresistance has been proposed previously and is most likely due to tumor cell survival and growth by paracrine action of SASP factors. Although, the precise molecular mechanism by which MYBBP1A regulates DNA damage induced senescence remains elusive and warrants further investigation, our study revealed an inverse regulation of MYBBP1A and AKT(Ser473) phosphorylation as a characteristic feature of senescent tumor cells. Moreover, the presence of MYBBP1A^{low}pAKT(Ser473)^{high} staining pattern serves as a promising biomarker for OPSCC patients at high-risk for treatment failure. Remarkably a significant correlation with progression-free or overall survival was not found considering pAKT(Thr308) levels, suggesting a more critical role of the mTOR/AKT pathway for the clinical behavior of OPSCCs with low MYBBP1A levels. This data proposes a model (Fig. 5.3) in which tumor cells with a MYBBP1A^{low} but pAkt(Ser473)^{high} protein pattern have a senescent-like phenotype and might critically contribute to tumor progression due to the emergence of highly malignant and/or therapy resistant tumor cells. Indeed, our data demonstrated that SCC-25 cells represent a bona fide *in vitro* model for malignant and invasive tumor cells, where loss of MYBBP1A and PI3K/AKT activation results in bypassing senescence and resume cancer progression, presumably in the setting of additional stochastic events. According to this data, additional markers to define pre-/post-senescence phenotypes would be an interesting starting point for further studies.

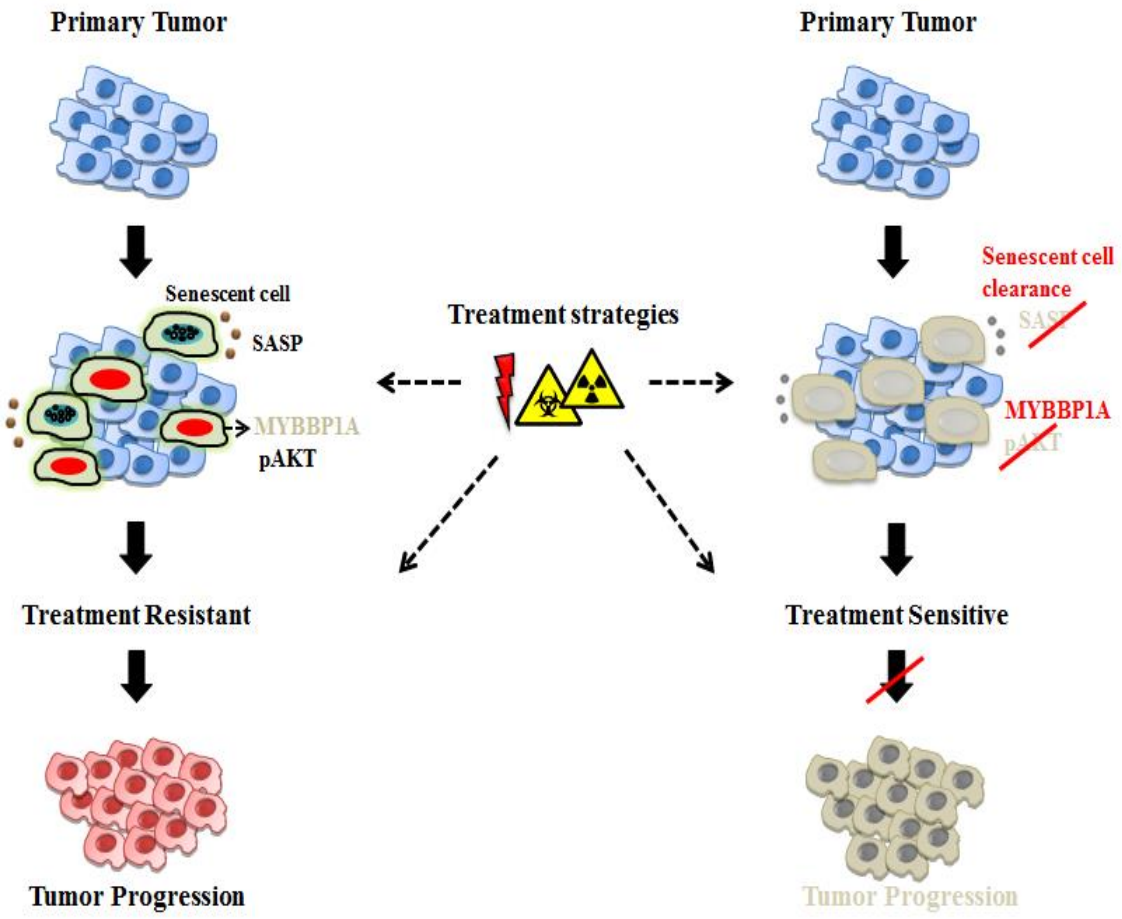

Figure 5.3: Schematic model of the novel MYBBP1A and PI3K/AKT cascade in HNSCC. Left panel: Model for attenuation of MYBBP1A and AKT phosphorylation following genotoxic stress promotes tumor progression due to a higher resistance to therapy and secretion of SASP factors. Right panel: Restoration of MYBBP1A protein or pharmacological inhibition of PI3K/mTOR/AKT pathway is an attractive new concept to eliminate the senescent cells, thus sensitize tumor cells for available treatment options resulting in better outcome for patients.

Altogether, this new data represents significant progress in our understanding of how the presence of senescent cells in malignant tumors are associated with a poor therapeutic index and provides a strong rationale for cancer therapeutics that prevents senescence by-pass, as emergent cells appear to have highly drug resistant phenotypes. Thus, the restoration of MYBBP1A function or the pharmacological inhibition of the PI3K/mTOR/AKT pathway is an attractive new concept to sensitize tumor cells for available treatment options, but also to establish new strategies for targeted therapy with the potential of elimination of senescent cells. Moreover, the obtained data strongly suggests that the abundance of MYBBP1A^{low}pAKT(Ser473)^{high} senescent

tumor cells in primary tumors, but also following tumor relapse, could serve as a reliable biomarker for treatment decision making and to stratify HNSCC patients at high risk for treatment failure. This might also be of clinical relevance for other human malignancies with similar etiology and treatment options. However, a better understanding of the underlying molecular principles with regard to the regulation and function of MYBBP1A and appropriate preclinical model systems resembling the complexity of the tumor tissue architecture are urgently needed. Despite the role of MYBBP1A in early embryogenesis, a critical function in adult tissue function or homeostasis has not been demonstrated yet. In this regard, the identification of MYBBP1A-dependent gene regulatory networks in cellular senescence could potentially open up new routes to identify a suitable druggable target other than MYBBP1A itself. Thus, potential therapeutic interventions could be combined with new strategies to facilitate the elimination of senescent cells as a novel avenue for treatment of malignant cancers and health span extension.

Bibliography

6 Bibliography

1. Friedman JM, Stavas MJ, Cmelak AJ. Clinical and scientific impact of human papillomavirus on head and neck cancer. World journal of clinical oncology. 2014;5(4):781-91.
2. Jemal A, Bray F, Center MM, Ferlay J, Ward E, Forman D. Global cancer statistics. CA: a cancer journal for clinicians. 2011;61(2):69-90.
3. Mehanna H, Paleri V, West CM, Nutting C. Head and neck cancer--Part 1: Epidemiology, presentation, and prevention. Bmj. 2010;341:c4684.
4. Kim L, King T, Agulnik M. Head and neck cancer: changing epidemiology and public health implications. Oncology. 2010;24(10):915-9, 24.
5. Mathers CD, Loncar D. Projections of global mortality and burden of disease from 2002 to 2030. PLoS medicine. 2006;3(11):e442.
6. Conway DI, Petticrew M, Marlborough H, Berthiller J, Hashibe M, Macpherson LM. Socioeconomic inequalities and oral cancer risk: a systematic review and meta-analysis of case-control studies. International journal of cancer Journal international du cancer. 2008;122(12):2811-9.
7. Hashibe M, Brennan P, Chuang SC, Boccia S, Castellsague X, Chen C, et al. Interaction between tobacco and alcohol use and the risk of head and neck cancer: pooled analysis in the International Head and Neck Cancer Epidemiology Consortium. Cancer epidemiology, biomarkers & prevention : a publication of the American Association for Cancer Research, cosponsored by the American Society of Preventive Oncology. 2009;18(2):541-50.
8. Chaturvedi AK, Engels EA, Anderson WF, Gillison ML. Incidence trends for human papillomavirus-related and -unrelated oral squamous cell carcinomas in the United States. Journal of clinical oncology : official journal of the American Society of Clinical Oncology. 2008;26(4):612-9.
9. Chaturvedi AK, Anderson WF, Lortet-Tieulent J, Curado MP, Ferlay J, Franceschi S, et al. Worldwide trends in incidence rates for oral cavity and oropharyngeal cancers. Journal of clinical oncology : official journal of the American Society of Clinical Oncology. 2013;31(36):4550-9.
10. Fakhry C, Westra WH, Li S, Cmelak A, Ridge JA, Pinto H, et al. Improved survival of patients with human papillomavirus-positive head and neck squamous cell carcinoma in a prospective clinical trial. Journal of the National Cancer Institute. 2008;100(4):261-9.
11. Kutler DI, Auerbach AD, Satagopan J, Giampietro PF, Batish SD, Huvos AG, et al. High incidence of head and neck squamous cell carcinoma in patients with Fanconi anemia. Archives of otolaryngology--head & neck surgery. 2003;129(1):106-12.
12. Marur S, Forastiere AA. Head and neck cancer: changing epidemiology, diagnosis, and treatment. Mayo Clinic proceedings. 2008;83(4):489-501.
13. Taghavi N, Yazdi I. Type of food and risk of oral cancer. Archives of Iranian medicine. 2007;10(2):227-32.
14. Leemans CR, Braakhuis BJ, Brakenhoff RH. The molecular biology of head and neck cancer. Nature reviews Cancer. 2011;11(1):9-22.
15. Pai SI, Westra WH. Molecular pathology of head and neck cancer: implications for diagnosis, prognosis, and treatment. Annual review of pathology. 2009;4:49-70.
16. Deshpande AM, Wong DT. Molecular mechanisms of head and neck cancer. Expert review of anticancer therapy. 2008;8(5):799-809.
17. Hanahan D, Weinberg RA. The hallmarks of cancer. Cell. 2000;100(1):57-70.
18. Negrini S, Gorgoulis VG, Halazonetis TD. Genomic instability--an evolving hallmark of cancer. Nature reviews Molecular cell biology. 2010;11(3):220-8.
19. Poeta ML, Manola J, Goldwasser MA, Forastiere A, Benoit N, Califano JA, et al. TP53 mutations and survival in squamous-cell carcinoma of the head and neck. The New England journal of medicine. 2007;357(25):2552-61.

20. Boyle JO, Hakim J, Koch W, van der Riet P, Hruban RH, Roa RA, et al. The incidence of p53 mutations increases with progression of head and neck cancer. Cancer research. 1993;53(19):4477-80.
21. Brennan JA, Boyle JO, Koch WM, Goodman SN, Hruban RH, Eby YJ, et al. Association between cigarette smoking and mutation of the p53 gene in squamous-cell carcinoma of the head and neck. The New England journal of medicine. 1995;332(11):712-7.
22. Brown CJ, Lain S, Verma CS, Fersht AR, Lane DP. Awakening guardian angels: drugging the p53 pathway. Nature reviews Cancer. 2009;9(12):862-73.
23. Millon R, Muller D, Schultz I, Salvi R, Ghnassia JP, Frebourg T, et al. Loss of MDM2 expression in human head and neck squamous cell carcinomas and clinical significance. Oral oncology. 2001;37(8):620-31.
24. Vogelstein B, Lane D, Levine AJ. Surfing the p53 network. Nature. 2000;408(6810):307-10.
25. Scheffner M, Werness BA, Huibregtse JM, Levine AJ, Howley PM. The E6 oncoprotein encoded by human papillomavirus types 16 and 18 promotes the degradation of p53. Cell. 1990;63(6):1129-36.
26. Agrawal N, Frederick MJ, Pickering CR, Bettegowda C, Chang K, Li RJ, et al. Exome sequencing of head and neck squamous cell carcinoma reveals inactivating mutations in NOTCH1. Science. 2011;333(6046):1154-7.
27. Stransky N, Egloff AM, Tward AD, Kostic AD, Cibulskis K, Sivachenko A, et al. The mutational landscape of head and neck squamous cell carcinoma. Science. 2011;333(6046):1157-60.
28. Schache AG, Liloglou T, Risk JM, Filia A, Jones TM, Sheard J, et al. Evaluation of human papilloma virus diagnostic testing in oropharyngeal squamous cell carcinoma: sensitivity, specificity, and prognostic discrimination. Clinical cancer research : an official journal of the American Association for Cancer Research. 2011;17(19):6262-71.
29. Smeets SJ, Braakhuis BJ, Abbas S, Snijders PJ, Ylstra B, van de Wiel MA, et al. Genome-wide DNA copy number alterations in head and neck squamous cell carcinomas with or without oncogene-expressing human papillomavirus. Oncogene. 2006;25(17):2558-64.
30. Cabelguenne A, Blons H, de Waziers I, Carnot F, Houllier AM, Soussi T, et al. p53 alterations predict tumor response to neoadjuvant chemotherapy in head and neck squamous cell carcinoma: a prospective series. Journal of clinical oncology : official journal of the American Society of Clinical Oncology. 2000;18(7):1465-73.
31. Suh Y, Amelio I, Guerrero Urbano T, Tavassoli M. Clinical update on cancer: molecular oncology of head and neck cancer. Cell death & disease. 2014;5:e1018.
32. Rothenberg SM, Ellisen LW. The molecular pathogenesis of head and neck squamous cell carcinoma. The Journal of clinical investigation. 2012;122(6):1951-7.
33. Weng AP, Ferrando AA, Lee W, Morris JPt, Silverman LB, Sanchez-Irizarry C, et al. Activating mutations of NOTCH1 in human T cell acute lymphoblastic leukemia. Science. 2004;306(5694):269-71.
34. Talora C, Sgroi DC, Crum CP, Dotto GP. Specific down-modulation of Notch1 signaling in cervical cancer cells is required for sustained HPV-E6/E7 expression and late steps of malignant transformation. Genes & development. 2002;16(17):2252-63.
35. Yugawa T, Handa K, Narisawa-Saito M, Ohno S, Fujita M, Kiyono T. Regulation of Notch1 gene expression by p53 in epithelial cells. Molecular and cellular biology. 2007;27(10):3732-42.
36. Dotto GP. Crosstalk of Notch with p53 and p63 in cancer growth control. Nature reviews Cancer. 2009;9(8):587-95.
37. Sharafinski ME, Ferris RL, Ferrone S, Grandis JR. Epidermal growth factor receptor targeted therapy of squamous cell carcinoma of the head and neck. Head & neck. 2010;32(10):1412-21.
38. Temam S, Kawaguchi H, El-Naggar AK, Jelinek J, Tang H, Liu DD, et al. Epidermal growth factor receptor copy number alterations correlate with poor clinical outcome in patients with head and neck squamous cancer. Journal of clinical oncology : official journal of the American Society of Clinical Oncology. 2007;25(16):2164-70.
39. Loeffler-Ragg J, Witsch-Baumgartner M, Tzankov A, Hilbe W, Schwentner I, Sprinzl GM, et al. Low incidence of mutations in EGFR kinase domain in Caucasian patients with head and neck squamous cell carcinoma. European journal of cancer. 2006;42(1):109-11.

40. Hynes NE, Lane HA. ERBB receptors and cancer: the complexity of targeted inhibitors. Nature reviews Cancer. 2005;5(5):341-54.
41. Saranath D, Chang SE, Bhoite LT, Panchal RG, Kerr IB, Mehta AR, et al. High frequency mutation in codons 12 and 61 of H-ras oncogene in chewing tobacco-related human oral carcinoma in India. British journal of cancer. 1991;63(4):573-8.
42. Lin SY, Makino K, Xia W, Matin A, Wen Y, Kwong KY, et al. Nuclear localization of EGF receptor and its potential new role as a transcription factor. Nature cell biology. 2001;3(9):802-8.
43. Engelman JA. Targeting PI3K signalling in cancer: opportunities, challenges and limitations. Nature reviews Cancer. 2009;9(8):550-62.
44. Liu P, Cheng H, Roberts TM, Zhao JJ. Targeting the phosphoinositide 3-kinase pathway in cancer. Nature reviews Drug discovery. 2009;8(8):627-44.
45. Franke TF. PI3K/Akt: getting it right matters. Oncogene. 2008;27(50):6473-88.
46. Sarbassov DD, Guertin DA, Ali SM, Sabatini DM. Phosphorylation and regulation of Akt/PKB by the rictor-mTOR complex. Science. 2005;307(5712):1098-101.
47. Liu P, Begley M, Michowski W, Inuzuka H, Ginzberg M, Gao D, et al. Cell-cycle-regulated activation of Akt kinase by phosphorylation at its carboxyl terminus. Nature. 2014;508(7497):541-5.
48. Liu P, Wang Z, Wei W. Phosphorylation of Akt at the C-terminal tail triggers Akt Activation. Cell cycle. 2014;13(14):2162-4.
49. Iglesias-Bartolome R, Martin D, Gutkind JS. Exploiting the head and neck cancer oncogenome: widespread PI3K-mTOR pathway alterations and novel molecular targets. Cancer discovery. 2013;3(7):722-5.
50. Luo J, Manning BD, Cantley LC. Targeting the PI3K-Akt pathway in human cancer: rationale and promise. Cancer cell. 2003;4(4):257-62.
51. Bussink J, van der Kogel AJ, Kaanders JH. Activation of the PI3-K/AKT pathway and implications for radioresistance mechanisms in head and neck cancer. The lancet oncology. 2008;9(3):288-96.
52. Psyrri A, Seiwert TY, Jimeno A. Molecular pathways in head and neck cancer: EGFR, PI3K, and more. American Society of Clinical Oncology educational book / ASCO American Society of Clinical Oncology Meeting. 2013:246-55.
53. Bian Y, Hall B, Sun ZJ, Molinolo A, Chen W, Gutkind JS, et al. Loss of TGF-beta signaling and PTEN promotes head and neck squamous cell carcinoma through cellular senescence evasion and cancer-related inflammation. Oncogene. 2012;31(28):3322-32.
54. Gallo O, Franchi A, Magnelli L, Sardi I, Vannacci A, Boddi V, et al. Cyclooxygenase-2 pathway correlates with VEGF expression in head and neck cancer. Implications for tumor angiogenesis and metastasis. Neoplasia. 2001;3(1):53-61.
55. Mineta H, Miura K, Ogino T, Takebayashi S, Misawa K, Ueda Y, et al. Prognostic value of vascular endothelial growth factor (VEGF) in head and neck squamous cell carcinomas. British journal of cancer. 2000;83(6):775-81.
56. Koontongkaew S, Amornphimoltham P, Monthanpisut P, Saensuk T, Leelakriangsak M. Fibroblasts and extracellular matrix differently modulate MMP activation by primary and metastatic head and neck cancer cells. Medical oncology. 2012;29(2):690-703.
57. Squarize CH, Castilho RM, Sriuranpong V, Pinto DS, Jr., Gutkind JS. Molecular cross-talk between the NFkappaB and STAT3 signaling pathways in head and neck squamous cell carcinoma. Neoplasia. 2006;8(9):733-46.
58. Argiris A, Karamouzis MV, Raben D, Ferris RL. Head and neck cancer. Lancet. 2008;371(9625):1695-709.
59. Chaturvedi AK, Engels EA, Pfeiffer RM, Hernandez BY, Xiao W, Kim E, et al. Human papillomavirus and rising oropharyngeal cancer incidence in the United States. Journal of clinical oncology : official journal of the American Society of Clinical Oncology. 2011;29(32):4294-301.

60. Boscolo-Rizzo P, Maronato F, Marchiori C, Gava A, Da Mosto MC. Long-term quality of life after total laryngectomy and postoperative radiotherapy versus concurrent chemoradiotherapy for laryngeal preservation. The Laryngoscope. 2008;118(2):300-6.
61. Sahu N, Grandis JR. New advances in molecular approaches to head and neck squamous cell carcinoma. Anti-cancer drugs. 2011;22(7):656-64.
62. Slaughter DP, Southwick HW, Smejkal W. Field cancerization in oral stratified squamous epithelium; clinical implications of multicentric origin. Cancer. 1953;6(5):963-8.
63. Tabor MP, Brakenhoff RH, van Houten VM, Kummer JA, Snel MH, Snijders PJ, et al. Persistence of genetically altered fields in head and neck cancer patients: biological and clinical implications. Clinical cancer research : an official journal of the American Association for Cancer Research. 2001;7(6):1523-32.
64. Braakhuis BJ, Tabor MP, Kummer JA, Leemans CR, Brakenhoff RH. A genetic explanation of Slaughter's concept of field cancerization: evidence and clinical implications. Cancer research. 2003;63(8):1727-30.
65. Behren A, Kamenisch Y, Muehlen S, Flechtenmacher C, Haberkorn U, Hilber H, et al. Development of an oral cancer recurrence mouse model after surgical resection. International journal of oncology. 2010;36(4):849-55.
66. Acuna Sanhueza GA, Faller L, George B, Koffler J, Misetic V, Flechtenmacher C, et al. Opposing function of MYBBP1A in proliferation and migration of head and neck squamous cell carcinoma cells. BMC cancer. 2012;12:72.
67. Favier D, Gonda TJ. Detection of proteins that bind to the leucine zipper motif of c-Myb. Oncogene. 1994;9(1):305-11.
68. Tavner FJ, Simpson R, Tashiro S, Favier D, Jenkins NA, Gilbert DJ, et al. Molecular cloning reveals that the p160 Myb-binding protein is a novel, predominantly nucleolar protein which may play a role in transactivation by Myb. Molecular and cellular biology. 1998;18(2):989-1002.
69. Kuroda T, Murayama A, Katagiri N, Ohta YM, Fujita E, Masumoto H, et al. RNA content in the nucleolus alters p53 acetylation via MYBBP1A. The EMBO journal. 2011;30(6):1054-66.
70. Hochstatter J, Holzel M, Rohrmoser M, Schermelleh L, Leonhardt H, Keough R, et al. Myb-binding protein 1a (Mybbp1a) regulates levels and processing of pre-ribosomal RNA. The Journal of biological chemistry. 2012;287(29):24365-77.
71. Yamauchi T, Keough RA, Gonda TJ, Ishii S. Ribosomal stress induces processing of Mybbp1a and its translocation from the nucleolus to the nucleoplasm. Genes to cells : devoted to molecular & cellular mechanisms. 2008;13(1):27-39.
72. Keough RA, Macmillan EM, Lutwyche JK, Gardner JM, Tavner FJ, Jans DA, et al. Myb-binding protein 1a is a nucleocytoplasmic shuttling protein that utilizes CRM1-dependent and independent nuclear export pathways. Experimental cell research. 2003;289(1):108-23.
73. Fan M, Rhee J, St-Pierre J, Handschin C, Puigserver P, Lin J, et al. Suppression of mitochondrial respiration through recruitment of p160 myb binding protein to PGC-1alpha: modulation by p38 MAPK. Genes & development. 2004;18(3):278-89.
74. Diaz VM, Mori S, Longobardi E, Menendez G, Ferrai C, Keough RA, et al. p160 Myb-binding protein interacts with Prep1 and inhibits its transcriptional activity. Molecular and cellular biology. 2007;27(22):7981-90.
75. Mori S, Bernardi R, Laurent A, Resnati M, Crippa A, Gabrieli A, et al. Myb-Binding Protein 1A (MYBBP1A) Is Essential for Early Embryonic Development, Controls Cell Cycle and Mitosis, and Acts as a Tumor Suppressor. PloS one. 2012;7(10):e39723.
76. Hara Y, Onishi Y, Oishi K, Miyazaki K, Fukamizu A, Ishida N. Molecular characterization of Mybbp1a as a co-repressor on the Period2 promoter. Nucleic acids research. 2009;37(4):1115-26.
77. Jones LC, Okino ST, Gonda TJ, Whitlock JP, Jr. Myb-binding protein 1a augments AhR-dependent gene expression. The Journal of biological chemistry. 2002;277(25):22515-9.
78. Owen HR, Elser M, Cheung E, Gersbach M, Kraus WL, Hottiger MO. MYBBP1a is a novel repressor of NF-kappaB. Journal of molecular biology. 2007;366(3):725-36.

79. Kumazawa T, Nishimura K, Kuroda T, Ono W, Yamaguchi C, Katagiri N, et al. Novel nucleolar pathway connecting intracellular energy status with p53 activation. The Journal of biological chemistry. 2011;286(23):20861-9.
80. Ono W, Akaogi K, Waku T, Kuroda T, Yokoyama W, Hayashi Y, et al. Nucleolar protein, Myb-binding protein 1A, specifically binds to nonacetylated p53 and efficiently promotes transcriptional activation. Biochemical and biophysical research communications. 2013;434(3):659-63.
81. Perrera C, Colombo R, Valsasina B, Carpinelli P, Troiani S, Modugno M, et al. Identification of Myb-binding protein 1A (MYBBP1A) as a novel substrate for aurora B kinase. The Journal of biological chemistry. 2010;285(16):11775-85.
82. Blasius M, Forment JV, Thakkar N, Wagner SA, Choudhary C, Jackson SP. A phospho-proteomic screen identifies substrates of the checkpoint kinase Chk1. Genome biology. 2011;12(8):R78.
83. Akaogi K, Ono W, Hayashi Y, Kishimoto H, Yanagisawa J. MYBBP1A suppresses breast cancer tumorigenesis by enhancing the p53 dependent anoikis. BMC cancer. 2013;13:65.
84. Hayflick L, Moorhead PS. The serial cultivation of human diploid cell strains. Experimental cell research. 1961;25:585-621.
85. Harley CB, Futcher AB, Greider CW. Telomeres shorten during ageing of human fibroblasts. Nature. 1990;345(6274):458-60.
86. Serrano M, Lin AW, McCurrach ME, Beach D, Lowe SW. Oncogenic ras provokes premature cell senescence associated with accumulation of p53 and p16INK4a. Cell. 1997;88(5):593-602.
87. Zhu J, Woods D, McMahon M, Bishop JM. Senescence of human fibroblasts induced by oncogenic Raf. Genes & development. 1998;12(19):2997-3007.
88. Alimonti A, Nardella C, Chen Z, Clohessy JG, Carracedo A, Trotman LC, et al. A novel type of cellular senescence that can be enhanced in mouse models and human tumor xenografts to suppress prostate tumorigenesis. The Journal of clinical investigation. 2010;120(3):681-93.
89. Courtois-Cox S, Genther Williams SM, Reczek EE, Johnson BW, McGillicuddy LT, Johannessen CM, et al. A negative feedback signaling network underlies oncogene-induced senescence. Cancer cell. 2006;10(6):459-72.
90. Young AP, Schlisio S, Minamishima YA, Zhang Q, Li L, Grisanzio C, et al. VHL loss actuates a HIF-independent senescence programme mediated by Rb and p400. Nature cell biology. 2008;10(3):361-9.
91. Campisi J, d'Adda di Fagagna F. Cellular senescence: when bad things happen to good cells. Nature reviews Molecular cell biology. 2007;8(9):729-40.
92. Collado M, Blasco MA, Serrano M. Cellular senescence in cancer and aging. Cell. 2007;130(2):223-33.
93. Kuilman T, Michaloglou C, Mooi WJ, Peeper DS. The essence of senescence. Genes & development. 2010;24(22):2463-79.
94. Toussaint O, Medrano EE, von Zglinicki T. Cellular and molecular mechanisms of stress-induced premature senescence (SIPS) of human diploid fibroblasts and melanocytes. Experimental gerontology. 2000;35(8):927-45.
95. Ben-Porath I, Weinberg RA. The signals and pathways activating cellular senescence. The international journal of biochemistry & cell biology. 2005;37(5):961-76.
96. van Deursen JM. The role of senescent cells in ageing. Nature. 2014;509(7501):439-46.
97. Campisi J. Senescent cells, tumor suppression, and organismal aging: good citizens, bad neighbors. Cell. 2005;120(4):513-22.
98. Pawlikowski JS, Adams PD, Nelson DM. Senescence at a glance. Journal of cell science. 2013;126(Pt 18):4061-7.
99. Aliouat-Denis CM, Dendouga N, Van den Wyngaert I, Goehlmann H, Steller U, van de Weyer I, et al. p53-independent regulation of p21Waf1/Cip1 expression and senescence by Chk2. Molecular cancer research : MCR. 2005;3(11):627-34.

100. Chen WS, Yu YC, Lee YJ, Chen JH, Hsu HY, Chiu SJ. Depletion of securin induces senescence after irradiation and enhances radiosensitivity in human cancer cells regardless of functional p53 expression. International journal of radiation oncology, biology, physics. 2010;77(2):566-74.
101. Burton DG, Krizhanovsky V. Physiological and pathological consequences of cellular senescence. Cellular and molecular life sciences : CMLS. 2014;71(22):4373-86.
102. Munoz-Espin D, Serrano M. Cellular senescence: from physiology to pathology. Nature reviews Molecular cell biology. 2014;15(7):482-96.
103. Munoz-Espin D, Canamero M, Maraver A, Gomez-Lopez G, Contreras J, Murillo-Cuesta S, et al. Programmed cell senescence during mammalian embryonic development. Cell. 2013;155(5):1104-18.
104. Dimri GP, Lee X, Basile G, Acosta M, Scott G, Roskelley C, et al. A biomarker that identifies senescent human cells in culture and in aging skin in vivo. Proceedings of the National Academy of Sciences of the United States of America. 1995;92(20):9363-7.
105. Rodier F, Campisi J. Four faces of cellular senescence. The Journal of cell biology. 2011;192(4):547-56.
106. Campisi J. Cellular senescence: putting the paradoxes in perspective. Current opinion in genetics & development. 2011;21(1):107-12.
107. Freund A, Laberge RM, Demaria M, Campisi J. Lamin B1 loss is a senescence-associated biomarker. Molecular biology of the cell. 2012;23(11):2066-75.
108. Coppe JP, Desprez PY, Krtolica A, Campisi J. The senescence-associated secretory phenotype: the dark side of tumor suppression. Annual review of pathology. 2010;5:99-118.
109. Freund A, Patil CK, Campisi J. p38MAPK is a novel DNA damage response-independent regulator of the senescence-associated secretory phenotype. The EMBO journal. 2011;30(8):1536-48.
110. Braig M, Lee S, Loddenkemper C, Rudolph C, Peters AH, Schlegelberger B, et al. Oncogene-induced senescence as an initial barrier in lymphoma development. Nature. 2005;436(7051):660-5.
111. Collado M, Gil J, Efeyan A, Guerra C, Schuhmacher AJ, Barradas M, et al. Tumour biology: senescence in premalignant tumours. Nature. 2005;436(7051):642.
112. Collado M, Serrano M. Senescence in tumours: evidence from mice and humans. Nature reviews Cancer. 2010;10(1):51-7.
113. Michaloglou C, Vredeveld LC, Soengas MS, Denoyelle C, Kuilman T, van der Horst CM, et al. BRAFE600-associated senescence-like cell cycle arrest of human naevi. Nature. 2005;436(7051):720-4.
114. Chen Z, Trotman LC, Shaffer D, Lin HK, Dotan ZA, Niki M, et al. Crucial role of p53-dependent cellular senescence in suppression of Pten-deficient tumorigenesis. Nature. 2005;436(7051):725-30.
115. Coppe JP, Patil CK, Rodier F, Krtolica A, Beausejour CM, Parrinello S, et al. A human-like senescence-associated secretory phenotype is conserved in mouse cells dependent on physiological oxygen. PloS one. 2010;5(2):e9188.
116. Schmitt CA, Fridman JS, Yang M, Lee S, Baranov E, Hoffman RM, et al. A senescence program controlled by p53 and p16INK4a contributes to the outcome of cancer therapy. Cell. 2002;109(3):335-46.
117. Xue W, Zender L, Miething C, Dickins RA, Hernando E, Krizhanovsky V, et al. Senescence and tumour clearance is triggered by p53 restoration in murine liver carcinomas. Nature. 2007;445(7128):656-60.
118. Hoenicke L, Zender L. Immune surveillance of senescent cells--biological significance in cancer- and non-cancer pathologies. Carcinogenesis. 2012;33(6):1123-6.
119. Krizhanovsky V, Yon M, Dickins RA, Hearn S, Simon J, Miething C, et al. Senescence of activated stellate cells limits liver fibrosis. Cell. 2008;134(4):657-67.
120. Jun JI, Lau LF. Cellular senescence controls fibrosis in wound healing. Aging. 2010;2(9):627-31.
121. Storer M, Mas A, Robert-Moreno A, Pecoraro M, Ortells MC, Di Giacomo V, et al. Senescence is a developmental mechanism that contributes to embryonic growth and patterning. Cell. 2013;155(5):1119-30.
122. Adams PD. Healing and hurting: molecular mechanisms, functions, and pathologies of cellular senescence. Molecular cell. 2009;36(1):2-14.

123. Campisi J. Aging, cellular senescence, and cancer. Annual review of physiology. 2013;75:685-705.
124. Janzen V, Forkert R, Fleming HE, Saito Y, Waring MT, Dombkowski DM, et al. Stem-cell ageing modified by the cyclin-dependent kinase inhibitor p16INK4a. Nature. 2006;443(7110):421-6.
125. Krishnamurthy J, Ramsey MR, Ligon KL, Torrice C, Koh A, Bonner-Weir S, et al. p16INK4a induces an age-dependent decline in islet regenerative potential. Nature. 2006;443(7110):453-7.
126. Baker DJ, Wijshake T, Tchkonia T, LeBrasseur NK, Childs BG, van de Sluis B, et al. Clearance of p16Ink4a-positive senescent cells delays ageing-associated disorders. Nature. 2011;479(7372):232-6.
127. Brack AS, Conboy MJ, Roy S, Lee M, Kuo CJ, Keller C, et al. Increased Wnt signaling during aging alters muscle stem cell fate and increases fibrosis. Science. 2007;317(5839):807-10.
128. Coppe JP, Patil CK, Rodier F, Sun Y, Munoz DP, Goldstein J, et al. Senescence-associated secretory phenotypes reveal cell-nonautonomous functions of oncogenic RAS and the p53 tumor suppressor. PLoS biology. 2008;6(12):2853-68.
129. Liu Y, El-Naggar S, Darling DS, Higashi Y, Dean DC. Zeb1 links epithelial-mesenchymal transition and cellular senescence. Development. 2008;135(3):579-88.
130. Krtolica A, Parrinello S, Lockett S, Desprez PY, Campisi J. Senescent fibroblasts promote epithelial cell growth and tumorigenesis: a link between cancer and aging. Proceedings of the National Academy of Sciences of the United States of America. 2001;98(21):12072-7.
131. Liu D, Hornsby PJ. Senescent human fibroblasts increase the early growth of xenograft tumors via matrix metalloproteinase secretion. Cancer research. 2007;67(7):3117-26.
132. Ono W, Hayashi Y, Yokoyama W, Kuroda T, Kishimoto H, Ito I, et al. The nucleolar protein Myb-binding protein 1A (MYBBP1A) enhances p53 tetramerization and acetylation in response to nucleolar disruption. The Journal of biological chemistry. 2014;289(8):4928-40.
133. Roesch Ely M, Nees M, Karsai S, Magele I, Bogumil R, Vorderwulbecke S, et al. Transcript and proteome analysis reveals reduced expression of calgranulins in head and neck squamous cell carcinoma. European journal of cell biology. 2005;84(2-3):431-44.
134. Holzinger D, Schmitt M, Dyckhoff G, Benner A, Pawlita M, Bosch FX. Viral RNA patterns and high viral load reliably define oropharynx carcinomas with active HPV16 involvement. Cancer research. 2012;72(19):4993-5003.
135. Koffler J, Holzinger D, Sanhueza GA, Flechtenmacher C, Zaoui K, Lahrmann B, et al. Submaxillary gland androgen-regulated protein 3A expression is an unfavorable risk factor for the survival of oropharyngeal squamous cell carcinoma patients after surgery. European archives of oto-rhino-laryngology : official journal of the European Federation of Oto-Rhino-Laryngological Societies. 2013;270(4):1493-500.
136. Michishita E, Nakabayashi K, Ogino H, Suzuki T, Fujii M, Ayusawa D. DNA topoisomerase inhibitors induce reversible senescence in normal human fibroblasts. Biochemical and biophysical research communications. 1998;253(3):667-71.
137. Leontieva OV, Blagosklonny MV. DNA damaging agents and p53 do not cause senescence in quiescent cells, while consecutive re-activation of mTOR is associated with conversion to senescence. Aging. 2010;2(12):924-35.
138. Yang J, Bogni A, Schuetz EG, Ratain M, Dolan ME, McLeod H, et al. Etoposide pathway. Pharmacogenetics and genomics. 2009;19(7):552-3.
139. te Poele RH, Okorokov AL, Jardine L, Cummings J, Joel SP. DNA damage is able to induce senescence in tumor cells in vitro and in vivo. Cancer research. 2002;62(6):1876-83.
140. Hoare M, Narita M. Transmitting senescence to the cell neighbourhood. Nature cell biology. 2013;15(8):887-9.
141. Rovillain E, Mansfield L, Caetano C, Alvarez-Fernandez M, Caballero OL, Medema RH, et al. Activation of nuclear factor-kappa B signalling promotes cellular senescence. Oncogene. 2011;30(20):2356-66.
142. Yu Z, Weinberger PM, Sasaki C, Egleston BL, Speier WFt, Haffty B, et al. Phosphorylation of Akt (Ser473) predicts poor clinical outcome in oropharyngeal squamous cell cancer. Cancer

epidemiology, biomarkers & prevention : a publication of the American Association for Cancer Research, cosponsored by the American Society of Preventive Oncology. 2007;16(3):553-8.
143. Hodkinson PS, Elliott T, Wong WS, Rintoul RC, Mackinnon AC, Haslett C, et al. ECM overrides DNA damage-induced cell cycle arrest and apoptosis in small-cell lung cancer cells through beta1 integrin-dependent activation of PI3-kinase. Cell death and differentiation. 2006;13(10):1776-88.
144. Jeon SJ, Seo JE, Yang SI, Choi JW, Wells D, Shin CY, et al. Cellular stress-induced up-regulation of FMRP promotes cell survival by modulating PI3K-Akt phosphorylation cascades. Journal of biomedical science. 2011;18:17.
145. Liu SQ, Yu JP, Yu HG, Lv P, Chen HL. Activation of Akt and ERK signalling pathways induced by etoposide confer chemoresistance in gastric cancer cells. Digestive and liver disease : official journal of the Italian Society of Gastroenterology and the Italian Association for the Study of the Liver. 2006;38(5):310-8.
146. Wu HM, Chi KH, Lin WW. Proteasome inhibitors stimulate activator protein-1 pathway via reactive oxygen species production. FEBS letters. 2002;526(1-3):101-5.
147. Skinner HD, Sandulache VC, Ow TJ, Meyn RE, Yordy JS, Beadle BM, et al. TP53 disruptive mutations lead to head and neck cancer treatment failure through inhibition of radiation-induced senescence. Clinical cancer research : an official journal of the American Association for Cancer Research. 2012;18(1):290-300.
148. Chuang HC, Yang LP, Fitzgerald AL, Osman A, Woo SH, Myers JN, et al. The p53-reactivating small molecule RITA induces senescence in head and neck cancer cells. PloS one. 2014;9(8):e104821.
149. Cahu J, Bustany S, Sola B. Senescence-associated secretory phenotype favors the emergence of cancer stem-like cells. Cell death & disease. 2012;3:e446.
150. Pommier Y, Leteurtre F, Fesen MR, Fujimori A, Bertrand R, Solary E, et al. Cellular determinants of sensitivity and resistance to DNA topoisomerase inhibitors. Cancer investigation. 1994;12(5):530-42.
151. Pommier Y, Tanizawa A, Kohn KW. Mechanisms of topoisomerase I inhibition by anticancer drugs. Advances in pharmacology. 1994;29B:73-92.
152. Rufini A, Tucci P, Celardo I, Melino G. Senescence and aging: the critical roles of p53. Oncogene. 2013;32(43):5129-43.
153. Vousden KH, Prives C. Blinded by the Light: The Growing Complexity of p53. Cell. 2009;137(3):413-31.
154. Brady CA, Jiang D, Mello SS, Johnson TM, Jarvis LA, Kozak MM, et al. Distinct p53 transcriptional programs dictate acute DNA-damage responses and tumor suppression. Cell. 2011;145(4):571-83.
155. Khoo KH, Verma CS, Lane DP. Drugging the p53 pathway: understanding the route to clinical efficacy. Nature reviews Drug discovery. 2014;13(3):217-36.
156. Brzostek-Racine S, Gordon C, Van Scoy S, Reich NC. The DNA damage response induces IFN. Journal of immunology. 2011;187(10):5336-45.
157. Morotti A, Cilloni D, Pautasso M, Messa F, Arruga F, Defilippi I, et al. NF-kB inhibition as a strategy to enhance etoposide-induced apoptosis in K562 cell line. American journal of hematology. 2006;81(12):938-45.
158. Campbell KJ, Witty JM, Rocha S, Perkins ND. Cisplatin mimics ARF tumor suppressor regulation of RelA (p65) nuclear factor-kappaB transactivation. Cancer research. 2006;66(2):929-35.
159. Janssens S, Tschopp J. Signals from within: the DNA-damage-induced NF-kappaB response. Cell death and differentiation. 2006;13(5):773-84.
160. Rodier F, Coppe JP, Patil CK, Hoeijmakers WA, Munoz DP, Raza SR, et al. Persistent DNA damage signalling triggers senescence-associated inflammatory cytokine secretion. Nature cell biology. 2009;11(8):973-9.
161. Chien Y, Scuoppo C, Wang X, Fang X, Balgley B, Bolden JE, et al. Control of the senescence-associated secretory phenotype by NF-kappaB promotes senescence and enhances chemosensitivity. Genes & development. 2011;25(20):2125-36.

162. Tilstra JS, Robinson AR, Wang J, Gregg SQ, Clauson CL, Reay DP, et al. NF-kappaB inhibition delays DNA damage-induced senescence and aging in mice. The Journal of clinical investigation. 2012;122(7):2601-12.
163. Sherr CJ, Weber JD. The ARF/p53 pathway. Current opinion in genetics & development. 2000;10(1):94-9.
164. Visintin R, Amon A. The nucleolus: the magician's hat for cell cycle tricks. Current opinion in cell biology. 2000;12(6):752.
165. Vivanco I, Sawyers CL. The phosphatidylinositol 3-Kinase AKT pathway in human cancer. Nature reviews Cancer. 2002;2(7):489-501.
166. Astle MV, Hannan KM, Ng PY, Lee RS, George AJ, Hsu AK, et al. AKT induces senescence in human cells via mTORC1 and p53 in the absence of DNA damage: implications for targeting mTOR during malignancy. Oncogene. 2012;31(15):1949-62.
167. Xu Y, Li N, Xiang R, Sun P. Emerging roles of the p38 MAPK and PI3K/AKT/mTOR pathways in oncogene-induced senescence. Trends in biochemical sciences. 2014;39(6):268-76.
168. Engelman JA, Luo J, Cantley LC. The evolution of phosphatidylinositol 3-kinases as regulators of growth and metabolism. Nature reviews Genetics. 2006;7(8):606-19.
169. Wang Q, Ding H, Liu B, Li SH, Li P, Ge H, et al. Addition of the Akt inhibitor triciribine overcomes antibody resistance in cells from ErbB2/Neu-positive/PTEN-deficient mammary tumors. International journal of oncology. 2014;44(4):1277-83.
170. Fukuchi K, Watanabe H, Tomoyasu S, Ichimura S, Tatsumi K, Gomi K. Phosphatidylinositol 3-kinase inhibitors, Wortmannin or LY294002, inhibited accumulation of p21 protein after gamma-irradiation by stabilization of the protein. Biochimica et biophysica acta. 2000;1496(2-3):207-20.
171. Will M, Qin AC, Toy W, Yao Z, Rodrik-Outmezguine V, Schneider C, et al. Rapid induction of apoptosis by PI3K inhibitors is dependent upon their transient inhibition of RAS-ERK signaling. Cancer discovery. 2014;4(3):334-47.
172. Britschgi A, Andraos R, Brinkhaus H, Klebba I, Romanet V, Muller U, et al. JAK2/STAT5 inhibition circumvents resistance to PI3K/mTOR blockade: a rationale for cotargeting these pathways in metastatic breast cancer. Cancer cell. 2012;22(6):796-811.
173. Nahalkova J, Tomkinson B. TPPII, MYBBP1A and CDK2 form a protein-protein interaction network. Archives of biochemistry and biophysics. 2014;564:128-35.
174. Carrassa L, Damia G. Unleashing Chk1 in cancer therapy. Cell cycle. 2011;10(13):2121-8.
175. Liu Y, Hawkins OE, Su Y, Vilgelm AE, Sobolik T, Thu YM, et al. Targeting aurora kinases limits tumour growth through DNA damage-mediated senescence and blockade of NF-kappaB impairs this drug-induced senescence. EMBO molecular medicine. 2013;5(1):149-66.
176. Damsky W, Micevic G, Meeth K, Muthusamy V, Curley DP, Santhanakrishnan M, et al. mTORC1 activation blocks BrafV600E-induced growth arrest but is insufficient for melanoma formation. Cancer cell. 2015;27(1):41-56.
177. Dhomen N, Reis-Filho JS, da Rocha Dias S, Hayward R, Savage K, Delmas V, et al. Oncogenic Braf induces melanocyte senescence and melanoma in mice. Cancer cell. 2009;15(4):294-303.
178. Kennedy AL, Morton JP, Manoharan I, Nelson DM, Jamieson NB, Pawlikowski JS, et al. Activation of the PIK3CA/AKT pathway suppresses senescence induced by an activated RAS oncogene to promote tumorigenesis. Molecular cell. 2011;42(1):36-49.
179. Vredeveld LC, Possik PA, Smit MA, Meissl K, Michaloglou C, Horlings HM, et al. Abrogation of BRAFV600E-induced senescence by PI3K pathway activation contributes to melanomagenesis. Genes & development. 2012;26(10):1055-69.
180. Nichols AC, Yoo J, Palma DA, Fung K, Franklin JH, Koropatnick J, et al. Frequent mutations in TP53 and CDKN2A found by next-generation sequencing of head and neck cancer cell lines. Archives of otolaryngology--head & neck surgery. 2012;138(8):732-9.
181. Pedrero JM, Carracedo DG, Pinto CM, Zapatero AH, Rodrigo JP, Nieto CS, et al. Frequent genetic and biochemical alterations of the PI 3-K/AKT/PTEN pathway in head and neck squamous cell carcinoma. International journal of cancer Journal international du cancer. 2005;114(2):242-8.

182. Massarelli E, Liu DD, Lee JJ, El-Naggar AK, Lo Muzio L, Staibano S, et al. Akt activation correlates with adverse outcome in tongue cancer. Cancer. 2005;104(11):2430-6.
183. Lim J, Kim JH, Paeng JY, Kim MJ, Hong SD, Lee JI, et al. Prognostic value of activated Akt expression in oral squamous cell carcinoma. Journal of clinical pathology. 2005;58(11):1199-205.
184. Amornphimoltham P, Patel V, Leelahavanichkul K, Abraham RT, Gutkind JS. A retroinhibition approach reveals a tumor cell-autonomous response to rapamycin in head and neck cancer. Cancer research. 2008;68(4):1144-53.
185. Amornphimoltham P, Sriuranpong V, Patel V, Benavides F, Conti CJ, Sauk J, et al. Persistent activation of the Akt pathway in head and neck squamous cell carcinoma: a potential target for UCN-01. Clinical cancer research : an official journal of the American Association for Cancer Research. 2004;10(12 Pt 1):4029-37.
186. Nathan CO, Amirghahari N, Abreo F, Rong X, Caldito G, Jones ML, et al. Overexpressed eIF4E is functionally active in surgical margins of head and neck cancer patients via activation of the Akt/mammalian target of rapamycin pathway. Clinical cancer research : an official journal of the American Association for Cancer Research. 2004;10(17):5820-7.
187. Tsao AS, McDonnell T, Lam S, Putnam JB, Bekele N, Hong WK, et al. Increased phospho-AKT (Ser(473)) expression in bronchial dysplasia: implications for lung cancer prevention studies. Cancer epidemiology, biomarkers & prevention : a publication of the American Association for Cancer Research, cosponsored by the American Society of Preventive Oncology. 2003;12(7):660-4.
188. Roy HK, Olusola BF, Clemens DL, Karolski WJ, Ratashak A, Lynch HT, et al. AKT proto-oncogene overexpression is an early event during sporadic colon carcinogenesis. Carcinogenesis. 2002;23(1):201-5.
189. Bettstetter M, Berezowska S, Keller G, Walch A, Feuchtinger A, Slotta-Huspenina J, et al. Epidermal growth factor receptor, phosphatidylinositol-3-kinase catalytic subunit/PTEN, and KRAS/NRAS/BRAF in primary resected esophageal adenocarcinomas: loss of PTEN is associated with worse clinical outcome. Human pathology. 2013;44(5):829-36.
190. Khan KH, Yap TA, Yan L, Cunningham D. Targeting the PI3K-AKT-mTOR signaling network in cancer. Chinese journal of cancer. 2013;32(5):253-65.
191. Porta C, Paglino C, Mosca A. Targeting PI3K/Akt/mTOR Signaling in Cancer. Frontiers in oncology. 2014;4:64.
192. Souroullas GP, Sharpless NE. mTOR signaling in melanoma: oncogene-induced pseudo-senescence? Cancer cell. 2015;27(1):3-5.
193. Razmik Mirzayans DM. Role of Therapy-Induced Cellular Senescence in Tumor Cells and its Modification in Radiotherapy: The Good, The Bad and The Ugly. Journal of Nuclear Medicine & Radiation Therapy. 2013;s6(01).
194. Roberson RS, Kussick SJ, Vallieres E, Chen SY, Wu DY. Escape from therapy-induced accelerated cellular senescence in p53-null lung cancer cells and in human lung cancers. Cancer research. 2005;65(7):2795-803.
195. Elmore LW, Di X, Dumur C, Holt SE, Gewirtz DA. Evasion of a single-step, chemotherapy-induced senescence in breast cancer cells: implications for treatment response. Clinical cancer research : an official journal of the American Association for Cancer Research. 2005;11(7):2637-43.
196. Gewirtz DA. Autophagy, senescence and tumor dormancy in cancer therapy. Autophagy. 2009;5(8):1232-4.
197. Wu PC, Wang Q, Grobman L, Chu E, Wu DY. Accelerated cellular senescence in solid tumor therapy. Experimental oncology. 2012;34(3):298-305.
198. Wang Q, Wu PC, Dong DZ, Ivanova I, Chu E, Zeliadt S, et al. Polyploidy road to therapy-induced cellular senescence and escape. International journal of cancer Journal international du cancer. 2013;132(7):1505-15.
199. Sun Y, Nelson PS. Molecular pathways: involving microenvironment damage responses in cancer therapy resistance. Clinical cancer research : an official journal of the American Association for Cancer Research. 2012;18(15):4019-25.

200. Marinov M, Ziogas A, Pardo OE, Tan LT, Dhillon T, Mauri FA, et al. AKT/mTOR pathway activation and BCL-2 family proteins modulate the sensitivity of human small cell lung cancer cells to RAD001. Clinical cancer research : an official journal of the American Association for Cancer Research. 2009;15(4):1277-87.
201. Hambardzumyan D, Becher OJ, Rosenblum MK, Pandolfi PP, Manova-Todorova K, Holland EC. PI3K pathway regulates survival of cancer stem cells residing in the perivascular niche following radiation in medulloblastoma in vivo. Genes & development. 2008;22(4):436-48.
202. Gordon RR, Nelson PS. Cellular senescence and cancer chemotherapy resistance. Drug resistance updates : reviews and commentaries in antimicrobial and anticancer chemotherapy. 2012;15(1-2):123-31.
203. Achuthan S, Santhoshkumar TR, Prabhakar J, Nair SA, Pillai MR. Drug-induced senescence generates chemoresistant stemlike cells with low reactive oxygen species. The Journal of biological chemistry. 2011;286(43):37813-29.
204. Shamma A, Takegami Y, Miki T, Kitajima S, Noda M, Obara T, et al. Rb Regulates DNA damage response and cellular senescence through E2F-dependent suppression of N-ras isoprenylation. Cancer cell. 2009;15(4):255-69.
205. Gewinner C, Wang ZC, Richardson A, Teruya-Feldstein J, Etemadmoghadam D, Bowtell D, et al. Evidence that inositol polyphosphate 4-phosphatase type II is a tumor suppressor that inhibits PI3K signaling. Cancer cell. 2009;16(2):115-25.
206. Dirac AM, Bernards R. Reversal of senescence in mouse fibroblasts through lentiviral suppression of p53. The Journal of biological chemistry. 2003;278(14):11731-4.
207. Sage J, Miller AL, Perez-Mancera PA, Wysocki JM, Jacks T. Acute mutation of retinoblastoma gene function is sufficient for cell cycle re-entry. Nature. 2003;424(6945):223-8.
208. Brown JP, Wei W, Sedivy JM. Bypass of senescence after disruption of p21CIP1/WAF1 gene in normal diploid human fibroblasts. Science. 1997;277(5327):831-4.
209. Chin L, Pomerantz J, Polsky D, Jacobson M, Cohen C, Cordon-Cardo C, et al. Cooperative effects of INK4a and ras in melanoma susceptibility in vivo. Genes & development. 1997;11(21):2822-34.
210. Yu H, McDaid R, Lee J, Possik P, Li L, Kumar SM, et al. The role of BRAF mutation and p53 inactivation during transformation of a subpopulation of primary human melanocytes. The American journal of pathology. 2009;174(6):2367-77.
211. Chao SK, Lin J, Brouwer-Visser J, Smith AB, 3rd, Horwitz SB, McDaid HM. Resistance to discodermolide, a microtubule-stabilizing agent and senescence inducer, is 4E-BP1-dependent. Proceedings of the National Academy of Sciences of the United States of America. 2011;108(1):391-6.
212. Kuilman T, Peeper DS. Senescence-messaging secretome: SMS-ing cellular stress. Nature reviews Cancer. 2009;9(2):81-94.
213. Coppe JP, Kauser K, Campisi J, Beausejour CM. Secretion of vascular endothelial growth factor by primary human fibroblasts at senescence. The Journal of biological chemistry. 2006;281(40):29568-74.
214. McConkey DJ, Choi W, Marquis L, Martin F, Williams MB, Shah J, et al. Role of epithelial-to-mesenchymal transition (EMT) in drug sensitivity and metastasis in bladder cancer. Cancer metastasis reviews. 2009;28(3-4):335-44.
215. Bhatia B, Multani AS, Patrawala L, Chen X, Calhoun-Davis T, Zhou J, et al. Evidence that senescent human prostate epithelial cells enhance tumorigenicity: cell fusion as a potential mechanism and inhibition by p16INK4a and hTERT. International journal of cancer Journal international du cancer. 2008;122(7):1483-95.
216. Bartholomew JN, Volonte D, Galbiati F. Caveolin-1 regulates the antagonistic pleiotropic properties of cellular senescence through a novel Mdm2/p53-mediated pathway. Cancer research. 2009;69(7):2878-86.
217. Roninson IB. Tumor cell senescence in cancer treatment. Cancer research. 2003;63(11):2705-15.
218. Shay JW, Roninson IB. Hallmarks of senescence in carcinogenesis and cancer therapy. Oncogene. 2004;23(16):2919-33.

219. Sidi R, Pasello G, Opitz I, Soltermann A, Tutic M, Rehrauer H, et al. Induction of senescence markers after neo-adjuvant chemotherapy of malignant pleural mesothelioma and association with clinical outcome: an exploratory analysis. European journal of cancer. 2011;47(2):326-32.
220. Waldman T, Zhang Y, Dillehay L, Yu J, Kinzler K, Vogelstein B, et al. Cell-cycle arrest versus cell death in cancer therapy. Nature medicine. 1997;3(9):1034-6.
221. Albert JM, Kim KW, Cao C, Lu B. Targeting the Akt/mammalian target of rapamycin pathway for radiosensitization of breast cancer. Molecular cancer therapeutics. 2006;5(5):1183-9.
222. Demidenko ZN, Zubova SG, Bukreeva EI, Pospelov VA, Pospelova TV, Blagosklonny MV. Rapamycin decelerates cellular senescence. Cell cycle. 2009;8(12):1888-95.
223. Mao Z, Tian X, Van Meter M, Ke Z, Gorbunova V, Seluanov A. Sirtuin 6 (SIRT6) rescues the decline of homologous recombination repair during replicative senescence. Proceedings of the National Academy of Sciences of the United States of America. 2012;109(29):11800-5.
224. Naylor RM, Baker DJ, van Deursen JM. Senescent cells: a novel therapeutic target for aging and age-related diseases. Clinical pharmacology and therapeutics. 2013;93(1):105-16.
225. Bykov VJ, Issaeva N, Shilov A, Hultcrantz M, Pugacheva E, Chumakov P, et al. Restoration of the tumor suppressor function to mutant p53 by a low-molecular-weight compound. Nature medicine. 2002;8(3):282-8.
226. Ovadya Y, Krizhanovsky V. Senescent cells: SASPected drivers of age-related pathologies. Biogerontology. 2014;15(6):627-42.

Confirmation

Herewith, I confirm that I have written this thesis independently using only results of my investigation unless otherwise stated.

Heidelberg, April 2015

Babitha George